

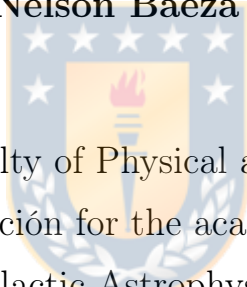


UNIVERSIDAD DE CONCEPCIÓN  
FACULTAD DE CIENCIAS FÍSICAS Y MATEMÁTICAS

# The First Deep Chemical Study of Globular Cluster NGC-2298

*The first spectroscopic prove of multiple population in this cluster*

Por: Ian Nelson Baeza Mardones



Thesis presented to the Faculty of Physical and Mathematical Sciences of  
the Universidad de Concepción for the academic degree of Magíster in  
Galactic Astrophysics.

November 2022

Concepción, Chile

Profesor Guía: Sandro Villanova



© 2022, Ian Baeza

Ninguna parte de esta tesis puede reproducirse o transmitirse bajo ninguna forma o por ningún medio o procedimiento, sin permiso por escrito del autor.

Se autoriza la reproducción total o parcial, con fines académicos, por cualquier medio o procedimiento, incluyendo la cita bibliográfica del documento.

No part of this thesis may be reproduced or transmitted in any form or by any means or process without written permission from the author.

Reproduction in whole or in part, for scholarly purposes, by any means or process, including bibliographic citation of the document, is authorized.



Dedicada a mi Madre, por su esfuerzo y persistencia tratando de siempre darme lo mejor

---

## AGRADECIMIENTOS

Me gustaría agradecer a todas las personas que me apoyaron durante el desarolllo de mi trabajo y con quienes encontre consuelo en aquellos momentos dificiles que la vida siempre nos presenta.

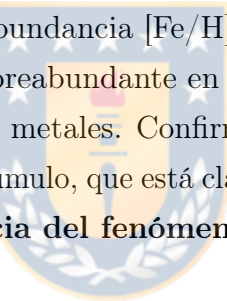
Me resulta imposible mencionar a todos aquellos me brindaron su ayuda pero es imposible para mi no mencionar al menos la constribución realizada por José Fernández Trincado, quien fue mi principal instructor en las tecnicas basicas de como usar el principal software en este estudio y por tanto le estoy muy agradecido pues sin el no hubiese sido capaz de llevar a cabo este proyecto.



## Resumen

Presentamos las primeras abundancias elementales detalladas de las estrellas del cúmulo globular pobre en metales NGC 2298. Basados en espectros de alta resolución en el infrarrojo cercano ( $R \sim 22,500$ ) de 12 miembros obtenidos durante la segunda fase del **Apache Point Observatory Galactic Evolution Experiment (APOGEE)** en el Observatorio Las Campanas como parte de la decimoséptima publicación de datos (DR 17) del Sloan Digital Sky Survey IV. Empleamos el **Código Automático de Bruselas para la Caracterización de Espectros de Alta Precisión (BACCHUS)**.

Encontramos una metalicidad media y mediana  $[Fe/H] = -1,76$  y  $-1,75$ , respectivamente, con una dispersión de estrella a estrella de 0,14 dex, que es compatible con los errores internos de medición. no encontramos ninguna evidencia de una dispersión intrínseca de la abundancia  $[Fe/H]$ . El enriquecimiento típico de elementos  $\alpha$  en NGC 2298 es sobreabundante en relación con el Sol, y sigue la tendencia de otros CGs pobres en metales. Confirmamos la existencia de una población enriquecida en Al en este cúmulo, que está claramente anticorrelacionada con el Mg, **indicando la prevalencia del fenómeno de población múltiple en NGC 2298.**

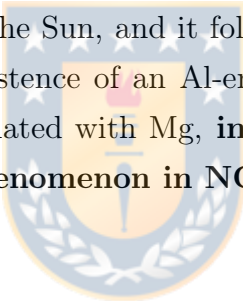


**Keywords** – NGC 2298, Cúmulo Globular, Poblaciones Estelares Multiples, Tesis de Magíster

## Abstract

We present **the first detailed elemental abundances of stars in the metal-poor globular cluster NGC 2298**. Based on near-infrared high-resolution ( $R \sim 22,500$ ) spectra of 12 members obtained during the second phase of the **Apache Point Observatory Galactic Evolution Experiment (APOGEE)** at Las Campanas Observatory as part of the seventeenth Data Release (DR 17) of the Sloan Digital Sky Survey IV. We employed the **Brussels Automatic Code for Characterizing High accuracy Spectra (BACCHUS)**.

We find a mean and median metallicity  $[Fe/H] = -1.76$  and  $-1.75$ , respectively, with a star-to-star spread of 0.14 dex, which is compatible with the internal measurement errors. we don't find any evidence for an intrinsic  $[Fe/H]$  abundance spread. The typical  $\alpha$ -element enrichment in NGC 2298 is overabundant relative to the Sun, and it follows the trend of other metal-poor GCs. We confirm the existence of an Al-enhanced population in this cluster, which is clearly anti-correlated with Mg, **indicating the prevalence of the multiple-population phenomenon in NGC 2298**.



# Contents

|   |            |
|---|------------|
| <b>AGRADECIMIENTOS</b>                                    | <b>i</b>   |
| <b>Resumen</b>  | <b>ii</b>  |
| <b>Abstract</b>   | <b>iii</b> |
| <b>1 Introduction</b>                                     | <b>1</b>   |
| 1.1 Basic Definitions . . . . .                           | 1          |
| 1.2 Globular Cluster . . . . .                            | 2          |
| 1.2.1 Globular Cluster in Milky Way . . . . .             | 3          |
| 1.3 Motivation . . . . .                                  | 4          |
| <b>2 Theoretical Framework</b>                            | <b>6</b>   |
| 2.1 Stars and Single Stellar Population . . . . .         | 6          |
| 2.1.1 Stellar stages . . . . .                            | 8          |
| 2.1.2 Nucleosynthesis . . . . .                           | 10         |
| 2.1.3 Isochrones . . . . .                                | 13         |
| 2.2 Spectroscopy: Characterizing spectral lines . . . . . | 14         |
| 2.2.1 Profiles . . . . .                                  | 15         |
| 2.2.2 Intrinsic effects and from the medium . . . . .     | 16         |
| 2.2.2.1 Natural Broadening . . . . .                      | 16         |
| 2.2.2.2 Doppler Broadening . . . . .                      | 17         |
| 2.2.2.3 Pressure Broadening . . . . .                     | 18         |
| 2.2.2.4 Granulation and Micro Turbulence . . . . .        | 18         |
| 2.2.3 Characterization of Lines . . . . .                 | 20         |
| 2.3 Multiple Stellar Population . . . . .                 | 22         |
| 2.3.1 Evidence of the Phenomena . . . . .                 | 24         |
| 2.3.1.1 Photometry of MPs . . . . .                       | 24         |
| 2.3.1.2 Spectroscopy of MPs . . . . .                     | 25         |
| 2.3.2 Models . . . . .                                    | 27         |
| 2.3.2.1 Multiple epoch of star formation . . . . .        | 28         |
| 2.3.2.1.1 Reverse Order Model . . . . .                   | 29         |
| 2.3.2.1.2 Early Star Formation Period (eSFP) . .          | 29         |
| 2.3.2.2 Single epoch of star formation . . . . .          | 30         |
| 2.3.2.2.1 Very Massive Stars (VMS) . . . . .              | 31         |

---

|          |   |           |
|----------|---|-----------|
| 2.3.3    | Predictions vs Reality of MPs . . . . .   | 32        |
| 2.4      | Data Information . . . . .  | 34        |
| 2.4.1    | Gaia Data Release 3 . . . . .   | 34        |
| 2.4.2    | APOGEE-2: The Apache Point Observatory Galactic Evolution Experiment II . . . . .   | 34        |
| 2.4.3    | BACCHUS: Brussels Automatic Code for Characterizing High accuracy Spectra . . . . . | 35        |
| <b>3</b> | <b>Methodology</b>  | <b>36</b> |
| 3.1      | Determination of likely Members . . . . .   | 36        |
| 3.1.1    | Vector Point Diagram and Position in the sky . . . . .                              | 36        |
| 3.1.1.1  | Cross-match and Contrast with preliminary values of ASCAP . . . . .                 | 38        |
| 3.2      | Inference of Atmospheric parameters . . . . .                                       | 41        |
| 3.2.1    | Micro Turbulence $\xi_{micro}$ . . . . .  | 46        |
| 3.3      | Conversion Vacuum to Air Wavelength from APOGEE spectra . . . . .                   | 46        |
| 3.4      | Running BACCHUS . . . . .   | 46        |
| 3.4.1    | Self Consistency of C-N-O . . . . .   | 47        |
| 3.4.2    | Central Values . . . . .  | 48        |
| <b>4</b> | <b>Analysis</b>   | <b>49</b> |
| 4.1      | Inputted Parameters on BACCHUS . . . . .  | 49        |
| 4.2      | Looking at the Central Values . . . . .   | 50        |
| 4.3      | Error Estimation . . . . .  | 51        |
| <b>5</b> | <b>Results</b>  | <b>53</b> |
| 5.1      | Abundances . . . . .  | 53        |
| 5.1.1    | CNO . . . . .   | 53        |
| 5.1.2    | Independence of Parameters . . . . .  | 55        |
| 5.1.3    | Multiple Stellar Population on NGC 2298 . . . . .                                   | 56        |
| 5.1.3.1  | The $\alpha$ elements Mg, Si, Ca . . . . .  | 57        |
| 5.1.3.2  | The odd-z element Al . . . . .  | 58        |
| 5.1.3.3  | Iron peak elements Fe and Ni . . . . .  | 58        |
| 5.1.4    | Contrast whit the Pipeline of APOGEE . . . . .                                      | 59        |
| <b>6</b> | <b>Conclusion</b>   | <b>61</b> |
|          | <b>Referencias</b>  | <b>63</b> |

# List of Tables

|   |    |
|---|----|
| 3.1.1 Photometric, kinematic, and astrometric properties of twelve likely members of NGC 2298 . . . . .         | 40 |
| 3.2.1 Photometric Correction, inferred values of reddening and distance   | 45 |
| 4.1.1 Atmospheric Parameters and classification of the targets.<br>(Summarized values of Fig (4.1.1)) . . . . . | 50 |
| 5.1.1 Estimated abundances for the selected sources, also are shown the results from ASCAP . . . . .            | 56 |
| 6.0.1 Our findings Vs Literature Values . . . . .   | 62 |



# List of Figures

|  |    |
|--|----|
| 1.2.1 Hubble composite image of globular cluster NGC 2298 . . . . .  | 3  |
| 2.1.1 Hertzsprung–Russell typical shape of Globular Cluster & Example<br>of evolution track of a single star . . . . .       | 7  |
| 2.1.2 Nucleosynthesis Chains . . . . .   | 11 |
| 2.1.3 S-process , R-process and Binding Energy . . . . .   | 12 |
| 2.1.4 Theoretical Isochrones PARSEC (Bressan et al., 2012) . . . . .   | 13 |
| 2.2.1 Types of spectra (Smith, 2007) . . . . .   | 14 |
| 2.2.2 Example of Voight functions (Ji, 2017) . . . . .   | 16 |
| 2.2.3 Thermal Broadening scheme (COSMOS, 2022) . . . . .   | 18 |
| 2.2.4 Snapshot of granulation simulation (González Manrique et al., 2020) .  | 19 |
| 2.2.5 Example of how granulation bend the spectral lines (Gray, 2005) .  | 21 |
| 2.2.6 Reference image of the optical depth to be considered of a Bisector<br>(González Manrique et al., 2020) . . . . .      | 22 |
| 2.3.1 Chromosome map and CMDs of NGC 2808 Latour et al. (2019) .   | 24 |
| 2.3.2 Spectroscopic measures of abundances by the group CAPOS<br>(Geisler et al., 2021b) . . . . .                           | 26 |
| 2.3.3 Schemes of models to explain the MP’s phenomena with multiple<br>epoch of star formation . . . . .                     | 28 |
| 2.3.4 Reverse Order Model, (modified image from Marcolini et al., 2009)  | 29 |
| 2.3.5 Simulation of eSFP model Wünsch et al. (2017) . . . . .  | 30 |
| 2.3.6 Schemes of models to explain the MP’s phenomena with a single<br>epoch of star formation . . . . .                     | 31 |
| 2.3.7 Scheme of VMS model Gieles et al. (2018) . . . . .   | 32 |
| 2.3.8 Summary of Models & Current estimation for most of GC in Milky<br>Way (images from Bastian and Lardo (2018)) . . . . . | 33 |
| 3.1.1 Individual probability of membership by Position in the Sky and<br>Proper Motion respectively . . . . .                | 37 |
| 3.1.2 Values of ASCAP contrasted with our criteria of selection of Members   | 39 |
| 3.2.1 Initial assignment of stellar stage & Color Consistency (most reliable<br>measures) . . . . .                          | 42 |
| 3.2.2 Sigma associated with each source . . . . .  | 44 |
| 3.2.3 Best Isochrone Fit, 3 Free parameters $\chi^2$ test . . . . .  | 45 |
| 3.4.1 Self consistency as described by Smith et al. (2013) . . . . .   | 47 |

|   |    |
|---|----|
| 3.4.2 Typical output of BACCHUS . . . . .   | 48 |
| 4.1.1 Kiel diagram (showing our inferred parameters) . . . . .  | 49 |
| 4.2.1 Example of the final fit of synthetic spectra to the real measures . . . . .  | 51 |
| 5.1.1 Summarized in this plot our findings and the final values report<br>(Globally and deferentially respectively) Baeza et al. (2022) . . . . . | 54 |
| 5.1.2 Linear Regression between stellar parameters and abundance<br>estimation (Baeza et al. (2022)) . . . . .                                    | 55 |
| 5.1.3 Final values of $[Fe/H]$ contrasted with the preliminary data of<br>ASCAP . . . . .   | 60 |



# Chapter 1

## Introduction

### 1.1 Basic Definitions

The basic notions and definitions to start talking about our main topic are listed

- **star(s):** are the fixed luminous point in the night sky which is a large, remote incandescent body like the sun, from the study of this object through their light, we know that the atmospheres of the vast majority of all stars are composed primarily of hydrogen, usually about 70-75%, Helium 24-27% and just < 3% for other elements (Basic notions of astrophysics are addressed in [Carroll and Ostlie, 2006](#))
- **Star Clusters:** when we talk about these objects we refer to groups of stars gravitationally bound. (for more generalized info see [Krumholz et al., 2019](#))
- **(Giant) Molecular Clouds:** Large structures composed principally of molecular hydrogen ( $H_2$ ) where the stars and star clusters are born. (for further info see [Heyer and Dame, 2015](#))
- **Photometry** is the act of measuring the flux within a limited wavelength range that we receive from celestial objects. The wavelength sensitive within the range it's characterized by a curve of Transmittance. The flux of a star is the sum of the star's contribution over all pixels illuminated by it. (for further details see [Walker \(2019\)](#), as e.g of this technique [Strömgren \(1966\)](#))

- **Spectroscopy:** This is a technique that consist in passing light through a slit and/or a prism to see its spectrum (light separate by wavelength). Exists three types of emission that can be measured, the continuous, absorption and emission. (this is addressed in section [2.2](#))

A *continuous spectrum* is simply the light in all wavelengths, like a rainbow, having no visibly peaks or gaps on the wavelength range measured, (thermal emission).

An *emission spectrum* are bright lines (emission lines) seen while atoms emits energy in their specific levels allowed or molecules in their specific range (seen while the atoms or molecules are exited, e.g. can be measured while are heated and passed through a spectrograph).

An *absorption spectrum* is the opposite to the emission line, are dark gaps in the continuum (absorption lines) produced by the resonance of photons with the specific levels of energy of atoms an molecules (seen while passing continuous radiation through a cold gas (atoms and/or molecules) relative to the continuum emission and then measured by the spectrograph).

The emission and absorption lines are unique for each element/molecule and their shape and intensity depends to different physical conditions (temperature, surface gravity, turbulence of the medium that produce them, etc.) (e.g. of this technique in infrared [Merrill and Ridgway, 1979](#)), (the past two item was inspired from [Frelijj Rubilar, 2017](#)).

## 1.2 Globular Cluster

Globular clusters (GCs) are larges groups of old stars with a very compact distribution reaching millions of stars contained within a few parsec cubic, they are important long-lived time capsules that provide information about the primordial evolutionary stages of their host galaxies. For several decades, GC stars have been known to exhibit star-to-star variations in specific elements (e.g., He, C, N, O, Na, Al), (such as lightelement ([Carretta et al., 2009b](#); [Schiavon et al., 2017](#); [Masseron et al., 2019](#); [Mészáros et al., 2020, 2021](#); [Geisler et al., 2021b](#)), and heavy-element ([Carretta and Bragaglia, 2021](#); [Fernández-Trincado et al., 2020c](#); [Marino et al., 2021](#))) this abundance spread is present over a wide range of metallicities, which

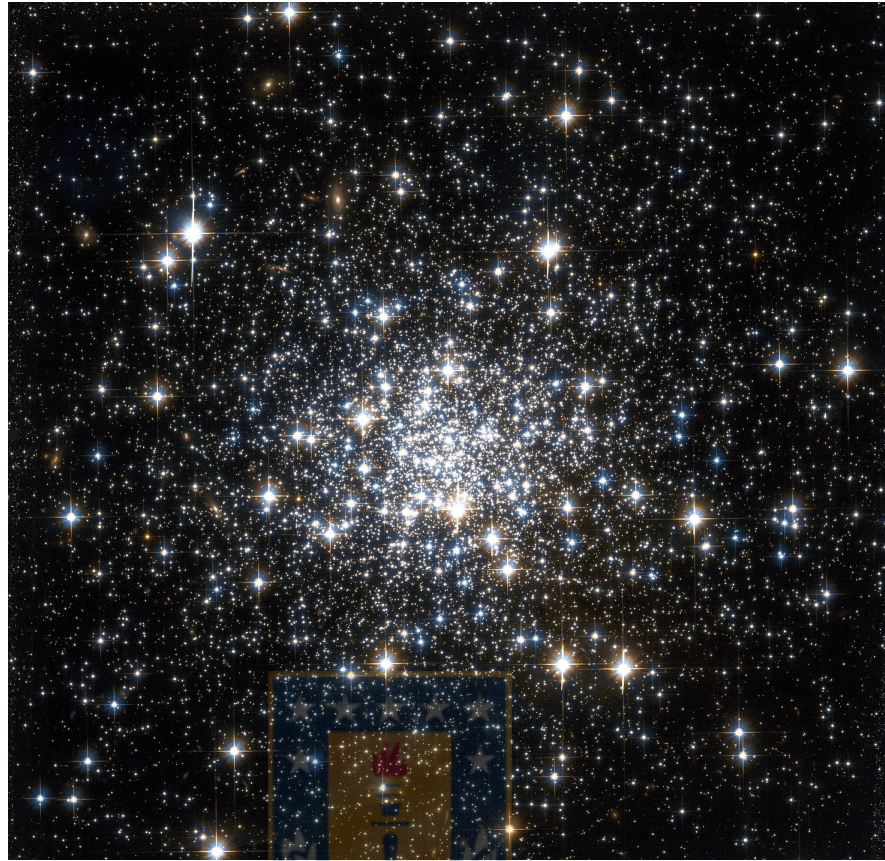


**Figure 1.2.1:** Hubble composite image of globular cluster NGC 2298

have been attributed to the Multiple stellar Populations (MPs) phenomenon (This phenomenon is observed in nearly all of the ancient GCs, for a thorough review, see ([Bastian and Lardo, 2018](#))), these variations can be evidenced spectroscopically and also photometrically.

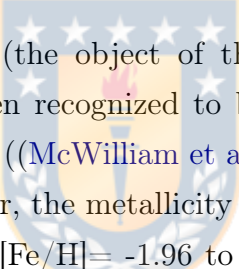
### 1.2.1 Globular Cluster in Milky Way

The ESA *Gaia* mission ([Gaia Collaboration et al., 2016, 2018, 2021](#)) has provided compelling evidence that the Milky Way (MW) was a cannibal Galaxy in its earlier years, some 8 to 10 Gyrs ago (see e.g., [Kruijssen et al., 2020](#)), and GCs have been formed when the Galaxy experienced a phase of rapid assembly ([Kruijssen et al., 2019, 2020](#)).

The building blocks of these early epochs have became part of the stellar populations of the MW (e.g. see the review of [Sandage \(1986\)](#)), and have been identified by numerous studies (see e.g., [Kraft, 1979](#)). Due the nature of GCs we could use them to trace how our galaxy had been evolved. Some of these events we

can found the debris of what were once believed to be massive ( $\gtrsim 10^8 M_{\odot}$ ) dwarf galaxies such as the *Gaia*-Enceladus-Sausage (Belokurov et al., 2018; Myeong et al., 2018; Helmi et al., 2018), Sequoia (Myeong et al., 2019), Helmi streams (Helmi et al., 1999), Kraken (Kruijssen et al., 2020), the disrupting Sagittarius dwarf galaxy (Ibata et al., 1994; Hasselquist et al., 2017, 2019; Antoja et al., 2020), and other minor sub-structures (Koppelman et al., 2019) some of which are likely associated either fully or partially dissolved or dissolving GCs (see e.g., Lind et al., 2015; Fernández-Trincado et al., 2016, 2017; Recio-Blanco et al., 2017; Fernández-Trincado et al., 2019a,b; Koch et al., 2019; Hanke et al., 2020; Fernández-Trincado et al., 2020a,b,d,e; Kundu et al., 2019a,b; Fernández-Trincado et al., 2021a,b; Koch-Hansen et al., 2021; Kundu et al., 2021, for instance).

## 1.3 Motivation



The southern cluster NGC 2298 (the object of this study), located in the constellation Puppis, has long been recognized to be among the most metal-poor GCs in the Milky Way (MW) ((McWilliam et al., 1992; Zhang et al., 2012; Dalessandro et al., 2012)). However, the metallicity estimates reported for this object have covered a range from  $[Fe/H] = -1.96$  to  $-1.71$  ((Frogel et al., 1983; McWilliam et al., 1992; Zinn and West, 1984; Geisler et al., 1995; Carretta and Gratton, 1997; Kraft and Ivans, 2003; Pritzl et al., 2005; Carretta et al., 2009b; Roediger et al., 2014)), creating some uncertainty regarding its status as one of the most metal-poor systems.

This cluster is also well known for its lack of a clear indication of MPs along the main sequence (MS) ((Piotto et al., 2015)), in contrast of what could be seen along the horizontal branch (HB) population ((Rani et al., 2021)), in near-UV/optical color-magnitude diagrams (CMDs). More significantly, its red-Giant branch (RGB) displays clear evidence for both first and second generation stars (e.g., (Milone et al., 2017)).

NGC 2298 is a particularly interesting GC, as its origin and nature still remains controversial. For instance, some studies have proposed that it is likely associated with the Monoceros progenitor galaxy ((Crane et al., 2003; Martin et al., 2004; Forbes and Bridges, 2010)) however, more recent studies conducted by (Massari et al., 2019) and (Malhan et al., 2022) have linked this GC to the Gaia-

Sausage/Enceladus merger (([Belokurov et al., 2018](#); [Helmi et al., 2018](#))). A few previous and more recent studies have also suggested the presence of extra-tidal features around NGC 2298 (([Leon et al., 2000](#); [Balbinot et al., 2011](#); [Carballo-Bello et al., 2018](#); [Sollima, 2020](#); [Ibata et al., 2021](#)) however, their existence has been questioned based on more recent investigations of deep imaging from the Dark Energy Camera (([Zhang et al., 2022](#)))).

While NGC 2298 has been widely studied photometrically (in the optical and UV), detailed spectroscopic information about it remains sparse (some spectroscopic studies have been performed, e.g., [McWilliam et al. \(1992\)](#); [Geisler et al. \(1995\)](#), but with short samples of stars or without a large variety of elements and without a resolution comparable to nowadays). Furthermore, high resolution spectroscopic evidence for the existence of multiple stellar populations in this GC has not been reported in the literature yet (evidenced as are showed in section [2.2](#)).

Due this it became imperative look for their chemical abundance, because using this as a signature and a window of the evolutionary path that the GC follow since was formed to nowadays, owing to unraveled nature yet of spread of this patterns in their chemistry (e.g. [Bastian and Lardo \(2018\)](#); [Renzini et al. \(2015\)](#)), we push forward the analysis of chemical spectra through the Apache Point Observatory Galactic Evolution Experiment (APOGEE,[Majewski et al. \(2017\)](#)) of the Sloan Digital Sky Survey-IV ([Blanton et al. \(2017\)](#)), which was provide large amount of information (due the nature of near infrared spectra which allow us to study previously inaccessible info in heavy obscured areas as Bulge of MW) recently analysed by group CAPOS (e.g. [Geisler \(2018\)](#); [Geisler et al. \(2021a\)](#); [Romero-Colmenares et al. \(2021\)](#)).

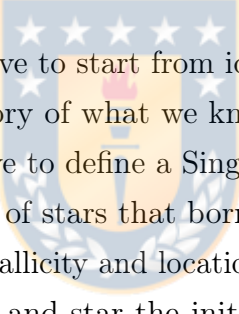
NGC 2298 is located at 15.1 kpc (([Baumgardt and Vasiliev, 2021](#))) from the Galactic center, it is an old ( 13.15 Gyr; ([Monty et al., 2018](#))) GC that lies in a region of relatively low foreground interstellar reddening, with  $E(B-V) \sim 0.14-0.16$  ([Kraft and Ivans \(2003\)](#); [Piotto et al. \(2015\)](#); [Monty et al. \(2018\)](#)), making it an excellent candidate for the study of MPs in GCs at a low Galactic latitude ( $b \sim -16^\circ$ ).

Therefore our aim is to study this GC to confirm the hypothesis that the phenomena of MPs is present in this cluster through high-resolution spectroscopy and confirm if this behaviour follow the trend of other GC in the same range of metallicity.

# Chapter 2

## Theoretical Framework

### 2.1 Stars and Single Stellar Population

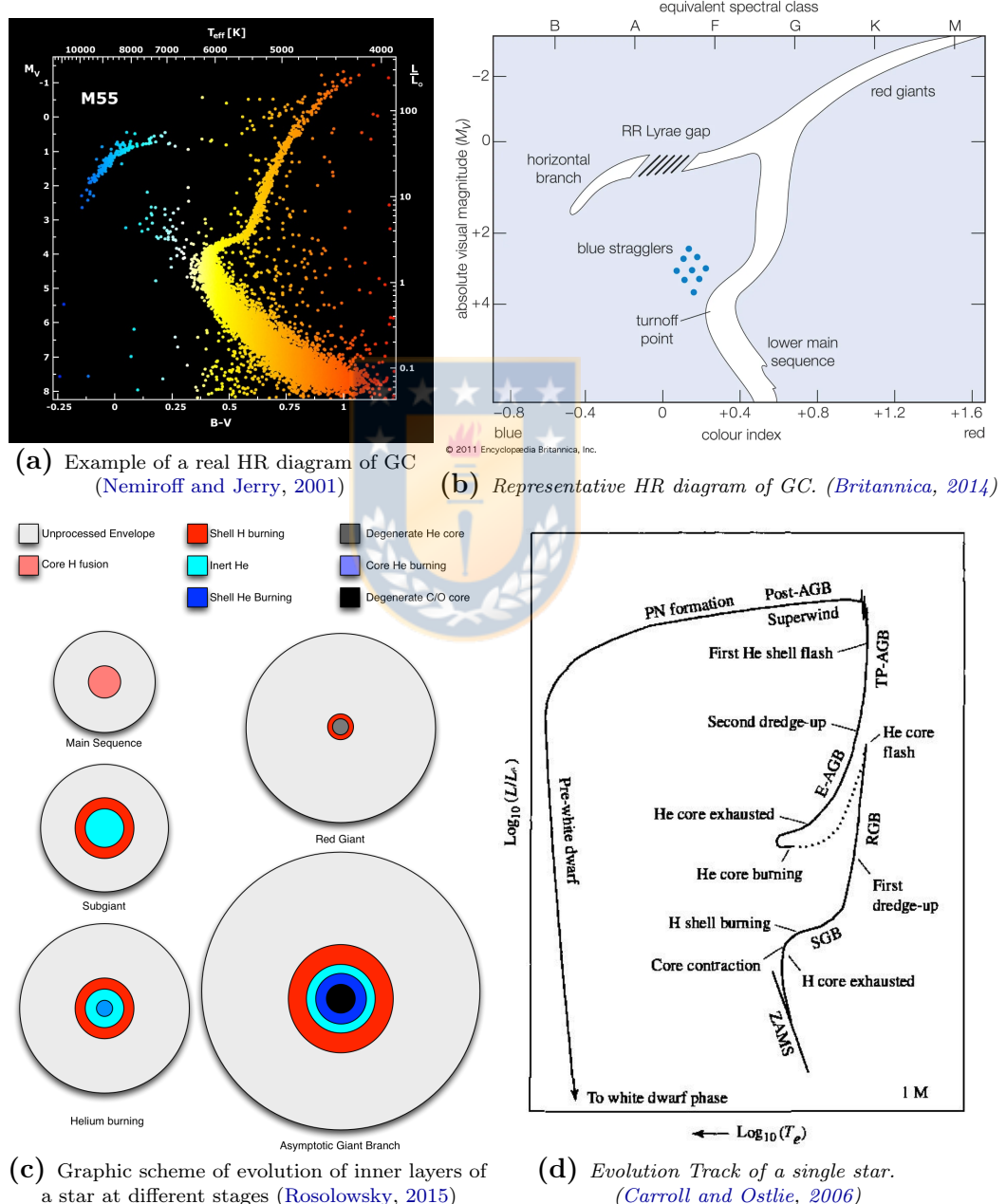


To understand reality we always have to start from idealized and simple models, so in order to understand the history of what we know and what we expect at the beginning from GC we first have to define a Single stellar population (SSP), this refers in simple terms a group of stars that born together (same age) with the same initial condition (such metallicity and location/environment) which only leaves as a difference between star and star the initial mass that was accreted for the formation of the star (Bruzual A., 2010), this characteristic will follow a specific distribution known as Initial Mass Function (IMF) this function primarily is dominated by probability (referring that it's less likely to have much mass in a single star) in second order response to the environment, the composition of the nebula, etc. (for further details in this topic we encourage to see Bastian et al. (2010)).

If we narrow down this idea of SSP to the GC we could imagine the physical phenomena which generate these objects, the idea consist in that a group of stars born from the same nebula (was assumed that due the time of collapse of nebula is very short in relative to the life of low mass star (as was aiming to study old stars) we can assume that the differential fragmentation of the nebula would not be a significant parameter in the final evolution, in futures sections we will see some models that within this time ranges significantly events could happen), then stars evolves at different timescales due the different initial mass. This was the

primordial idea behind GC (Milone and Marino, 2022; Bastian and Lardo, 2018), this due the characteristic pattern that we can distinguish in the HR-diagram which could directly be related with the evolution track theorized (see fig 2.1.1).

**Figure 2.1.1:** Hertzsprung–Russell typical shape of Globular Cluster & Example of evolution track of a single star



The evolution track of a single star it is pretty well understood through our understanding of physics (such as nuclear, thermodynamics, mechanic statistics,

etc. Maercker, 2009; Bressan et al., 2012; Boeltzig et al., 2016; Gratton et al., 2019) (exists as an exception to this affirmation at the final stages when massive stars dies ( $> 10\odot$ ), it is not always clearly which path the star will follow or which are the most significant parameters (apart from the mass of course) that will indicate how the star will die, e.g. see Pejcha (2020)), we know and expect specific behaviors in specific condition that are reached at the different evolutionary stages of a star as can be look in detail in fig 2.1.1d.

### 2.1.1 Stellar stages

The main stages/phases of the stars (to the purpose of this thesis we just address Post-Zero-Age-Main-Sequence Stellar Evolution until late type of Asymptotic Giant Branch, for further info about this stages or the ones not addressed here see e.g. Bruzual A. (2010); Carroll and Ostlie (2006); Eldridge (2008); Pejcha (2020); Krumholz et al. (2019); Maercker (2009); Rosolowsky (2015); Nomoto et al. (2013); Pagel (2009)) are defined through our current knowledge of physics, in simple terms,

(contrast the following information with the figures 2.1.1 and 2.1.1c)

- **Zero-Age Main Sequence (ZAMS):** is a diagonal line in the HR-diagram where stars depending of their initial masses first reach the main sequence and begin equilibrium hydrogen burning
- **Main Sequence (MS):** refers to a star while is burning Hydrogen in their core in Hydro-Thermal equilibrium
- **Turn Off:** this term is used to refers at the phase in the HR diagram were the stars have exhausted the hydrogen in their cores
- **Sub Giant Branch<sup>1</sup> (SGB):** is the phase that occurs after the Turn-Off point, due the sudden decrease of energy the core contracts rapidly causing that the envelope of the star starts to expand and make the temperature cools, resulting in redward movement on the HR-diagram.
- **Red Giant Branch<sup>1</sup> (RGB):** this stage happens after the SGB, it starts when the temperature of the star become stable again, this phase generate

---

<sup>1</sup>We use the term "*Branch*" due usually we look at these as a group in the HR-diagram and could be understood as a ramification

strong convection between layers (this mixture of elements it is called first dredge-up) and becomes more efficiently with the time which it's reflected in the HR-diagram moving above (becoming more bright).

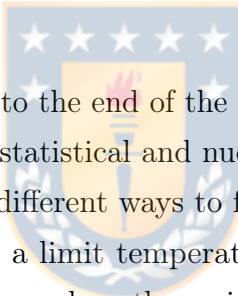
- **Helium Core Flash:** This phase (also known as Helium Flash) is a violent process and mark the end of the RGB stage, as the name indicates it is when the star starts to burn Helium in the core, this generate dramatically the temperature of the star which in the HR-diagram could be appreciate as a abrupt jump to left (the bluer/hotter)
- **Horizontal Branch<sup>1</sup> (HB):** This stage refers when the star is fusing Helium in their core, usually this stage is divided in three parts the blueward portion (B-HB, which is an analogous to the MS) an intermediate area of instability in the envelopes (RR Lyrae Gap) and the redward portion (R-HB) , the main difference between the R-HB and the B-HB is if the core of the star is still fusing Helium (because this stage is a much shorter to the previous stages). Moreover in the HR-diagram the look as a horizontal trend evolving from the B-HB to the R-HB.
- **Early Asymptotic Giant Branch<sup>12</sup> (E-AGB):** Named like this because the characteristic behaviour is approaching to the RGB asymptotically (becomes brighter and cooler), also is it's very analogous process to the RGB phase, happens after the HB and starts when the Hydrogen layer that was fusing becomes almost inactive. In this stage the stars shows strong convection between layers again (named as Second dredge-up)
- **Thermal Pulsing Asymptotic Giant Branch<sup>12</sup> (TP-AGB):** on certain point the Hydrogen layer reignites and becomes the main source of energy, during this process the Helium shell begins to turn off and turn on in a quasi-periodic pattern (this due the Hydrogen generates Helium, the Helium is being accumulated and at certain point ignites and fuse quickly until diminishes the quantity enough to turn off, and this repetitively), this periodicity is a function of the mass of the star , also again due the fusion in shell outside the core the star experiments again strong convection between layers (which is known as the third dredge-up)

---

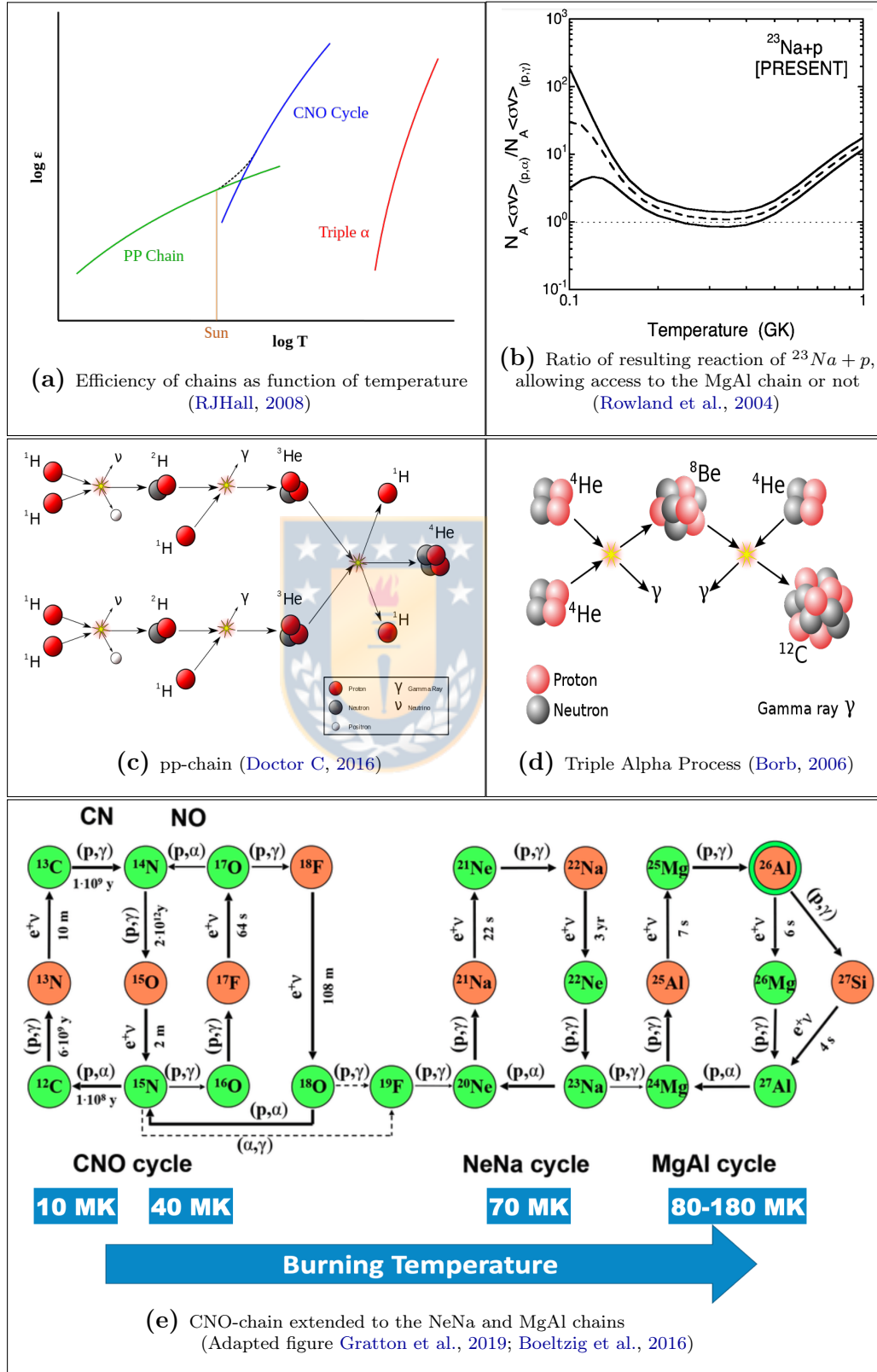
<sup>2</sup>This phases are known for a mass lost (the outer layer when the shell of H or He ignites are not in thermal-Hydrostatic equilibrium hence part of these are expelled)

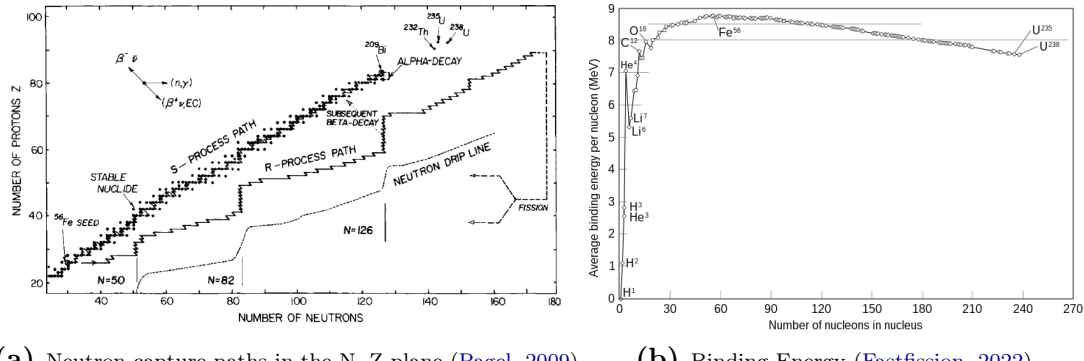
- **Post-AGB, White Dwarf, Supernova:** Here depending of the mass of the star will evolve differently, if is a relative low mass star most of the outer layers are being expelled and the star likely will become a white dwarf, instead if is a more massive star at certain point some of the pulsations of the star will be aggressive enough to make the star collapse here a Supernova event could occur or a direct collapse in certain cases the remnant of the star on these cases are neutron stars or black holes
- **Blue Stragglers (BS):** they are blue stars that locate above the turn-off point and are brighter and bluer, our understanding of these objects it's note clear (are not directly related with a normal stellar evolution) the most likely scenarios appear to be mass exchange with a binary star companion, or collisions between two stars, extending the star's main-sequence lifetime

### 2.1.2 Nucleosynthesis



Bypassing the last stages (previous to the end of the life of stars) and the BS, we know what occurs inside a star (in statistical and nucleosynthesis terms [Nomoto et al. \(2013\); Pagel \(2009\)](#)), exists different ways to fuse material depending the stage and the mass (which implies a limit temperature that can be reached in the core or the layers), in fig (2.1.2) we show the main chains that fuse Hydrogen and Helium moreover on which range relative to the other cycles this are effective (dominant, see fig 2.1.2a). For low mass stars the pp-chain (fig 2.1.2c) (and their variations) it's the main source of energy, and at the stages it's present along all the life of the star, for more massive stars CNO cycle and their extension to the NeNa or even the MgAl chains (fig 2.1.2e) become the dominant source of energy (look at the different temperatures needed to reach different cycles, also the specific panel (2.1.2b) indicates at which temperatures become relevant the initial combustion for the MgAl chain), the at later stages the combustion of Helium is carried out by the Triple Alpha process (fig 2.1.2d) (Also the "Alpha process" /"Alpha Ladder" which fuse Helium cores with other elements and produce the heavy elements), for even more massive stars another combustion become relevant (e.g. Carbon Burning could occur but I don't address this on this thesis due the most important chains for old stars are already mentioned).

**Figure 2.1.2:** Nucleosynthesis Chains

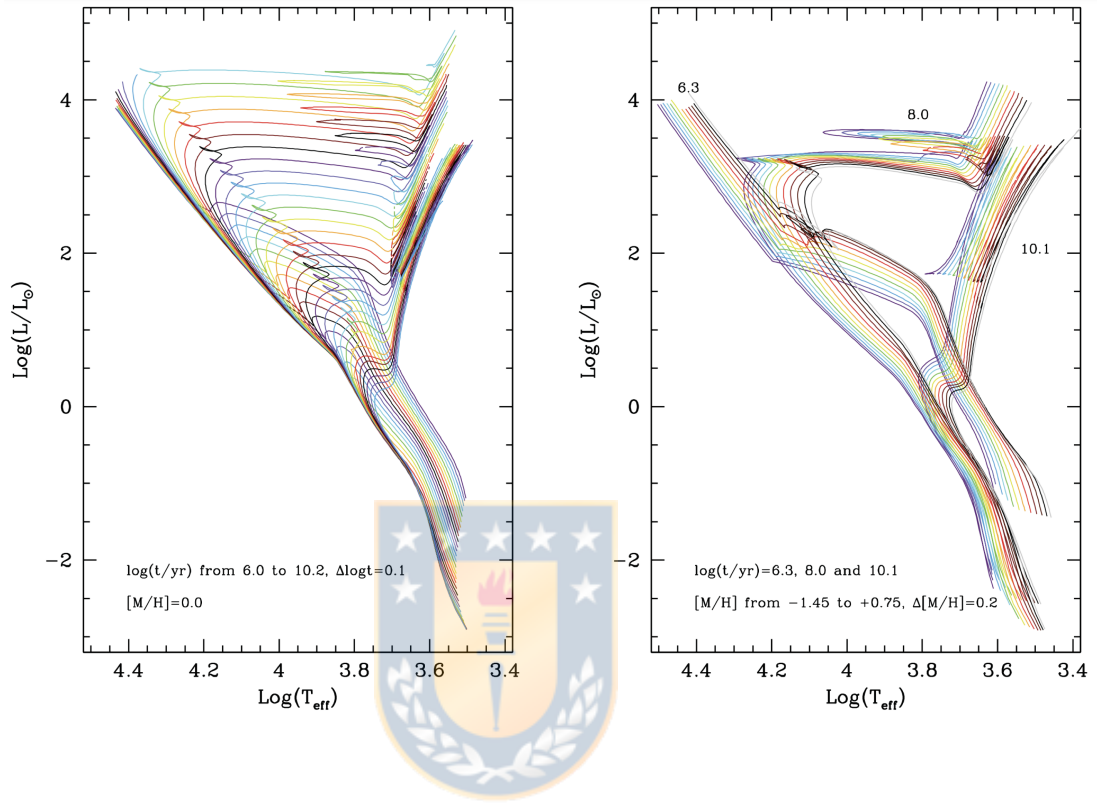
**Figure 2.1.3:** S-process , R-process and Binding Energy(a) Neutron capture paths in the  $N, Z$  plane (Pagel, 2009)

(b) Binding Energy (Fastfission, 2022)

On the other hand, we also had the s-process and the r-process which generates heavier elements (see fig 2.1.3), due the lack of charge of the neutron they could interact with the nuclei freely just requires a probabilistic event of collide with them , the differences between r and s process it's just the density of the neutron (increasing the probability of collide), r-process occur in violent events (e.g. Super Novas) and the s-process occurs along the lifetime of the star (it is believed to be most relevant in AGB) , these process are ubiquitous for all the elements (which means the only factors that have to consider is the cross section of the nuclei and neutrons and the density of them in the environment), and the production of heavier elements it's ruled by the valley of stability (see 2.1.3a) which is the range where atoms become (relative) stable and elements far from this quickly decays to this area, and the binding Energy (see 2.1.3b) which gradually (far elements with more protons will decay quickly) will make the heavier than Iron elements decay down until become Iron.(Pagel, 2009; Schatz, 2004; Nomoto et al., 2013)

### 2.1.3 Isochrones

**Figure 2.1.4:** Theoretical Isochrones PARSEC (Bressan et al., 2012)



As long as we know how the star evolves and which process occurs inside them we are able to model how it's expected that a SSP (a group of stars within a range of masses with an specific initial composition and given a certain time of evolution) it's expected to behave, this kind of model are called Isochrones (see fig 2.1.4), through these kind of model we could retrieve most of the info of a star as the initial mass, lost mass, evolutionary stage, current chemical composition (within the same SSP considering the variations in stages due normal nucleosynthesis it's not expected to have spread over 0.2 dex, Marigo et al. (2017)), with these parameters also we could retrieve their synthetic spectra and analyse how they should be look through specific filters using the specific passband of the filter and a standardized distance.(Bressan et al., 2012; Marigo et al., 2017; Nguyen et al., 2022)

Photometrically (when we look at the HR-diagram) exists two section with a very useful sensitivity, the Turn-Off point which is very sensitive to the age of the sample (in a same sample of mass distribution the stars will start to run out of

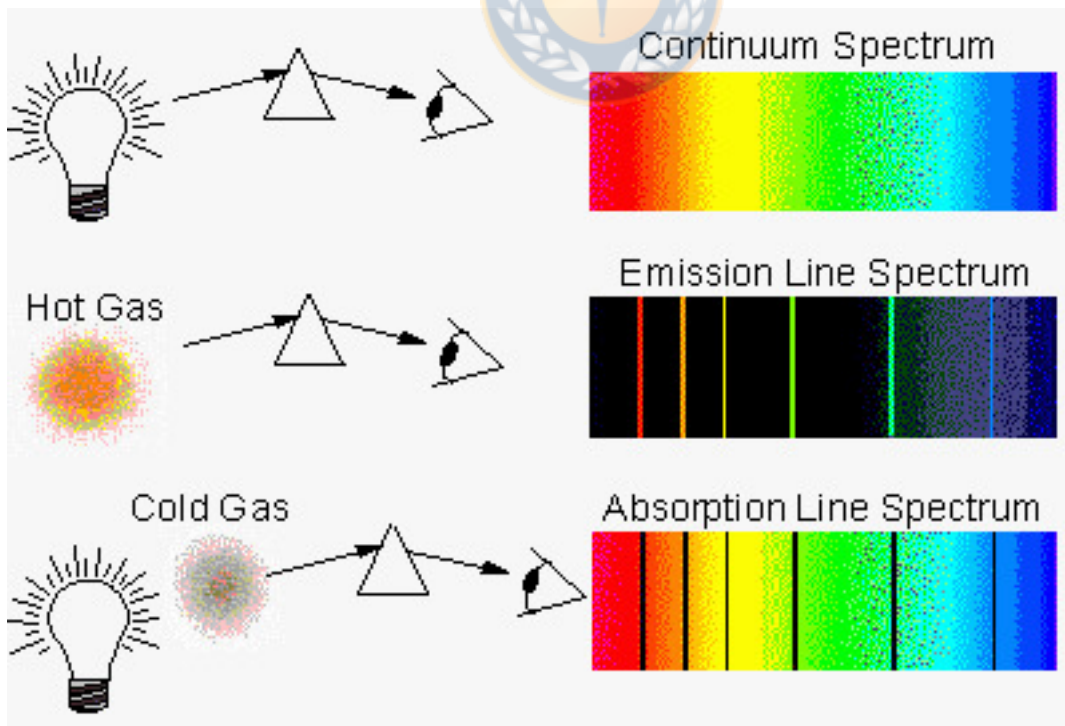
Hydrogen at very specific time from the start of the combustion), and the RGB and AGB stars which are very sensitive to the metallicity (due during these stages have strong convection between layers, dredge-up's, the absorption that causes the elements become more significantly at this stages, which means more metallicity implies a redder stages).

## 2.2 Spectroscopy: Characterizing spectral lines

Due this technique is the cornerstone of our study we will dedicate this section to know how the lines are characterized.

Spectroscopy is defined as the set of methods used to study the spectrum of an object, as was mentioned in the Introduction there are two types of *line* spectra, emission and absorption, these are produced due to the quantum nature of the atoms and the interference of the medium with respect to the light source as shown in the fig (2.2.1)

**Figure 2.2.1:** Types of spectra (Smith, 2007)



Line shapes observed in spectroscopy are measurements corresponding to the absorption or emission corresponding to an energy change in an atom, molecule

or ion, these characteristic shapes are also known as spectral line profiles.

### 2.2.1 Profiles

Ideal line shapes are used to represent this phenomena the typical shapes include Gaussian (the classic normal distribution, usually used to describes a randomness),

$$G(x, \mu, \sigma) := \frac{1}{\sigma\sqrt{2\pi}} \cdot e^{-\frac{1}{2}\left(\frac{x-\mu}{\sigma}\right)^2} \quad (2.2.1)$$

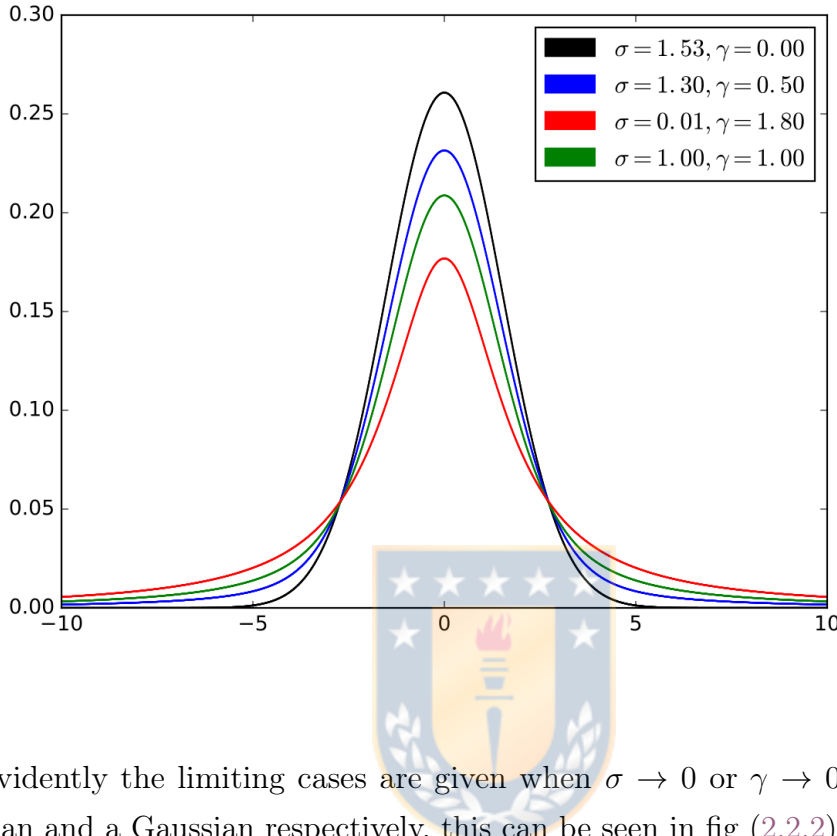
Lorentzian function (also known as Cauchy-Lorentz distribution), is more accentuated in the center and has long "wings" compared to the normal distribution.

$$L(x, \mu, \gamma) := \frac{\gamma}{\pi((x-\mu)^2 + \gamma^2)} \quad (2.2.2)$$

and more generally Voigth functions (which is a convolution between the past two shapes),

$$V(x, \mu, \sigma, \gamma) \equiv \int_{-\infty}^{+\infty} G(x', \mu, \sigma) \cdot L(x' - x, \mu, \gamma) dx' \quad (2.2.3)$$

**Figure 2.2.2:** Example of Voigth functions (Ji, 2017)



where evidently the limiting cases are given when  $\sigma \rightarrow 0$  or  $\gamma \rightarrow 0$  become a Lorentzian and a Gaussian respectively, this can be seen in fig (2.2.2).

## 2.2.2 Intrinsic effects and from the medium

However, the real shapes of the lines are determined by several parameters, primarily understanding that the process of line formation is described through the quantization of the energy transitions of an atom or molecule, we know that this would imply a delta function at a certain wavelength, an event that we know is not the case, due to several phenomena that in the first instance widen the line such as

### 2.2.2.1 Natural Broadening

This broadening is a direct consequence of the quantum nature of this phenomenon, since the lines themselves cannot be infinitely thin as a consequence of the Heisenberg uncertainty principle.

When the electron ( $\bar{e}$ ) occupies a state, it remains in it a  $\Delta t$  and depending on the

energy of this state this cannot be exact, from the same principle we can extract that the widening that the line will have will be given by

$$\Delta\lambda \approx \frac{\lambda^2}{2\pi c} \left( \frac{1}{\Delta t_i} - \frac{1}{\Delta t_f} \right) \quad (2.2.4)$$

where  $\lambda$  is the central value of the line,  $\Delta t_i$  is the lifetime in the initial state and  $\Delta t_f$  is the lifetime in the final state. This widening implies a literal width in the range where the profile occurs.([Hummer and Rybicki, 1971](#))

### 2.2.2.2 Doppler Broadening

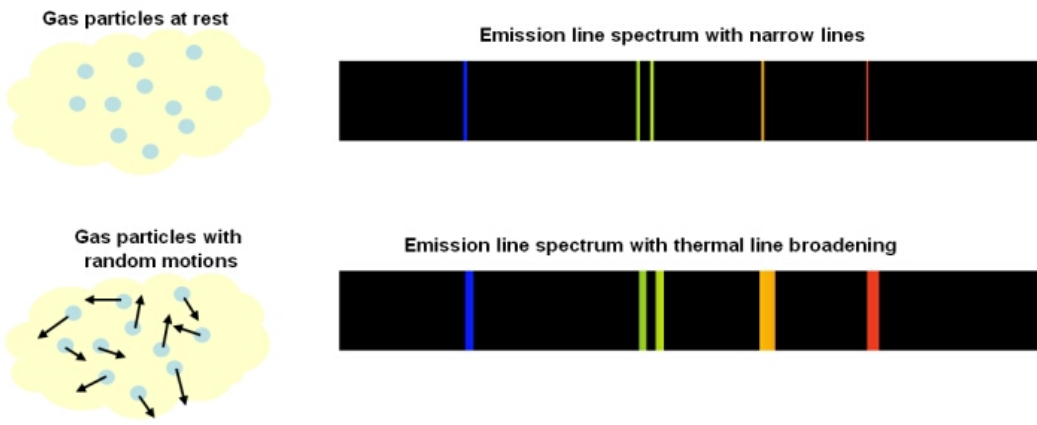
This broadening occurs by the nature of the material that composes, that is to say, this happen by effect of the velocities of the atoms that can compose a gas (in a gas in equilibrium for example the distribution of these velocities is given by the statistical physics according to the distribution of Maxwell's velocities). Atoms having velocities when absorbing or emitting will generate a contribution shifted from the expected center of emission by redshift or blueshift (see fig ([2.2.3](#))), this will be reflected in emissions at longer wavelengths and shorter wavelengths than the emission value.

The expected broadening is associated with the most probable velocity of the gas and can be described by

$$\Delta\lambda \approx \frac{2\lambda}{c} \sqrt{\frac{2k_B T}{m}} \quad (2.2.5)$$

with the term under the root the most probable velocity of a gas at equilibrium at a given temperature. This broadening can be profiled by fitting a Gaussian curve.([van Regemorter, 1965](#); [Hummer and Rybicki, 1971](#))

**Figure 2.2.3:** Thermal Broadening scheme ([COSMOS, 2022](#))



### 2.2.2.3 Pressure Broadening

This broadening occurs because the states of atoms and ions can be perturbed by collisions and perturbations in their electric field, this ends up shortening the  $\Delta t$  of the electronic transitions and therefore affects the natural broadening, this broadening can be described by

$$\Delta\lambda = \frac{\lambda^2}{c} \frac{\rho\sigma}{\pi} \sqrt{\frac{2k_B T}{m}} \quad (2.2.6)$$

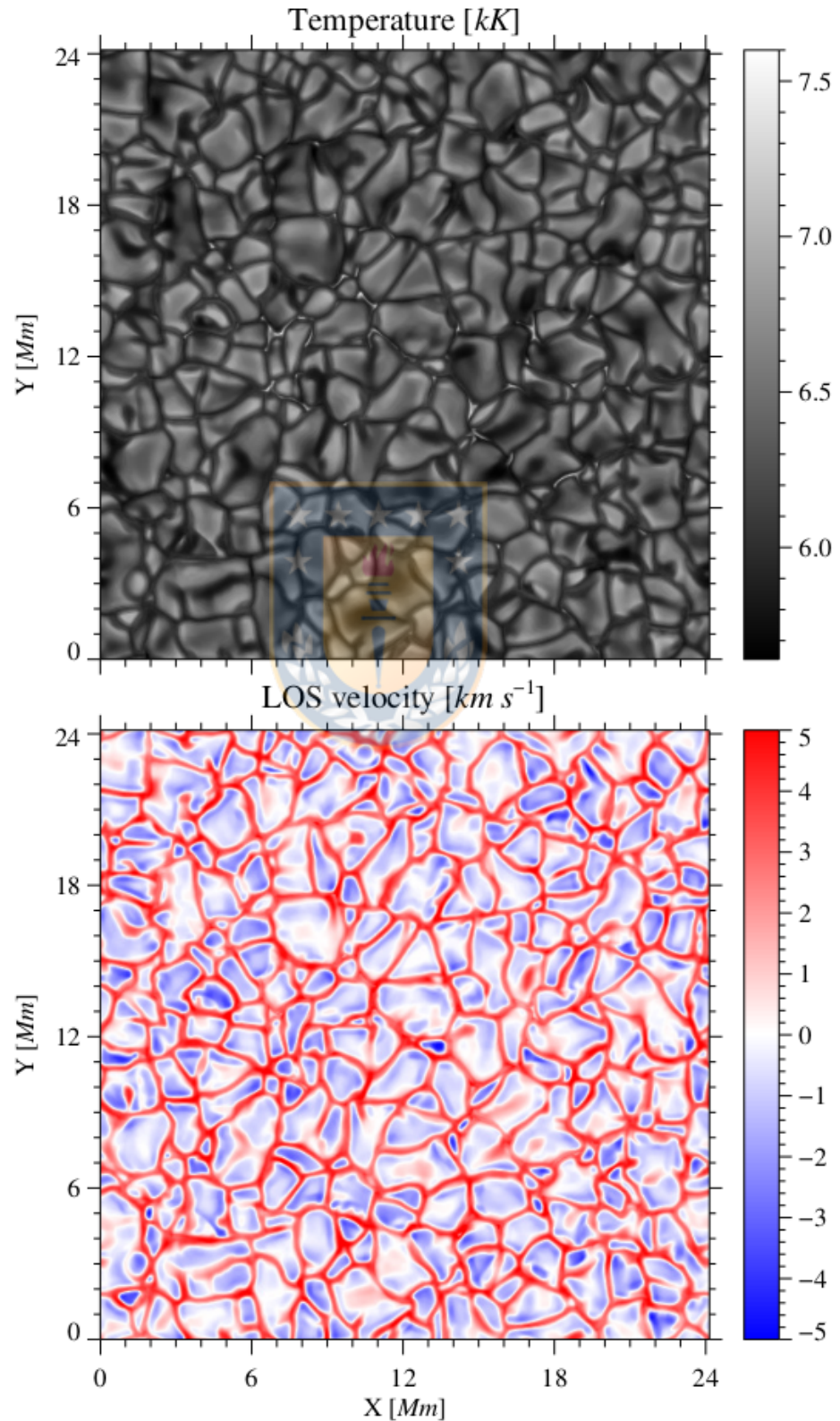
where  $\rho$  is the density of the atoms of the element under consideration (for a specific line one has to consider the amount of atoms in the ionization state required to form that line (Saha equation)), and  $\sigma$  is the "collision cross section" value that imposes a limit for an interaction to occur between atoms or molecules (collision or interference through the electric field) and in a simple way of see measures the probability of interactions. Also this broadening can be profiled through a Lorentzian curve. ([van Regemorter, 1965](#); [Hummer and Rybicki, 1971](#))

### 2.2.2.4 Granulation and Micro Turbulence

The surfaces of stars are not flat and static, for example, the photosphere of the Sun is not smooth, instead shows a structure in the form of "grains of rice" (see fig 2.2.4), usually called granulation, which is expected to be normal in any star (more present and significant in some than others).

It is an effect caused by columns of gases rising from the lower, hotter layers of

**Figure 2.2.4:** Snapshot of granulation simulation (González Manrique et al., 2020)



the star into the upper atmosphere, due to convective movements of the gas that composes it. Each granule has individual dimensions and consists of a structure in constant motion and, therefore, ephemeral.

These granules will affect the observed spectrum due to a Doppler effect, where the converging areas of the granules will generate a contribution to one side of the spectrum, while the diverging areas of the gas create the main contribution (see fig (2.2.5)). Taking the fig (2.2.4) as a reference, we can understand that the blue parts of the lower panel, i.e. the granules will form the blueshifted contribution due to the fact that with respect to our line of sight the material is coming out of the interior with a velocity towards us, while the red areas of the same lower panel are the "Cool-Lane" mentioned in fig (2.2.5) whose contribution is in the red wing of the profile due to the opposite situation, the material is moving towards the interior of the star and with respect to our line of sight it is moving away from us.

These phenomena can be bounded and/or standardized on the basis of important parameters of the star such as surface gravity ( $\log(G)$ ) and effective temperature ( $T_{eff}$ ) of the star, thus treating these deviations as a generalized problem of the star and by encompassing everything it is appropriated as a characteristic of the star studied which is called micro-turbulence, some studies have characterized for certain types of stars the value of micro-turbulence which is used in the analysis of spectra giving a degree of deviation expected in the lines. (see e.g. for FGK stars [Mott et al., 2020](#))

### 2.2.3 Characterization of Lines

The asymmetries in the lines in their last level of characterization are described and interpreted through an element called Bisector (this can be seen in the figure 2.2.5), this can only be measured when we have a high resolution and is based in simple terms on calculating the midpoint between the blue wing and the red wing according to the given definition that goes back to [Gray \(1988\)](#)

Because different parts of each line are formed at different depths, we can estimate how these velocity fields vary with depth (see Fig 2.2.6). Bisector measurements can be performed to estimate temporal patterns [Polster et al. \(2018\); Baldry et al. \(1999\)](#), in general some of these have also been standardized according to the spectral type of the stars discriminating particularities of the star system

**Figure 2.2.5:** Example of how granulation bend the spectral lines (Gray, 2005)

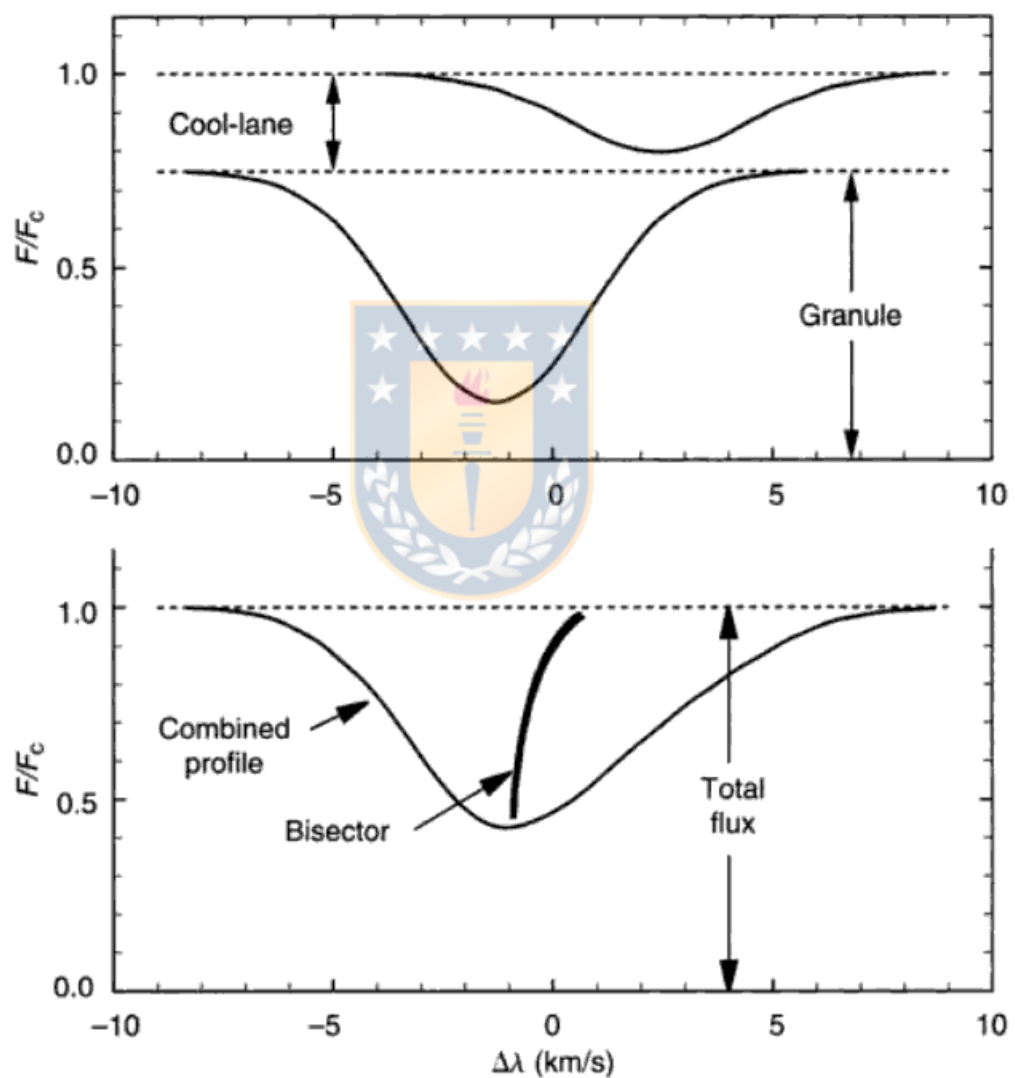
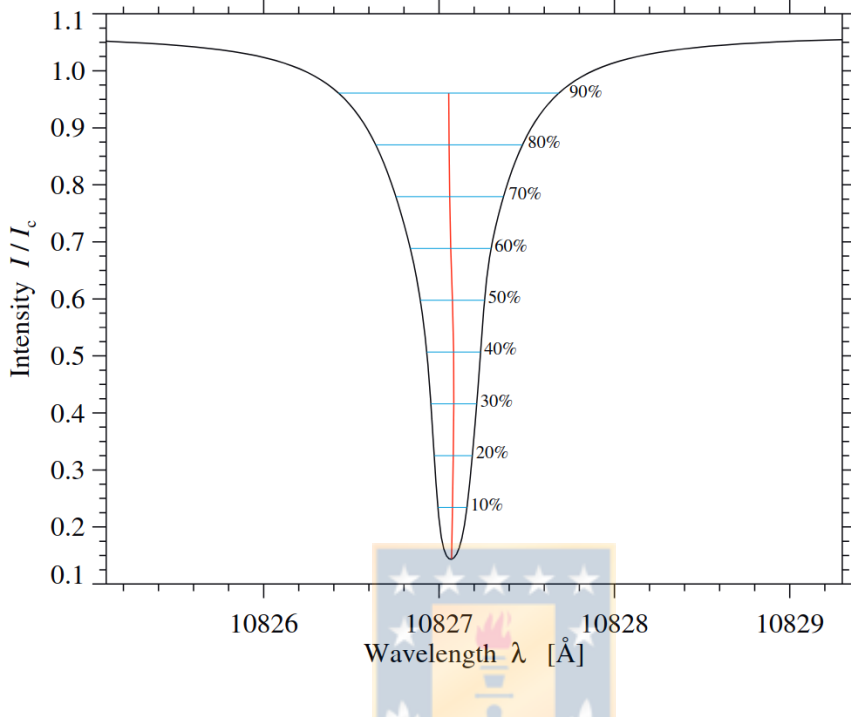


**Figure 2.2.6:** Reference image of the optical depth to be considered of a Bisector (González Manrique et al., 2020)



Dall et al. (2006); Mott et al. (2020), and recent studies have shown that such approximations can be further decomposed to understand in detail what influences the discrepancies Gray (2010).

In more detailed but highly limited studies the Bisector can be used to measure and estimate the Granulation itself, as shown in González Manrique et al. (2020), where they obtain a good estimate of this with simulations.

## 2.3 Multiple Stellar Population

As we mentioned in the previous sections due the compactness of GCs was believed that they born from the same nebula and was expected that they should have the same initial conditions (as Age and Chemical composition), instead when we reach the enough resolution in our spectrographs We found that this is far from reality and even nowadays the opposite phenomena (show a MPs) it's considered the way to define what it is a GC.(Carretta et al., 2010)

In specific MPs phenomena refers to have more than one population of stars inside of the GC. This phenomena is usually associated and understood through the idea

of a first generation of stars that "pollutes" the environment where the second generation of stars are being formed, however this remains unclear and object of study in the current Astronomy.([Milone and Marino, 2022](#); [Bastian and Lardo, 2018](#))

Moreover the  $2^{nd}$  generation inside of GC are an specific kind of stars that we can not found outside them, their chemistry it's only founded within this objects hence it's expected to be born inside of them (and currently even if we found them outside we associated to be born inside of them and explained as runaways ,[Bastian and Lardo \(2018\)](#)).

The most generalized characteristic with the MPs are the correlation (increases together) and anti-correlation (while one increase the amount the other decreases) between elements (this should be take carefully due this patterns had a great variability cluster to cluster and their individual chemistry becomes almost a distinguishable signature of them), the most important features that have from empirical evidence are

- **Fe/H** remains constant star to star within the GC
- **C+N+O** remains constant star to star within the cluster
- **N and C** are anticorrelated
- **Na and O** are anticorrelated
- **Mg and Al** are anticorrelated (it's more common in more massive and metal poor GC)
- **Li abundance** there are stars that doesn't show Na Li anticorrelation (which is not expected to happen naturally)
- **Na,N and He** are correlated (in some level of enhancement of the He, this variation had a significant impact in the HB morphology)
- **Fraction of enriched stars and mass of the GC** are correlated (this was been recently questioned in [Dondoglio et al. \(2022\)](#))
- **Extension of the spread in N, Na, O and He** are correlated
- **MPs have not been found in massive clusters with ages less than 2 Gyr**

- MPs are found in the full range of GC metallicities
- He enriched stars tends to be in towards the center of the GC

(To see some studies where this affirmations have been evidenced you can take a look to [Geisler et al., 2021b](#); [Baeza et al., 2022](#); [Fernández-Trincado et al., 2020c](#); [Bastian and Lardo, 2018](#); [Milone and Marino, 2022](#); [Zhang et al., 2012](#); [Mészáros et al., 2020, 2021](#); [Masseron et al., 2016, 2019](#))

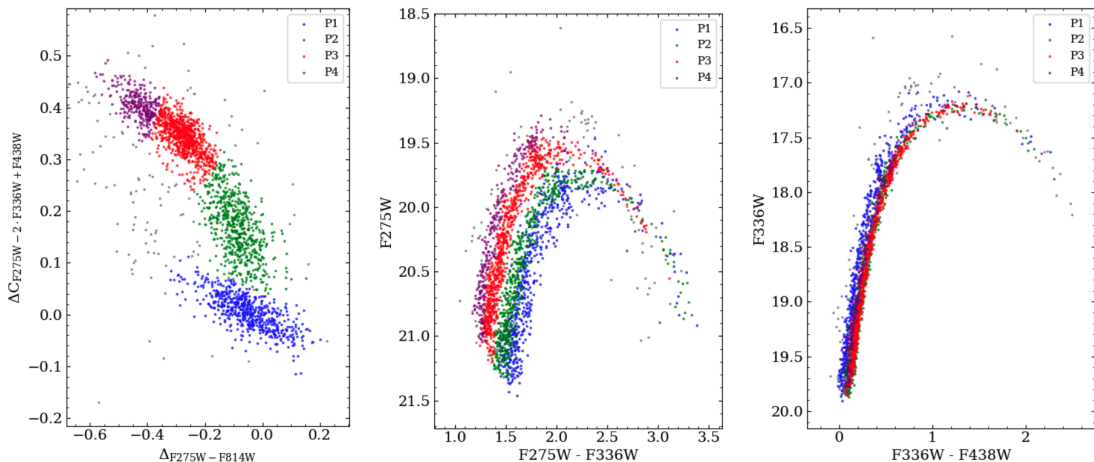
### 2.3.1 Evidence of the Phenomena

As astronomers we make use of the light to study the universe, for these objects there's not the exception and a multi-wavelength and multi-technique approach are commonly used to study them. Recently measures in the infrared had allow us to study the previous inaccessible Bulge information and the Gaia mission has provided the astrometry needed to independently of the chemistry determine the members of GC. ([Majewski et al., 2017](#); [Blanton et al., 2017](#); [Ahumada et al., 2020](#); [Gaia Collaboration et al., 2022, 2021, 2018, 2016](#); [Bastian and Lardo, 2018](#))

#### 2.3.1.1 Photometry of MPs

Evidence for this MP in GC can be found in the HR diagram as was mentioned before, if stars have different compositions different stellar tracks should be generated, and in the area of RGB and AGB will have a stronger impact due the dredge-up's on these stages. ([Carroll and Ostlie, 2006](#); [Bastian and Lardo, 2018](#))

**Figure 2.3.1:** Chromosome map and CMDs of NGC 2808 [Latour et al. \(2019\)](#)



The best photometric evidence it's retrieved thanks to the Hubble Space Telescope (HST, see for a more detailed view [Oesch et al., 2018](#)) which have filters with bands that are centered in absorption, emission and continuum separately (those filters were made on purpose at molecular bands that are affected by the MPs phenomena<sup>1</sup>) due this the characteristics in the HR-diagram will be accentuated (due the different stellar tracks will have different emissions/absorption, etc.), also a specific color-color diagram is commonly used with these filters which allow to directly separate the different populations of stars, this map is usually called Chromosome map (see fig [2.3.1](#)) (named in this way due the precision of this technique that it's like read the DNA of the Globular Cluster).

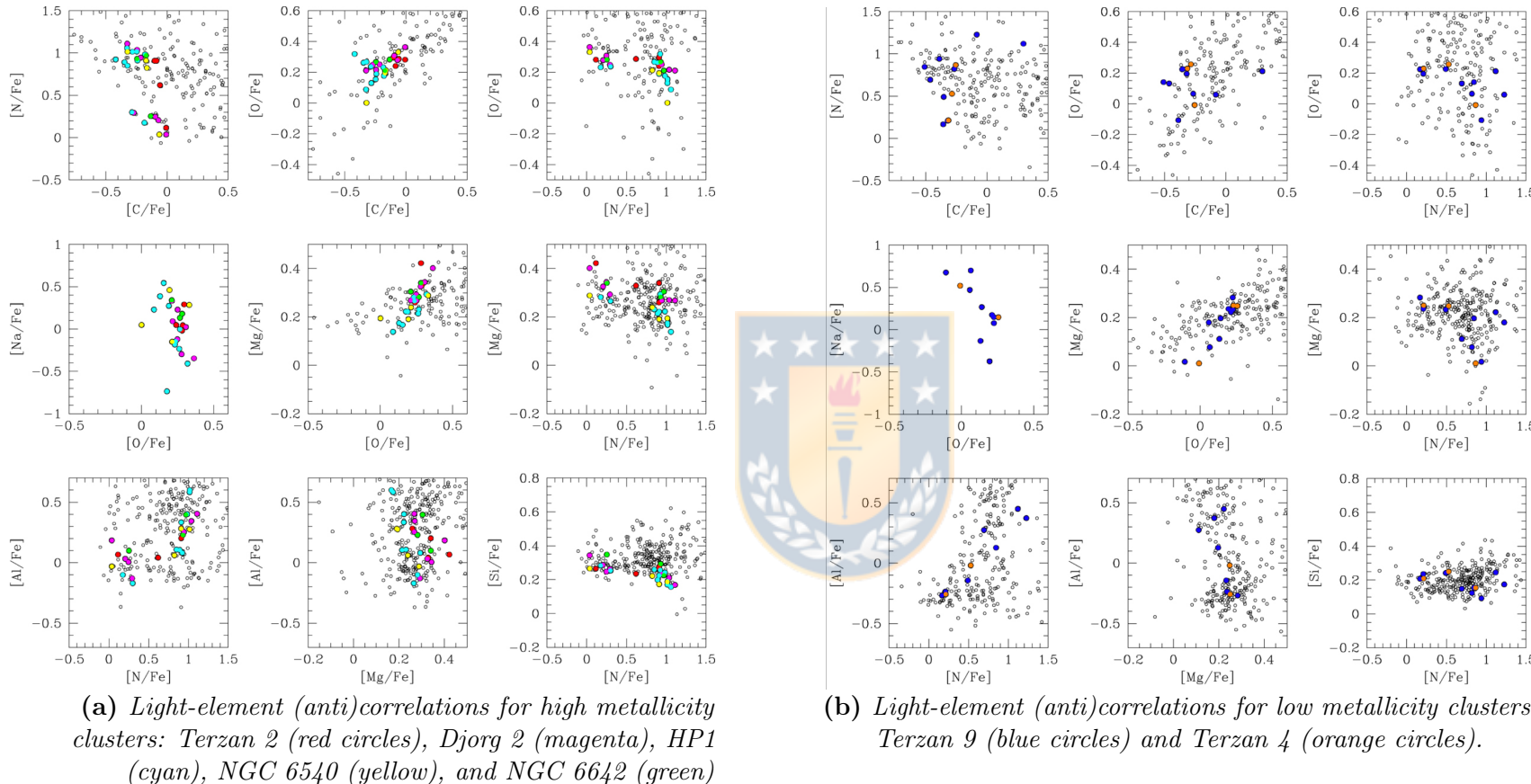
### 2.3.1.2 Spectroscopy of MPs

The main and strong evidence of MPs it's the direct measure of them by the difference in their chemistry and evidence the common patterns before mentioned (and also look for new ones), this is done through spectroscopy at different wavelength, some examples could be seen in the Fig [2.3.2](#) which are separate in two groups the High and Low metallicity range. [Geisler et al. \(2021b\)](#); [Masseron et al. \(2016, 2019\)](#); [Baeza et al. \(2022\)](#)

---

<sup>1</sup>passbands could be seen in their webpage <https://hst-docs.stsci.edu/wfc3ihb/chapter-6-uv-vis-imaging-with-wfc3/6-5-uv-vis-spectral-elements>

**Figure 2.3.2:** Spectroscopic measures of abundances by the group CAPOS (Geisler et al., 2021b)



Comparison objects (empty circles) from Masseron et al. (2019) and Mészáros et al. (2020)

### 2.3.2 Models

Most of the explanations as was mentioned before are associated with the idea of two populations where the first one contaminate the second one, however another ideas have arisen since no one of the models are even near to explain the phenomena (mainly due the wide variations in the behaviour cluster-cluster), in this section my aim is to give a notion of which models have been created to explain MPs and therefore how we look at the origin of this phenomena, we are not going to address this deeply, hence for a fully coverage of this topic we encourage to see the review of [Bastian and Lardo \(2018\)](#) (article which was our guidance to write this section) where this topic is addressed properly and also we recommend to take a look the original papers of the models ([D'Ercole et al., 2008](#); [Ventura and D'Antona, 2009](#); [D'Ercole et al., 2016](#); [Bekki et al., 2017](#); [Decressin et al., 2007b,a](#); [Krause et al., 2013](#); [Chantereau et al., 2016](#); [de Mink et al., 2009](#); [Jiang et al., 2017](#); [Bastian et al., 2013](#); [Cassisi and Salaris, 2014](#); [Wijnen et al., 2016](#); [Hopkins, 2014](#); [Marcolini et al., 2009](#); [Sánchez-Blázquez et al., 2012](#)).

Some of the typical problems that surges when we try to figured out how MP was formed are

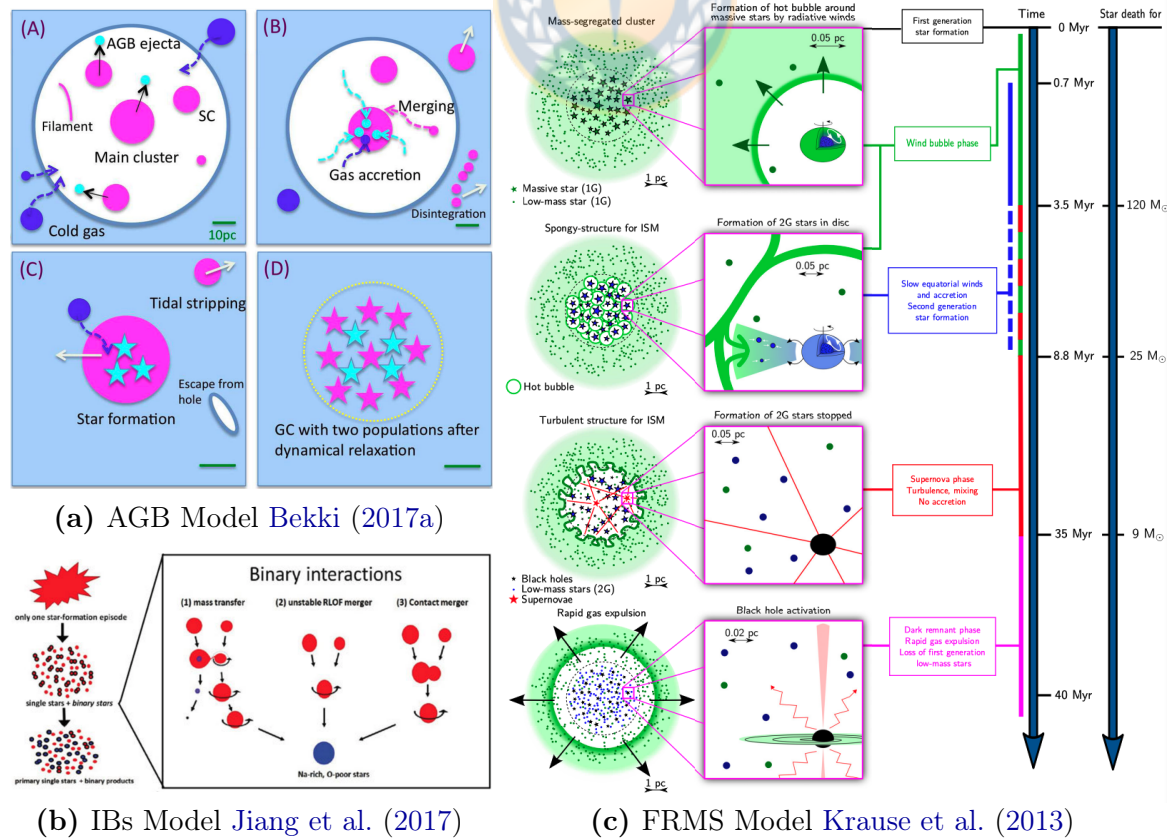
- **Dilution:** the current measures show some inconsistencies between expected abundances (e.g. Li should be depleted in the presence of Na, but this it's not always the case), therefore most of the models have been established the primordial material as the chemistry of the first generation stars then for the second generation this material is mixed with the material produced by first generation.
- **Discrete and Continuous spread:** this means that the models must have the ability of create smooth spread or clustered by generations spreads.
- **Mass Budget** this refers to the problem that surges when we try to explain this phenomena as multi-epoch of star formation, that even if all the mass produced of the proposed polluters were accreted can not explain the amount of stars of "second generation"
- **Young Massive Clusters (YMC) constrain:** within the accessible universe we had the lucky of being able of resolve some YMC, hence we could at least constraining some of the characteristics on early epochs. (e.g.

the measures suggest that spread of the age it' expected to be less than  $\sim 20\text{Myr}$ , the gas is efficiently removed at any stage)

### 2.3.2.1 Multiple epoch of star formation

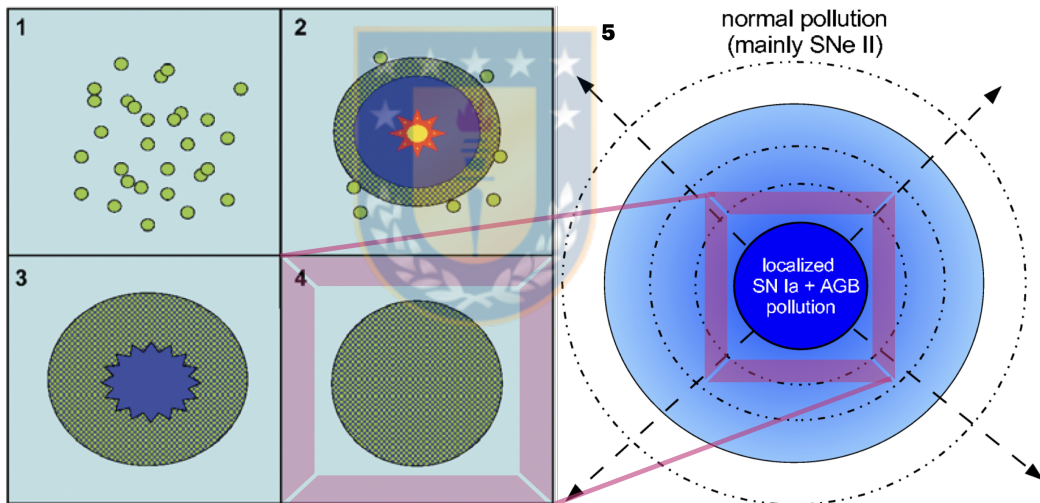
The most common model are the ones which consider two (or more) generation of stars, the most studied candidate as a polluter are the AGB stars polluters (D'Ercole et al., 2008; Ventura and D'Antona, 2009; D'Ercole et al., 2016; Bekki et al., 2017), another similar model consider Fast Rotating Massive Stars (FRMS) can expel material and then being acrated by the next generation (Decressin et al., 2007b,a; Krause et al., 2013; Chantereau et al., 2016) and also was proposed to explain in this way that the stars due the crowd could present in a very common way Interacting Binaries (IBs) , which includes mass transfer and colision between them to explain the M<P phenomena (de Mink et al., 2009; Jiang et al., 2017), an schematic representation of these models can be found in the fig (2.3.3)

**Figure 2.3.3:** Schemes of models to explain the MP's phenomena with multiple epoch of star formation



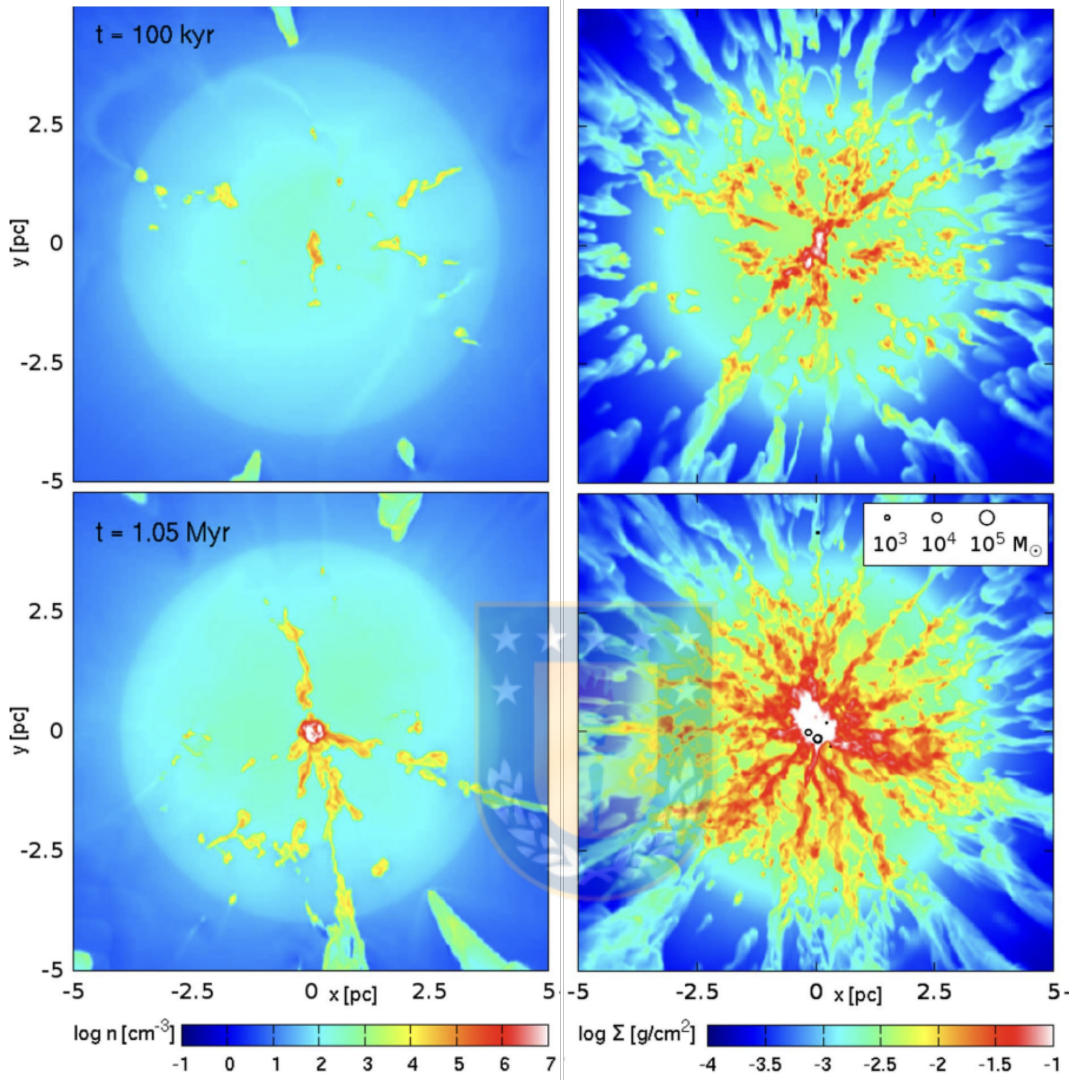
**2.3.2.1.1 Reverse Order Model** is also a multi epoch star formation model but with the peculiarity of consider as the commonly associated second generation as the first one, consist in have an already polluted environment which then is enriched by a Super Nova type Ia , after the cooling of the gas/dust at the center of the cluster begins the formation of the initial population, then when the firsts Supernova type II happen they mix the material remaining the Fe and the C+N+O constant. IN the fig (2.3.4) this model is represented in their initial condition and subsequent evolution, the first generation in this cluster is generated just in the center (dark blue area) and the second after the firsts Supernova type II exploded and mixes the inner and outer material.([Marcolini et al., 2009](#); [Sánchez-Blázquez et al., 2012](#))

**Figure 2.3.4:** Reverse Order Model, (modified image from [Marcolini et al., 2009](#))



**2.3.2.1.2 Early Star Formation Period (eSFP)** is a model which also contemplates multiple times the star formation but the difference consist in assuming extreme conditions for the Giant Molecular Cloud (these environments could be evidenced in other galaxies at high redshift) where the stars were formed, the idea is that due the high density the cloud will generate giant stars that within a very few Myr will strip off they outer layers polluting the environment , a simulation of the first Myr of this model could be seen in fig (2.3.5) in this figure could be appreciates how in very few time, giant stars have been surges in the center of the cloud.

**Figure 2.3.5:** Simulation of eSFP model [Wünsch et al. \(2017\)](#)

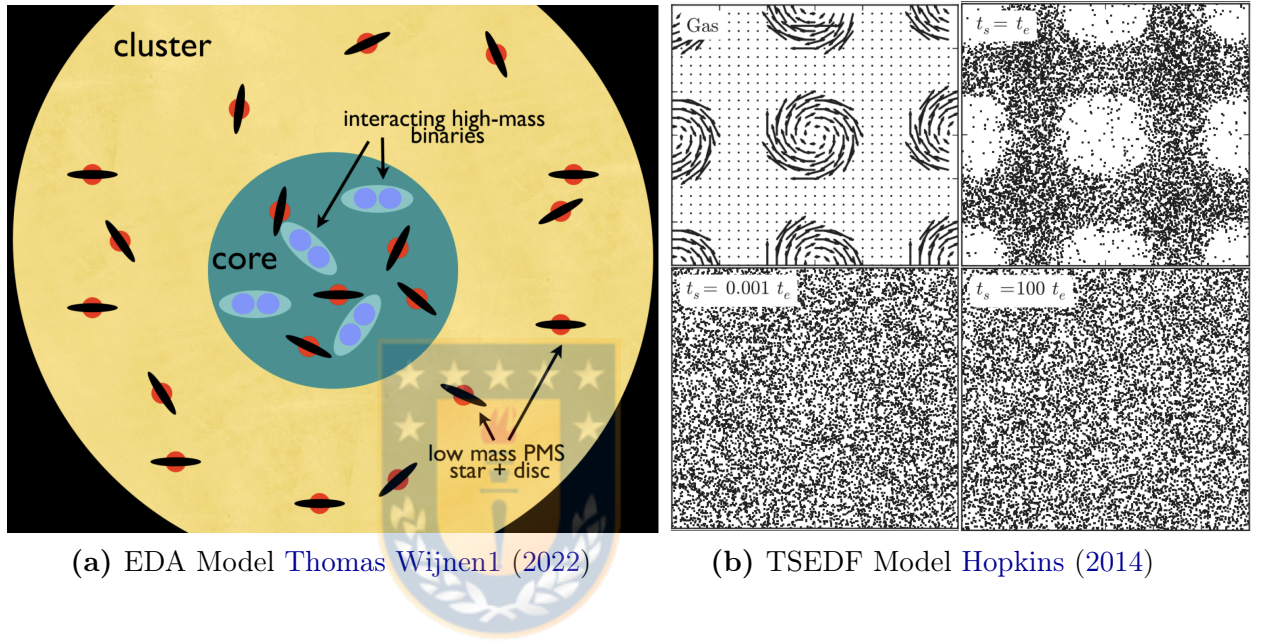


### 2.3.2.2 Single epoch of star formation

On the other hand are proposed models where the formation of MPs happen during ongoing stars formation as the Early Disc Accretion (EDA) scenario where the stars combine properties of the model of IBs and FRMS and during the accretion of material these stars pollutes the environment [Bastian et al. \(2013\)](#); [Cassisi and Salaris \(2014\)](#); [Wijnen et al. \(2016\)](#) an schematic representation of this model is shown in fig (2.3.6a) where we can see that due the likeliness of interaction this process would be carried in the center of the GC, also we have the Turbulent Separation of Elements During GC Formation (TSEDF) which consist in a natural separation of the gas and the large dust grains (which will generate different

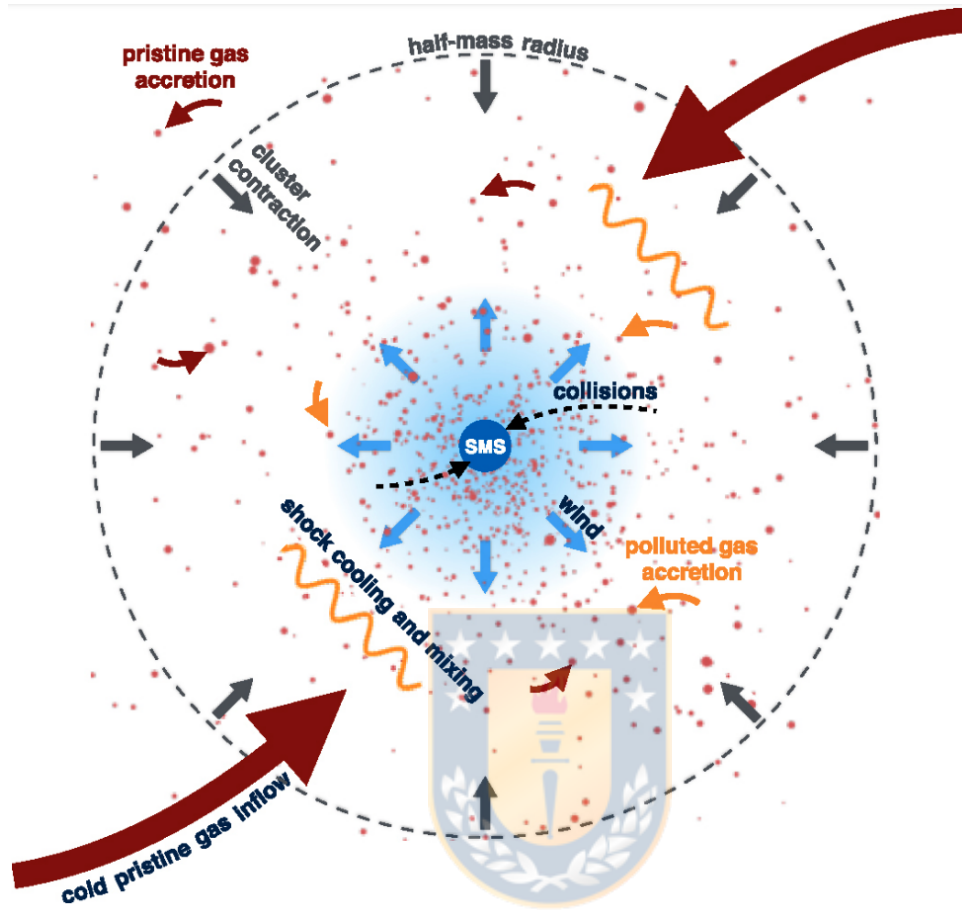
chemistry depending of the position of the star) due strong turbulence they could move separately Hopkins (2014), a simulation of how this model should work can be found in the fig (2.3.6b) where can be appreciated how heavy grains are expected to be displaced from the areas of initial turbulence.

**Figure 2.3.6:** Schemes of models to explain the MP's phenomena with a single epoch of star formation



**2.3.2.2.1 Very Massive Stars (VMS)** (also called Supermassive Star (SMS)) is a model which consists in the collision of stars to form a Very Massive Star at early stages of the collapse of the Giant Molecular Cloud, the cold, pristine gas accumulates in the center, causing the cluster to contract. The increased stellar density causes stellar collisions, forming an VMS/SMS at the center of the cluster. The VMS/SMS blows a wind enriched in hot hydrogen products that interacts and mixes with the incoming gas. The mixed material subsequently accumulates in the stars, enriching them with polluted material explaining in this way the MP phenomena, a schematic vie of this model could be seen in the fig (2.3.7). (Gieles et al., 2018)

**Figure 2.3.7:** Scheme of VMS model Gieles et al. (2018)



### 2.3.3 Predictions vs Reality of MPs

After go through a variety of models we should take a look and contrast how much likely these are, if they represent what our measures could tell us.

In fig (2.3.8a) it's showed a table taken from Bastian and Lardo (2018) where is displayed at what point the model could explain our measures and relations (the represent that can be the opposite under different or extreme conditions), from a quick look we can say that our understanding of the formation of MPs phenomena is still far to be good, this is a current problem in the modern astrophysics and we should push forward different way to explain this phenomena.

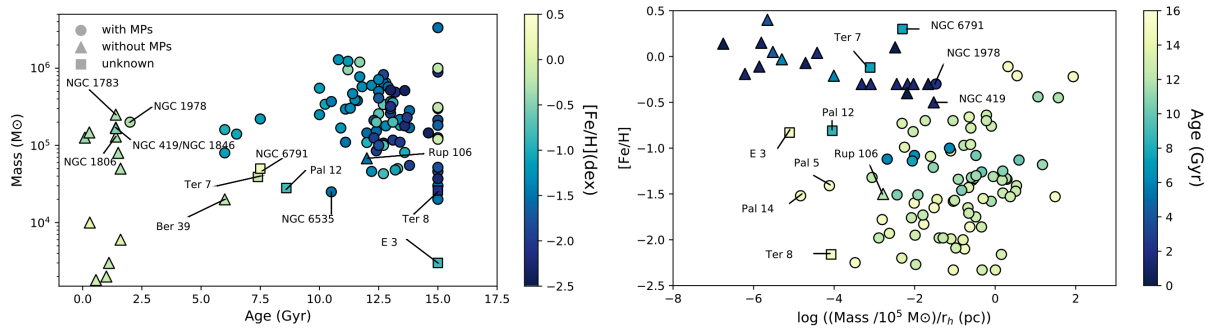
What we really know is the empirical evidence and trustful information is indeed the best way to asset this problem, in the fig (2.3.8b) we could get a summary of what we know about these GC as systems and in the fig (2.3.2) we could see some examples of the behaviour intrinsic to these objects, through this figures we

could find most of the initial characteristic that were mentioned at the beginning of this section, from this section we conclude that further studies would be need to explain this phenomena.

**Figure 2.3.8:** Summary of Models & Current estimation for most of GC in Milky Way (images from Bastian and Lardo (2018))

|               | (near) Ubiquity | Abundances | Li correlations | Variety/stochasticity | Mg-Al | Discreteness | Mass budget | enriched correlation with GC mass | He spread correlation with GC mass | YMCs | Age Trend |
|---------------|-----------------|------------|-----------------|-----------------------|-------|--------------|-------------|-----------------------------------|------------------------------------|------|-----------|
| AGB           | ✗               | ✗*         | ✗*              | ✗                     | ✓*    | ✗*           | ✗*          | ✗                                 | ✗*                                 | ✗    | ✗         |
| FRMS          | ✗               | ✗*         | ✗               | ✗                     | ✗     | ✗            | ✗           | ✗                                 | ✗                                  | ✗    | ✗         |
| VMS           | ✗               | ✗*         | ✗               | ?                     | ✗*    | ✗            | ✓*          | ✓*                                | ✓*                                 | ✓    | ✗         |
| EDA           | ✗               | ✗*         | ✗               | ✗                     | ✗     | ✗            | ✗           | ✗                                 | ✗                                  | ✓*   | ✗         |
| Reverse Order | ✗               | ✗*         | ✗               | ?                     | ?     | ✗            | ✓*          | ✗                                 | ✗                                  | ✗    | ✗         |
| eSF Period    | ✗               | ✗*         | ✗               | ✗                     | ✗     | ✗            | ✗           | ✗                                 | ✗                                  | ✓    | ✗         |

(a) Models accuracy considering different parameters (modified image)

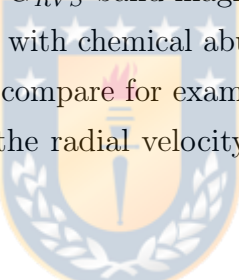


(b) Summarise knowledge of GC as systems

## 2.4 Data Information

### 2.4.1 Gaia Data Release 3

*Gaia* is a space mission that provides astrometry, photometry, and spectroscopy of billion stars in the Milky Way (MW). *Gaia* Data Release 3 (*Gaia* DR3) has been released on 13 June 2022, hence is the most recent release. *Gaia* DR3 combines the already published *Gaia* EDR3 data products with new data products for the same set of observations and time. The *Gaia* DR3 represents a significant advance over *Gaia* Data Release 2 with parallax and proper motions precisions increased (by 30% & by factor of 2 respectively). The DR3 photometry also features increased precision, but above all much better homogeneity across colour, magnitude, and celestial position. *Gaia* DR3 in comparison with *Gaia* EDR3 provides more set of data such as: sources with mean  $G_{RVS}$ -band magnitudes; sources with radial velocity; mean RVS spectra; sources with chemical abundances from RVS spectra; among others, that will allow us to compare for example our metallicities results and membership probability with the radial velocity data. ([Gaia Collaboration et al., 2022, 2021, 2018, 2016](#))



### 2.4.2 APOGEE-2: The Apache Point Observatory Galactic Evolution Experiment II

The APOGEE-2 survey ([Majewski et al., 2017](#)) is one of the internal programs of the Sloan Digital Sky Survey-IV ([Blanton et al., 2017; Ahumada et al., 2020](#)) developed to provide precise radial velocities ( $RV < 1 \text{ km s}^{-1}$ ) and detailed chemical abundances for an unprecedented large sample of giant stars, aiming to unveil the dynamical structure and chemical history of the entire MW galaxy.

The APOGEE-2 instruments (capable of observing up to 300 objects simultaneously) are high-resolution ( $R \sim 22,500$ ), near-infrared (NIR) spectrographs ([Wilson et al., 2019](#)) observing all the components of the MW (halo, disc, and bulge) from the Northern Hemisphere on the 2.5m telescope at Apache Point Observatory ([Gunn et al., 2006](#), APO, APOGEE-2N;) and the Southern Hemisphere on the Irénée du Pont 2.5m telescope ([Bowen and Vaughan, 1973](#)) at Las Campanas Observatory (LCO, APOGEE-2S). Each instrument records most of the  $H$ -band ( $1.51\mu\text{m} - 1.69\mu\text{m}$ ) on three detectors, with coverage

gaps between  $\sim 1.58\text{--}1.59\mu\text{m}$  and  $\sim 1.64\text{--}1.65\mu\text{m}$ , and with each fiber subtending a  $\sim 2''$  diameter on-sky field of view in the northern instrument and  $1.3''$  in the southern.

DR 17 is the final release of APOGEE-2 data from SDSS-III/SDSS-IV. We used our access to the internal version of DR 17. It includes all APOGEE data, including data taken at APO through November 2020 and at LCO through January 2021. The dual APOGEE-2 instruments have observed more than 650,000 stars throughout the MW, targeting these objects with selections detailed in [Zasowski et al. \(2017\)](#), [Santana et al. \(2021\)](#) and [Beaton et al. \(2021\)](#) (For our target we had 365 stars in the field of view dedicated to study NGC 2298). These papers also give a detailed overview of the targeting strategy of the APOGEE-2 survey. Spectra are reduced as described in [Nidever et al. \(2015\)](#), and analyzed using the APOGEE Stellar Parameters and Chemical Abundance Pipeline (ASPCAP; [García Pérez et al., 2016](#)), and the libraries of synthetic spectra described in [Zamora et al. \(2015\)](#). The accuracy and precision of the atmospheric parameters and chemical abundances are extensively analyzed in [Holtzman et al. \(2018\)](#), [Jönsson et al. \(2018\)](#), and [Jönsson et al. \(2020\)](#), while details regarding the customised *H*-band line list are fully described in [Shetrone et al. \(2015\)](#), [Hasselquist et al. \(2016\)](#), [Cunha et al. \(2017\)](#), and [Smith et al. \(2021\)](#).

#### 2.4.3 BACCHUS: Brussels Automatic Code for Characterizing High accuracy Spectra

This is the software used to perform the analysis of high resolution spectra developed by [Masseron et al. \(2016\)](#), this software use the models of MARCS (is the acronym for Model Atmospheres in a Radiative and Convective Scheme [Gustafsson et al., 2008](#)) is composite by a grid of one-dimensional, hydrostatic, plane-parallel and spherical LTE model atmospheres and based in the previous software Turbospectrum ([Plez, 2012](#)) which is a 1D LTE spectrum synthesis code and covers 600 molecules, is fast with many lines, and uses the treatment of line broadening.

# Chapter 3

## Methodology

### 3.1 Determination of likely Members

To determine the membership probability we used the Gaia data, we decide to use astrometric parameters such as the proper motion and the sky position to infer the most likely members, we use the general approach of 2D-Gaussian mixture model (GMM), this model considers that the distribution of proper motions of the stars in a cluster's region can be represented by two elliptical bi-variate Gaussians, meanwhile for the spatial distribution we can use a flat distribution for the field stars and one elliptical bi-variate Gaussian. This is a very common approach to determine likely members ([Tian et al. \(1998\)](#); [Griggio and Bedin \(2022\)](#); [Xiang et al. \(2021\)](#); [Çakmak and Karataş \(2022\)](#))

#### 3.1.1 Vector Point Diagram and Position in the sky

We define the probability of membership as

$$Prob_C(i) = \frac{\Phi_C(i)}{\Phi(i)}, \text{with } \Phi = \Phi_C + \Phi_F \quad (3.1.1)$$

, this means that we always be considering two distribution to describe the complete sample, one for the field and another component for our GC.

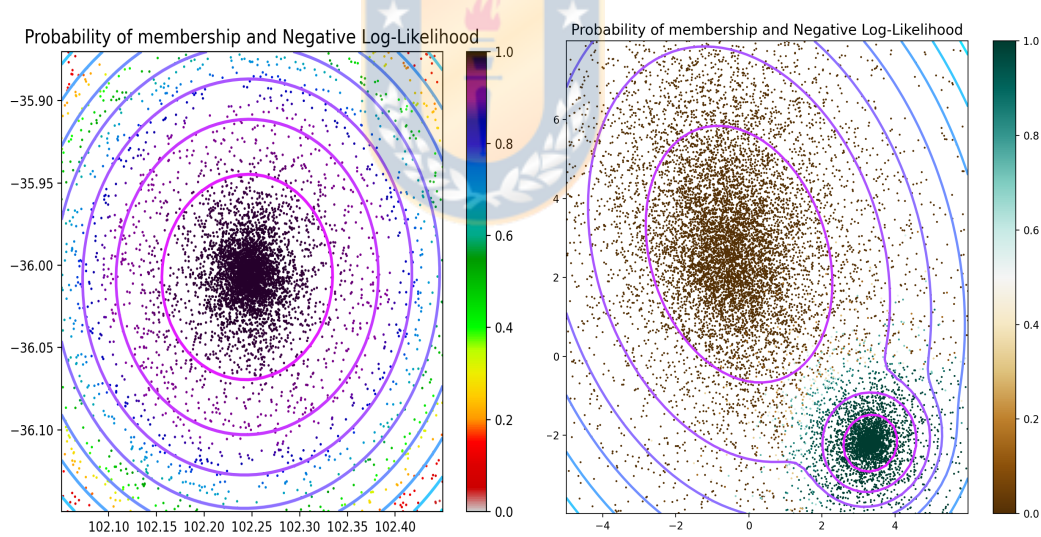
Due in both of our criteria used 2D-Gaussian result useful define it as follows,

$$\mathcal{N}(\vec{X}|\vec{\mu}, \Sigma) = \frac{1}{(2\pi)^{1/2}} \frac{1}{|\Sigma|^{1/2}} \exp\left\{-\frac{1}{2}(\vec{X} - \vec{\mu})^T \Sigma^{-1} (\vec{X} - \vec{\mu})\right\} \quad (3.1.2)$$

where the variables  $\vec{X}$  are the values of each source,  $\vec{\mu}$  refers to the center of the Gaussian and  $\Sigma$  to the covariance matrix ( $\Sigma^{-1}$  is known as the "precision" or "concentration" matrix and gives us information about the dispersion of our variables and the correlation between them).

For the spatial distribution we define the distribution of field as  $\Phi_F^r = \frac{1}{\pi r_{max}^2}$  ( $r_{max}$  in this case corresponds to 40 arc-min which is the total area that we downloaded surrounding the GC from the Gaia archive) and a 2D-Gaussian ( $\mathcal{N}_{Spatial}^C$ ). Meanwhile for the Vector Point Diagram (VPD) we use two 2D-Gaussian one for the field ( $\mathcal{N}_{VPD}^F$ ) an another for the Cluster ( $\mathcal{N}_{VPD}^C$ ).

**Figure 3.1.1:** Individual probability of membership by Position in the Sky and Proper Motion respectively



**On the Left panel:** we can see the log likelihood levels and the probability computed for our proposed model of the projection in the sky. (x-axis and y-axis are the right ascension and declination respectively) **On the Right panel:** we can see also the likelihood contour levels and the probability for our proposed model to the vector point diagram (the x-axis and yaxis are the pmra & pmdec from Gaia respectively) .(this computations were made with [Pedregosa et al. \(2011\)](#))

In the fig (3.1.1) we show our results of this GMM approach to determine likely members the centers vectors and the covariance matrix's were obtained through machine learning, with the easy and accessible python package Scikit-Learn

(Pedregosa et al. (2011)), which have already trained networks to perform the clustering analysis and in specific for GMM<sup>1</sup>. Using this tool we determine that for the field (take in account that the variables are the Right Ascension (RA) and Declination (Dec) and both of them are in degrees units)

$$\vec{\mu}_{Spatial}^C = \begin{pmatrix} 102.24503905 \\ -36.0071558811 \end{pmatrix}, \quad \Sigma_{Spatial}^C = \begin{bmatrix} 5.438e^{-3} & 5.725e^{-5} \\ 5.725e^{-5} & 2.648e^{-3} \end{bmatrix} \quad (3.1.3)$$

on the other hand for the VPD we got (consider that the variables are the proper motions given by Gaia, that means  $PMRA = \alpha \cos(\delta)$  [ $mas \cdot yr^{-1}$ ] and  $PMDec = \delta$  [ $mas \cdot yr^{-1}$ ])

$$\vec{\mu}_{VPD}^C = \begin{pmatrix} 3.33257 \\ -2.20978 \end{pmatrix} \quad \Sigma_{VPD}^C = \begin{bmatrix} 0.34166 & +0.02554 \\ +0.02554 & 0.32945 \end{bmatrix} \quad (3.1.4)$$

$$\vec{\mu}_{VPD}^F = \begin{pmatrix} -0.26936 \\ 2.58955 \end{pmatrix} \quad \Sigma_{VPD}^F = \begin{bmatrix} 3.52199 & -1.02109 \\ -1.02109 & 5.72170 \end{bmatrix} \quad (3.1.5)$$

these values are in good agreement with the literature (e.g Goldsbury et al. (2010); Baumgardt and Vasiliev (2021)). Then considering that the spatial distribution and the movement of the stars are independent each other our total probability is  $Prob(x_i) = \prod_j P(x_i)_j$

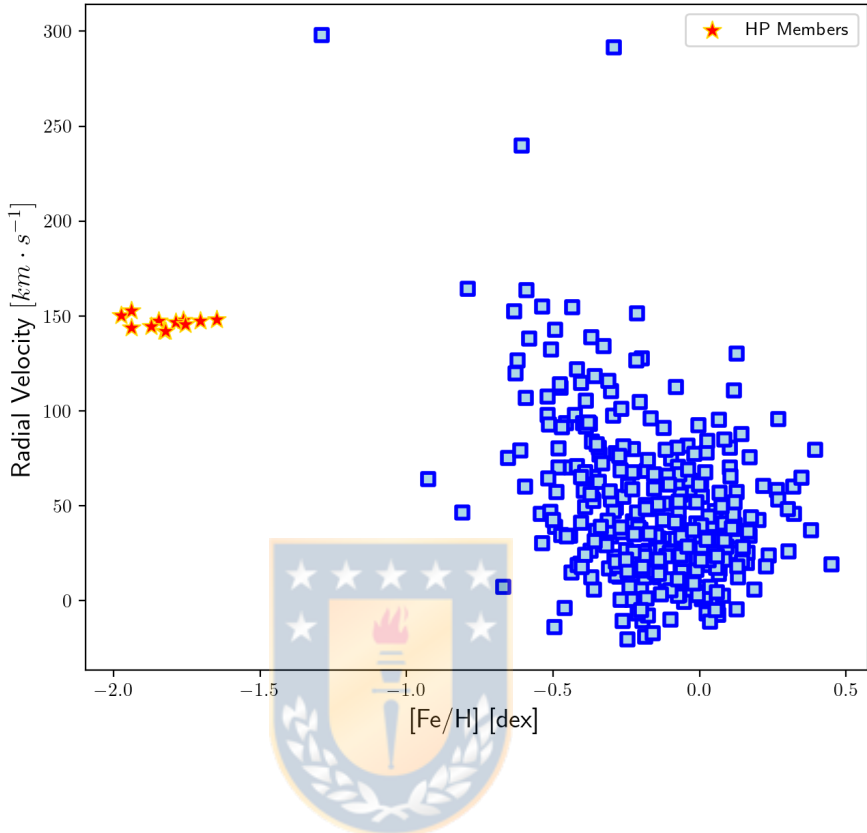
### 3.1.1.1 Cross-match and Contrast with preliminary values of ASCAP

Once we obtain our values of probability for each source we cross-matched our samples, after doing this we notice that in the APOGEE data twelve stars had a probability over 0.95.

---

<sup>1</sup>for further information you can see the webpage of the package [link to Scikit-Learn GMM](#)

**Figure 3.1.2:** Values of ASCAP contrasted with our criteria of selection of Members



With our candidates ready we decide to contrast with the values of ASCAP, as can be seen in the fig (3.1.2) our guesses are in good agreement whit those values of the pipeline due we can evidence a clear clustering in the radial velocities of our candidates and also are well separated in the preliminary values of Iron content. Therefore, with this information we can confidently work with these twelve stars as members of CG NGC 2298, the basic information of our twelve members is showed in the table 3.1.1.

**Table 3.1.1:** Photometric, kinematic, and astrometric properties of twelve likely members of NGC 2298.

| APOGEE ID          | $\alpha$     | $\delta$       | J      | H      | $K_s$  | G      | $(G_{BP}-G_{RP})$ | RV                | $\mu_\alpha \cos(\delta)$ | $\mu_\delta$        | $SNR^*$      |
|--------------------|--------------|----------------|--------|--------|--------|--------|-------------------|-------------------|---------------------------|---------------------|--------------|
|                    | hh:mm:ss     | dd:mm:ss       | [mag]  | [mag]  | [mag]  | [mag]  | [mag]             | $km \cdot s^{-1}$ | $mas \cdot yr^{-1}$       | $mas \cdot yr^{-1}$ | $pixel^{-1}$ |
| 2M06485459-3559151 | 6:48:54.5923 | -35:59:15.1764 | 11.927 | 11.296 | 11.133 | 13.896 | 1.551             | 147.35            | 3.184                     | -2.211              | 156          |
| 2M06485872-3600006 | 6:48:58.7201 | -36:00:00.6876 | 11.805 | 11.184 | 10.989 | 13.755 | 1.509             | 147.611           | 3.282                     | -2.184              | 174          |
| 2M06485886-3558262 | 6:48:58.8672 | -35:58:26.2056 | 11.933 | 11.304 | 11.171 | 13.88  | 1.512             | 146.718           | 3.357                     | -2.148              | 166          |
| 2M06485916-3600503 | 6:48:59.1636 | -36:00:50.346  | 11.854 | 11.257 | 11.074 | 13.802 | 1.521             | 142.108           | 3.339                     | -2.25               | 169          |
| 2M06490301-3559100 | 6:49:03.0122 | -35:59:10.0248 | 11.862 | 11.209 | 11.061 | 13.809 | 1.518             | 145.759           | 3.347                     | -2.138              | 157          |
| 2M06490382-3600299 | 6:49:03.8208 | -36:00:29.9376 | 13.173 | 12.591 | 12.494 | 14.972 | 1.365             | 152.961           | 3.405                     | -2.238              | 109          |
| 2M06490734-3558013 | 6:49:07.3498 | -35:58:01.308  | 11.658 | 11.008 | 10.858 | 13.64  | 1.546             | 144.482           | 3.305                     | -2.139              | 190          |
| 2M06491677-3557505 | 6:49:16.7743 | -35:57:50.58   | 12.227 | 11.602 | 11.454 | 14.074 | 1.442             | 148.226           | 3.314                     | -2.204              | 139          |
| 2M06485140-3600380 | 6:48:51.4013 | -36:00:38.0124 | 12.197 | 11.602 | 11.459 | 13.938 | 1.381             | 147.958           | 3.27                      | -2.066              | 138          |
| 2M06485619-3602261 | 6:48:56.1934 | -36:02:26.1996 | 13.105 | 12.593 | 12.46  | 14.781 | 1.266             | 150.24            | 3.378                     | -2.191              | 112          |
| 2M06485888-3601165 | 6:48:58.8886 | -36:01:16.5072 | 11.072 | 10.392 | 10.215 | 13.09  | 1.629             | 144.044           | 3.383                     | -2.189              | 254          |
| 2M06485948-3559426 | 6:48:59.4816 | -35:59:42.6264 | 12.555 | 12.018 | 11.862 | 14.4   | 1.352             | 141.928           | 3.432                     | -2.244              | 116          |

\* this parameter is the signal to noise ratio of the star given by APOGEE, all our sample is over 100 which implies very reliable measures

## 3.2 Inference of Atmospheric parameters

The next task to perform is get reliable Atmospheric parameters (which are need as initial guesses to model the atmospheres with BACCHUS, see section 2.4.3), we decide to do this through the fit of the Isochrone (see section 2.1.3) to the Gaia photometry (since already we have associated likely members to perform a fit), and then an interpolation ot get the parameters that we needed ( $T_{eff}$  and  $\log(G)$ ).

To perform the fit of the isochrone we first have to know the best parameters to generate this one, due the large uncertainties in the previous studies of the metallicity of this GC we decided to perform a  $\chi^2$  test to determine the best metallicity that fits our data and also to get the reddening and distance modulus, to achieve this we developed a software that try a different isochrones in a range of different position and return the best position through a  $\chi^2$  test, for our purpose we define the value the value of the test as

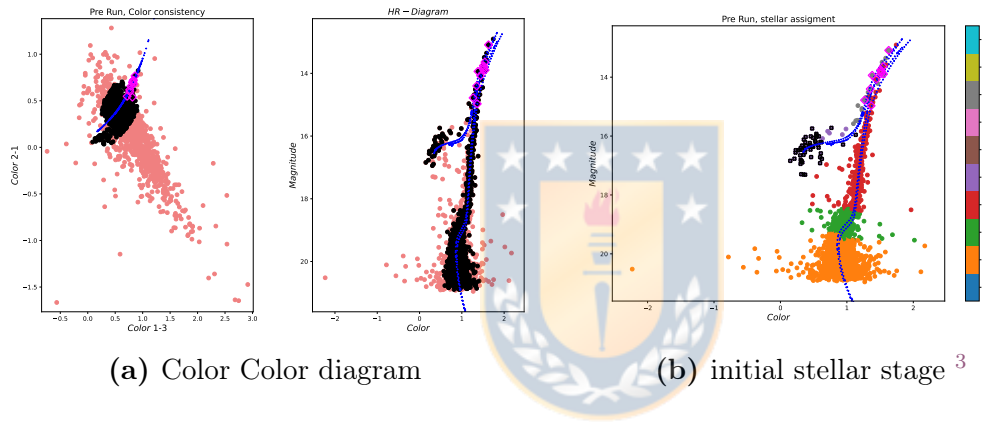
$$\chi^2 = \frac{1}{N-3} \left( \sum_i \left( \frac{C_i - I_i^{color}}{\sigma_i^{color}} \right)^2 + \sum_i \left( \frac{M_i - I_i^{Mag}}{\sigma_i^{mag}} \right)^2 \right) \quad (3.2.1)$$

where  $N$  is the number of sources that effectively are being fitted (the  $-3$  value it's due we are fitting 3 variables),  $C_i$  is the color of each source,  $M_i$  is the magnitude of each source,  $\sigma_i^{color}$  and  $\sigma_i^{mag}$  are the associated dispersion of each source in their color and in their magnitude and  $I_i^{color}$  and  $I_i^{Mag}$  are the values of color and magnitude of the isochrone which are the nearest to each source (square distance), for our purpose we took a sample of 400 isochrones of [Marigo et al. \(2017\)](#) varying values of MH between -2 to -1.6 with step of 0.01 dex and we fix an Age of 13.15 Gyr ([Monty et al., 2018](#)).

The way that this software works consist in two runs, first we move the extremes isochrones (values of MH=-2 dex and -1.6 dex) an look the best fit simultaneously to pre-assign a stellar stage (in this first iteration all the stars have a common sigma for color an another for the magnitude, and are the intrinsic dispersion of the sample), once the initial stellar stage is assigned we trim the data twice, first we look in a color-color diagram and look for a consistency in the color trend if the sources are farther than 0.25 mag (square distance) the stars are discarded

(most of this spread it's explained due that Gaia measures perform a pseudo-color correction for faint or not well resolved source through astrometry<sup>2</sup>), then the next trim that we perform is to the HB stars which are not well fitted though SSP model as the isochrones that we are using, so in order to have comparable data we keep all the HB that are inside of the range of all the HB stars in the isochrones that we gonna test (assuming the initial values of reddening and distance modulus, an also letting stars within a range of 0.1 mag in color and 0.3 mag in magnitude), these steps could be seen in the fig (3.2.1).

**Figure 3.2.1:** Initial assignment of stellar stage & Color Consistency (most reliable measures)



After the sample of stars is cut out letting us a comparable set, the stars are grouped by stellar stage and in this way per stage is assigned a value for the deviation associated with each source (except for the HB stars where the value in color is used the median value of other stars in the same range of magnitude), the value is computed per stage as the standard deviation of distance between the value and the nearest point of the isochrone, this means

$$\sigma_{Stellar-Stage} = \sqrt{\frac{\sum_i^{stage} (X_i^{stage} - \mu^{stage})^2}{n^{stage}}} \quad (3.2.2)$$

where  $n^{stage}$  is the number of the sources associated with the stage,  $X_i^{stage} = C_i - I_i^{Color}$ ,  $\mu^{stage} = \sum_i X_i^{stage}/n^{stage}$ , this value is multiplied by a factor which is defined as function of magnitudes of the sub-sample (stellar stage) as this means

---

<sup>2</sup>for further details see [link to pseudo-color info Gaia webpage](#)

<sup>3</sup>the numbers which indicates the stage associated with each source are the identifiers that are used in isochrones of Marigo et al. (2017) can be seen in [http://stev.oapd.inaf.it/cmd\\_3.4/faq.html](http://stev.oapd.inaf.it/cmd_3.4/faq.html)

that for each source the color deviation is

$$\sigma_i^{color} = \sigma_i^{Stellar-Stage} \times \left( 0.5 + \frac{M_i}{M_i^{Max-Stage}} \right) \quad (3.2.3)$$

with  $M^{Max-Stage}$  the maximum value of magnitude in the stage and the other values on the equation as was defined before (this in simple terms make that the brighter source of the stage had around 0.5 times the standard deviation of the associated stage and this factor increases smoothly to the fainter sources which will have around 1.5 standard deviation of the associated stage), for the magnitude we use a the same technique as the factor for the color but globally, so for each source we have that the mag deviation is

$$\sigma_i^{Mag} = \sigma_{Sample}^{Mag} \times \left( 0.5 + \frac{M_i}{M^{Max-Sample}} \right) \quad (3.2.4)$$

with  $M^{Max-Sample}$  the highest value of magnitude in the sample that effectively we are fitting, and where

$$\sigma_{Sample}^{Mag} = \sqrt{\frac{\sum_i^{Sample} (Y_i^{Sample} - \mu^{Sample})^2}{n^{Sample}}} \quad (3.2.5)$$

where  $n^{Sample}$  is the number of the sources in the whole sample,  $Y_i^{Sample} = M_i - I_i^{Mag}$ ,  $\mu^{Sample} = \sum_i Y_i^{Sample} / n^{Sample}$ , our results of the sigma estimation are showed in the fig (3.2.2).

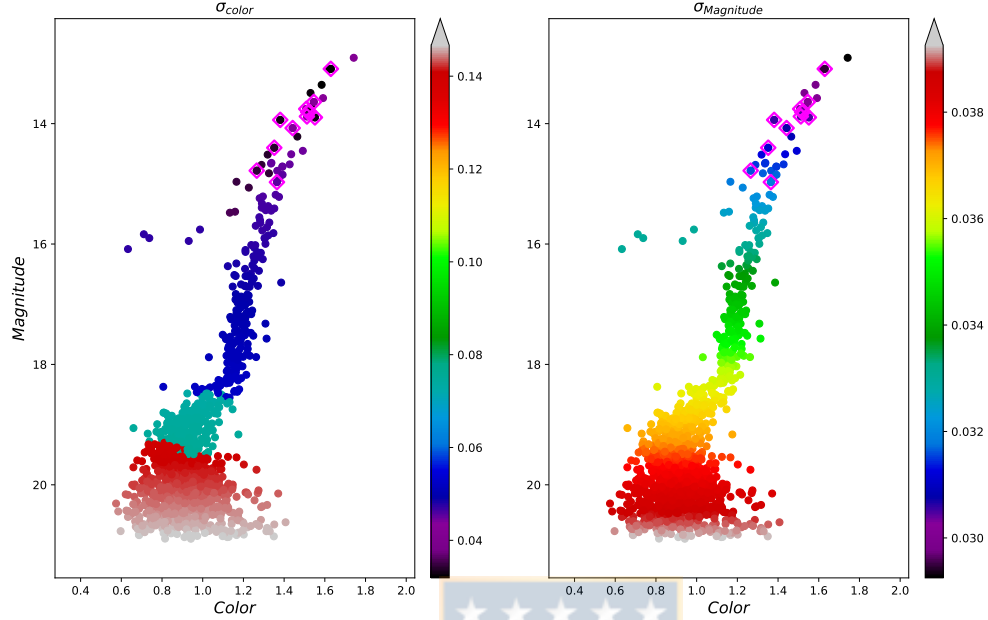
After getting the comparable sample and the assignation of values the second iteration start looking for the best fit, we interpolate each stellar stage in the isochrone and generate more point in each one in pro of getting best matches for each source, also for each Isochrone we tested the same range of reddening and distance modulus, the reddening is tested assigning a value of visual absorption and using the conversion between wavelength suggested in the webpage of the Isochrones <sup>4</sup>, for the last release of Gaia these values are

$$\frac{A_G}{A_V} = 0.83627, \quad \frac{A_{G_BP}}{A_V} = 1.08337, \quad \frac{A_{G_RP}}{A_V} = 0.63439 \quad (3.2.6)$$

---

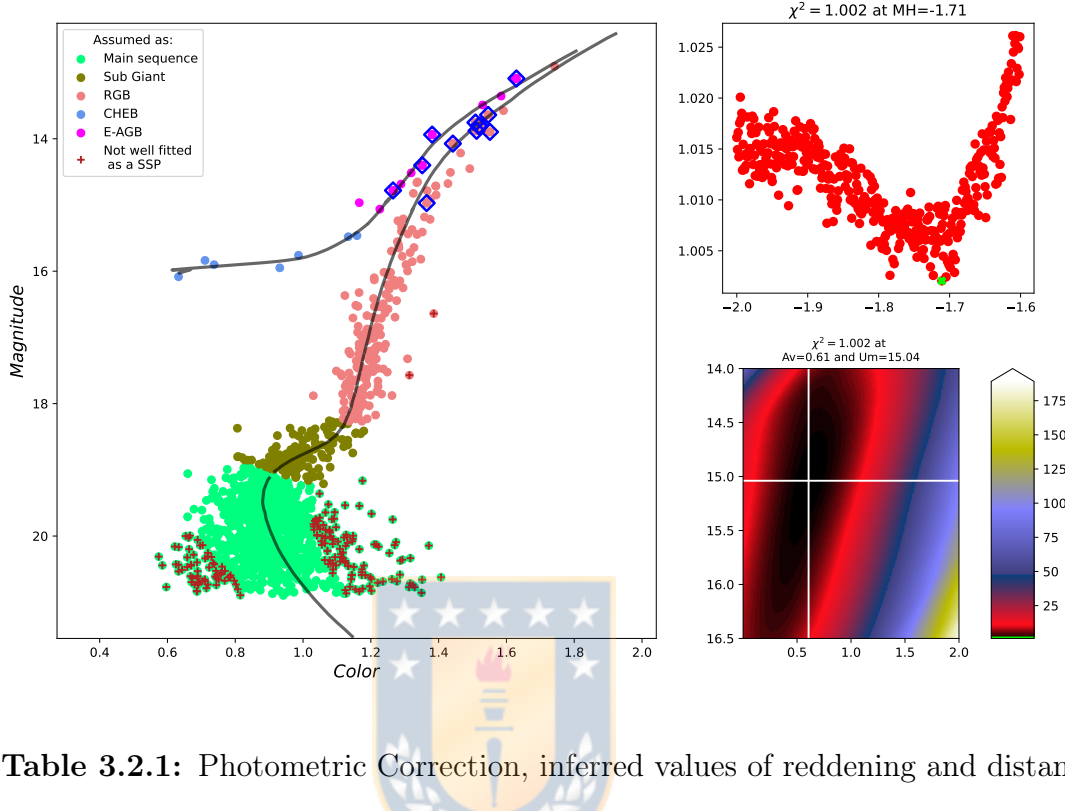
<sup>4</sup>Isochrone webpage [http://stev.oapd.inaf.it/cgi-bin/cmd\\_3.7](http://stev.oapd.inaf.it/cgi-bin/cmd_3.7)

**Figure 3.2.2:** Sigma associated with each source



Our best fit of Isochrone is showed in the fig (3.2.3), our twelve members are highlighted (edge of blue diamonds), the beside panels show the 3 free parameter  $\chi^2$  test (for each of the red point which are the isochrones (x-axis MH) we have a plane as is showed below), top panel the values obtained of best fit in each MH, below the map of reddening and distance modulus the white cross indicate where is the best value.

With this fit we could assign ideal values to our twelve members, these values are summarized in the table 3.2.1, where we show the de-reddened values of magnitude and color, also report the differential reddening and distance inferred. Also with these values we are able to get the atmospheric parameter through the interpolation of the Isochrone since these theoretical model have values expected for the specific magnitudes and color given an Age a metallicity and a stellar stage.

**Figure 3.2.3:** Best Isochrone Fit, 3 Free parameters  $\chi^2$  test**Table 3.2.1:** Photometric Correction, inferred values of reddening and distance

| APOGEE ID          | $G_0$  | $(G_{BP} - G_{RP})_0$ | $A_V$ | Distance [pc] |
|--------------------|--------|-----------------------|-------|---------------|
| 2M06485459-3559151 | 13.299 | 1.231                 | 0.714 | 10283.335     |
| 2M06485872-3600006 | 13.226 | 1.241                 | 0.597 | 10282.694     |
| 2M06485886-3558262 | 13.339 | 1.222                 | 0.647 | 10283.818     |
| 2M06485916-3600503 | 13.273 | 1.237                 | 0.633 | 10283.882     |
| 2M06490301-3559100 | 13.281 | 1.235                 | 0.632 | 10283.220     |
| 2M06490382-3600299 | 14.408 | 1.062                 | 0.674 | 10283.900     |
| 2M06490734-3558013 | 13.129 | 1.272                 | 0.611 | 10283.071     |
| 2M06491677-3557505 | 13.574 | 1.174                 | 0.598 | 10282.580     |
| 2M06485140-3600380 | 13.468 | 1.129                 | 0.561 | 10282.709     |
| 2M06485619-3602261 | 14.289 | 1.001                 | 0.588 | 10282.704     |
| 2M06485888-3601165 | 12.617 | 1.375                 | 0.566 | 10282.692     |
| 2M06485948-3559426 | 13.865 | 1.064                 | 0.640 | 10283.902     |

### 3.2.1 Micro Turbulence $\xi_{micro}$

There's a parameter that the isochrones models that we use doesn't have integrated yet , this is the micro-turbulence this parameter is associated (as the names indicates) with the atmospheric turbulence in the surface of the star, as we see in section 2.2.2.4 this parameter must be considered to characterize the spectral profile, we perform the estimation of this parameter through the equation

$$\xi_{micro} = 0.998 + 3.16 \times 10^{-4} \cdot X - 0.253 \cdot Y - 2.86 \times 10^{-4} \cdot X \cdot Y + 0.165 \cdot Y^2 \quad (3.2.7)$$

where  $X = T_{eff} - 5500$  [K] and  $Y = \log(g) - 4.0$ , this equation was taken from (Mott et al., 2020), and it's useful for FGK stars.

## 3.3 Conversion Vacuum to Air Wavelength from APOGEE spectra

The wavelength calibration of the APOGEE data is done using vacuum wavelengths. However, the wavelengths of atomic transitions are usually quoted at standard temperature and pressure (Air), to convert to the Air wavelength we use the expression an values showed in Edlen (1953)<sup>5</sup>

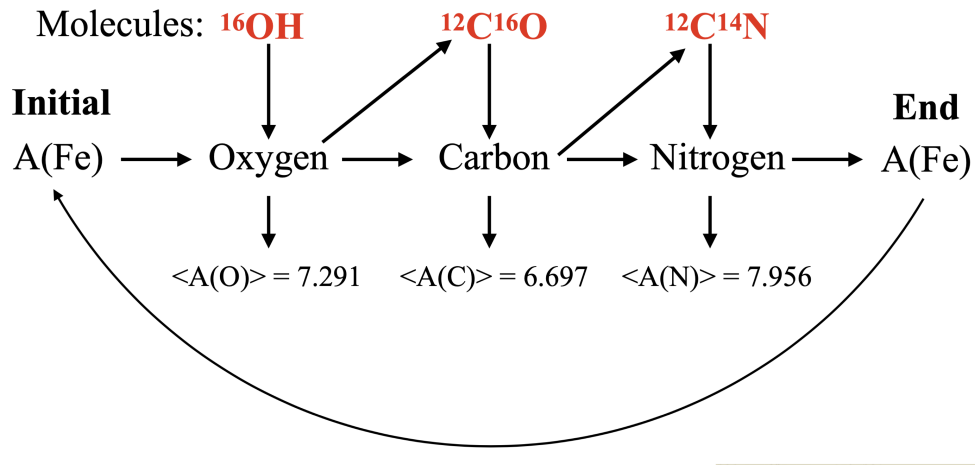
## 3.4 Running BACCHUS

Once our spectra are ready for our twelve reliable cluster members and our initial guesses of  $T_{eff}$ ,  $\log(G)$  and  $\xi_{micro}$  are established, we are able to start compute the abundances of each source, BACCHUS works with different steps first we have to load the stellar parameters to create the atmospheric model, then we use a element from which we have multiple lines to get a value of equivalent width (eqw, this is the width of a projected rectangle with a height equal to the relative continuum (1) that create the same area that the one enclosed by the absorption line, this is done automatically by the software), value which will be assumed

---

<sup>5</sup>APOGEE works with other values nevertheless variation between them at this wavelength are negligible. <https://www.sdss.org/dr12/irspec/spectra/#vacuum>

**Figure 3.4.1:** Self consistency as described by Smith et al. (2013)



equal for all the elements at the time of compute the abundance, then we can start the abundance computation.

The way we proceed was, first loading the parameters for the star then we use the Silicon (Si) to obtain the eqw (usually Iron is used for this purpose but due our cluster is very metal poor the lines weren't strong enough to make a reliable estimation of this parameter).

### 3.4.1 Self Consistency of C-N-O

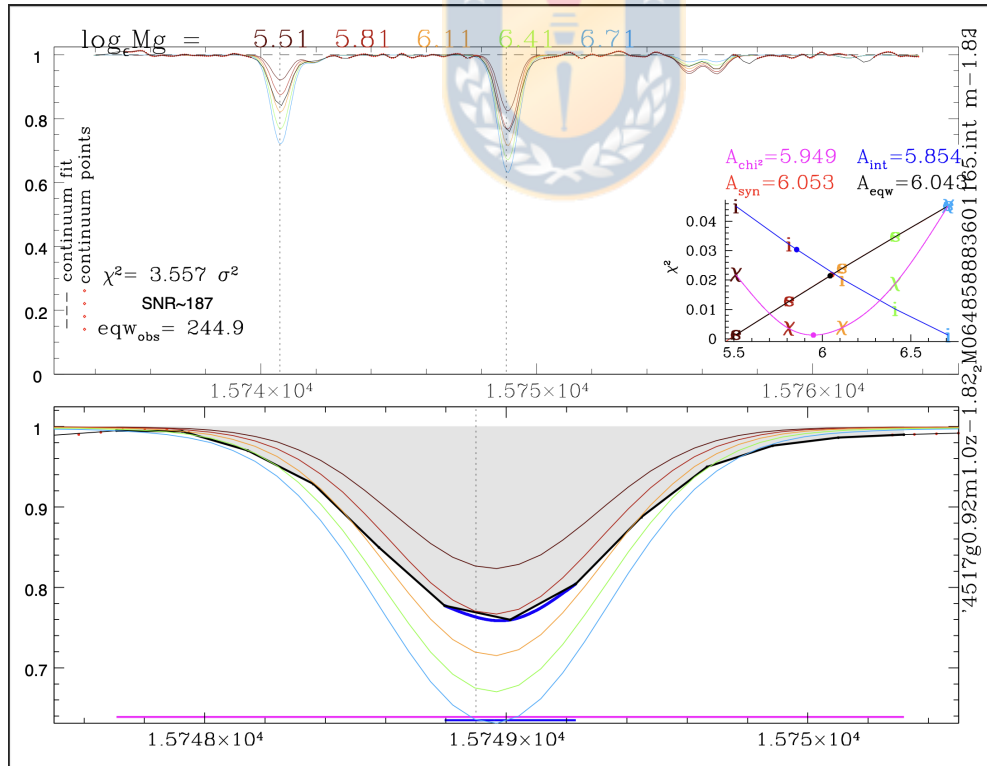
Then we have to consider the CNO analysis apart, since in the range that we are working the estimation of these elements came from molecules that are related between them because are made from the same atoms (this means use CO to set the carbon abundance, OH provides an O abundance, and CN provide N abundance), hence using a reliable measure (e.g. the element that we use to determine the eqw) we determine values for O and we fix this value then we determine C and fixed this value and then N and also is fixed, after this we reanalyse our reliable measure if it is different from the initial value we re-analyze the CNO lines in the same way. This process is repeated until the C, O and N abundances yield consistent abundances (which means reach a similar value to the initial guess of our reliable measure, see fig 3.4.1 for a schematic representation of this process called self-consistency, this procedure was explained in Smith et al. (2013)). After this we can compute the abundance for a variety of elements, these steps are made for each star.

BACCHUS computes abundances for each line therefore we have to check out which of the lines are reliable (it mean that have a expected Voight profile for most of the elements, the exception are those who are measure through molecules as CNO) and if the convolution converge, this is done bye eye, the software creates pdf files with the measures and the models also show info about the convergence of the convolution of the models in fig 3.4.2 you can see a typical output and a very good line of Mg where all the methods converges.

### 3.4.2 Central Values

In order to retrieve the final values due until now we compute abundances deferentially for each line we use the mean value along the measures of all lines for each element and we check if this value fits the data properly (we have to generate apart a model in BACCHUS indicating the value that we estimated).

**Figure 3.4.2:** Typical output of BACCHUS



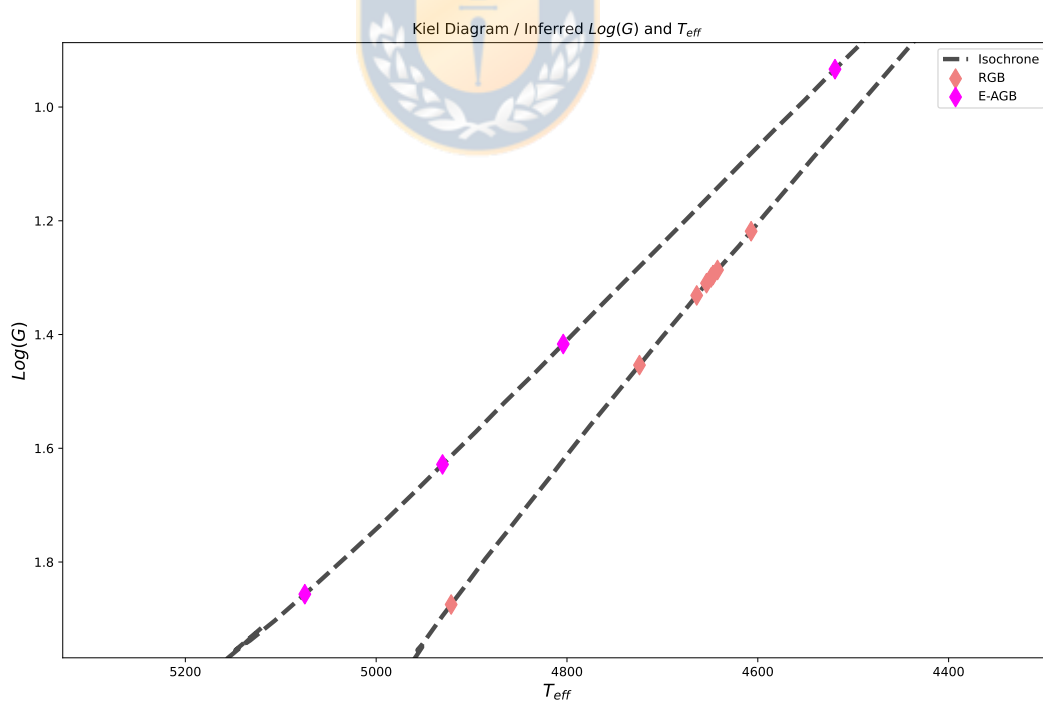
Finally we do this for all the lines of each element we just have to contrast the values with the solar values (to make it comparable), we use the values of Asplund et al. (2021).

# Chapter 4

## Analysis

### 4.1 Inputted Parameters on BACCHUS

Figure 4.1.1: Kiel diagram (showing our inferred parameters)



With the described procedure in the section 3.2 we obtain the atmospheric values showed in the Kiel diagram (see 4.1.1) and which values are summarized (plus the micro-turbulence  $\xi_{\text{micro}}$ ) in the table 4.1.1,

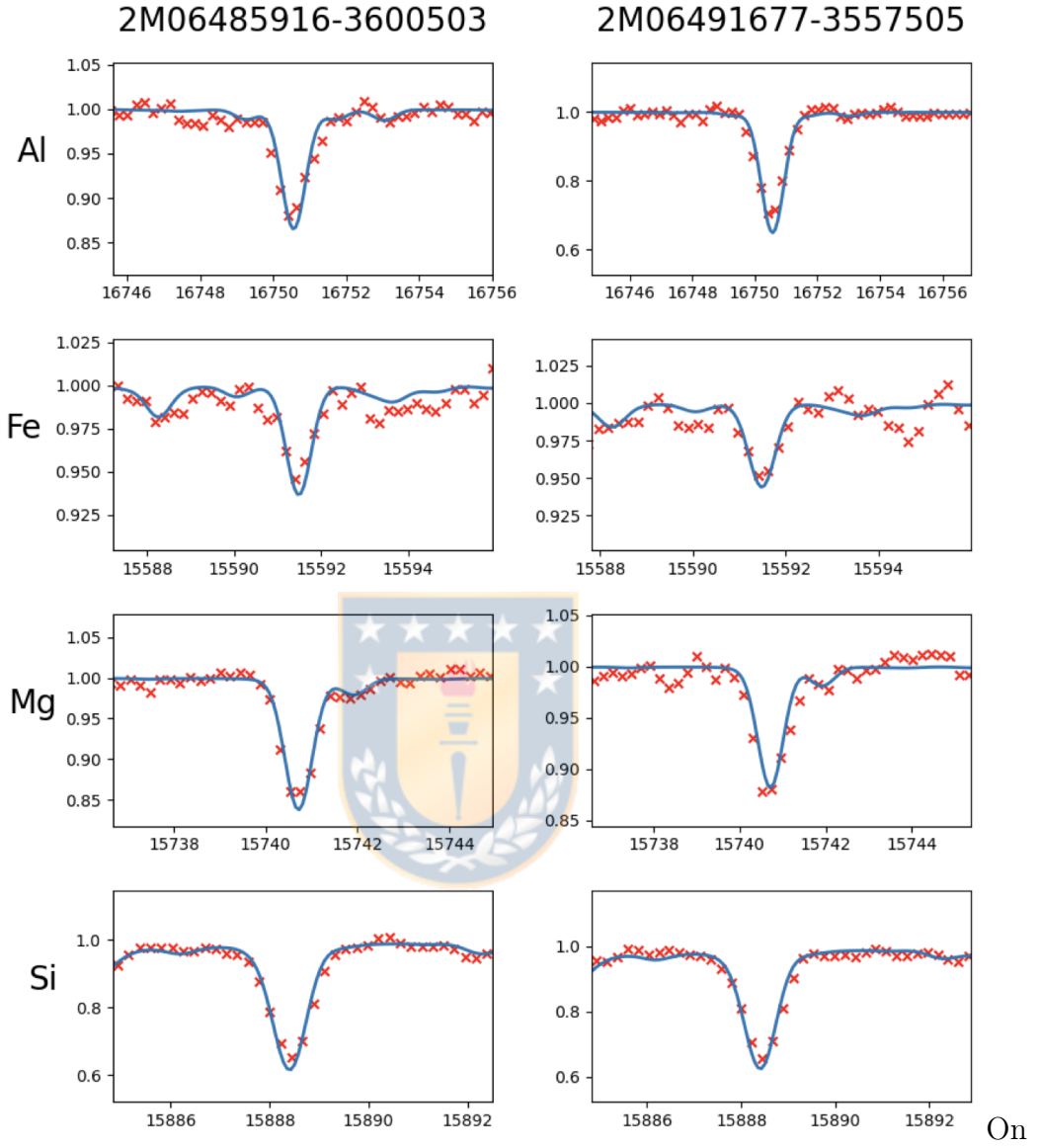
**Table 4.1.1:** Atmospheric Parameters and classification of the targets.  
(Summarized values of Fig (4.1.1))

| APOGEE ID          | $T_{eff}$ | $\log(g)$ | $\xi_{micro}$ | class |
|--------------------|-----------|-----------|---------------|-------|
| 2M06485459-3559151 | 4685      | 1.343     | 1.958         | RGB   |
| 2M06485872-3600006 | 4652      | 1.276     | 1.984         | RGB   |
| 2M06485886-3558262 | 4683      | 1.339     | 1.96          | RGB   |
| 2M06485916-3600503 | 4663      | 1.298     | 1.975         | RGB   |
| 2M06490301-3559100 | 4665      | 1.302     | 1.974         | RGB   |
| 2M06490382-3600299 | 4943      | 1.895     | 1.75          | RGB   |
| 2M06490734-3558013 | 4620      | 1.211     | 2.007         | RGB   |
| 2M06491677-3557505 | 4733      | 1.443     | 1.92          | RGB   |
| 2M06485140-3600380 | 4795      | 1.394     | 2.03          | AGB   |
| 2M06485619-3602261 | 5059      | 1.842     | 1.901         | AGB   |
| 2M06485888-3601165 | 4517      | 0.9164    | 2.17          | AGB   |
| 2M06485948-3559426 | 4935      | 1.636     | 1.957         | AGB   |

## 4.2 Looking at the Central Values

With the atmospheric values we are able to compute the abundances using BACCHUS as is described in the section 3.4.

**Figure 4.2.1:** Example of the final fit of synthetic spectra to the real measures



blue the final synthetic spectra, the red crosses are the measurements, sorted by star by columns and by element in rows

As was mentioned in 3.4.2, in the fig (4.2.1) we show two examples of final fit comparing the synthetic spectra with the measures.

## 4.3 Error Estimation

Once we determine the central values of each element (our best fit with just our best lines), we have to estimate the uncertainty for each element, these ones was

calculated as the root squared sum of the individual uncertainties due to the errors in each atmospheric parameter under the assumption that these individual uncertainties are independent. The reported uncertainty for each chemical species is

$$\sigma^2 = \sigma_{mean}^2 + \sigma_{[X/H],\epsilon_i}^2 + \sigma_{[X/H],Logg}^2 + \sigma_{[X/H],T_{eff}}^2 \quad (4.3.1)$$

as is described in (Fernández-Trincado et al., 2019c), we variate the values of our initial guesses as  $T_{eff} \pm 100 [K]$ ,  $\log(G) \pm 0.3$  (the  $\xi_{micro}$  is varied according the values of  $T_{eff}$  and  $\log(G)$  for these changes using the same equation (3.2.7)) and finally  $\xi_{micro} \pm 0.05$ . For each of these changes (6 in total) we have to do the same procedure indicated in section 3.4, re-estimate values and get the concatenate dispersion (the central values and the specific variation), this is done globally as GC value (this means doing separately by variation as is show in the equation 4.3.1) and then by star considering all the variations of parameters to get the spread of each abundance (this means considering all the values that we got for each star along all the variation of parameters and simply get the standard deviation of the values).

# Chapter 5

## Results

### 5.1 Abundance

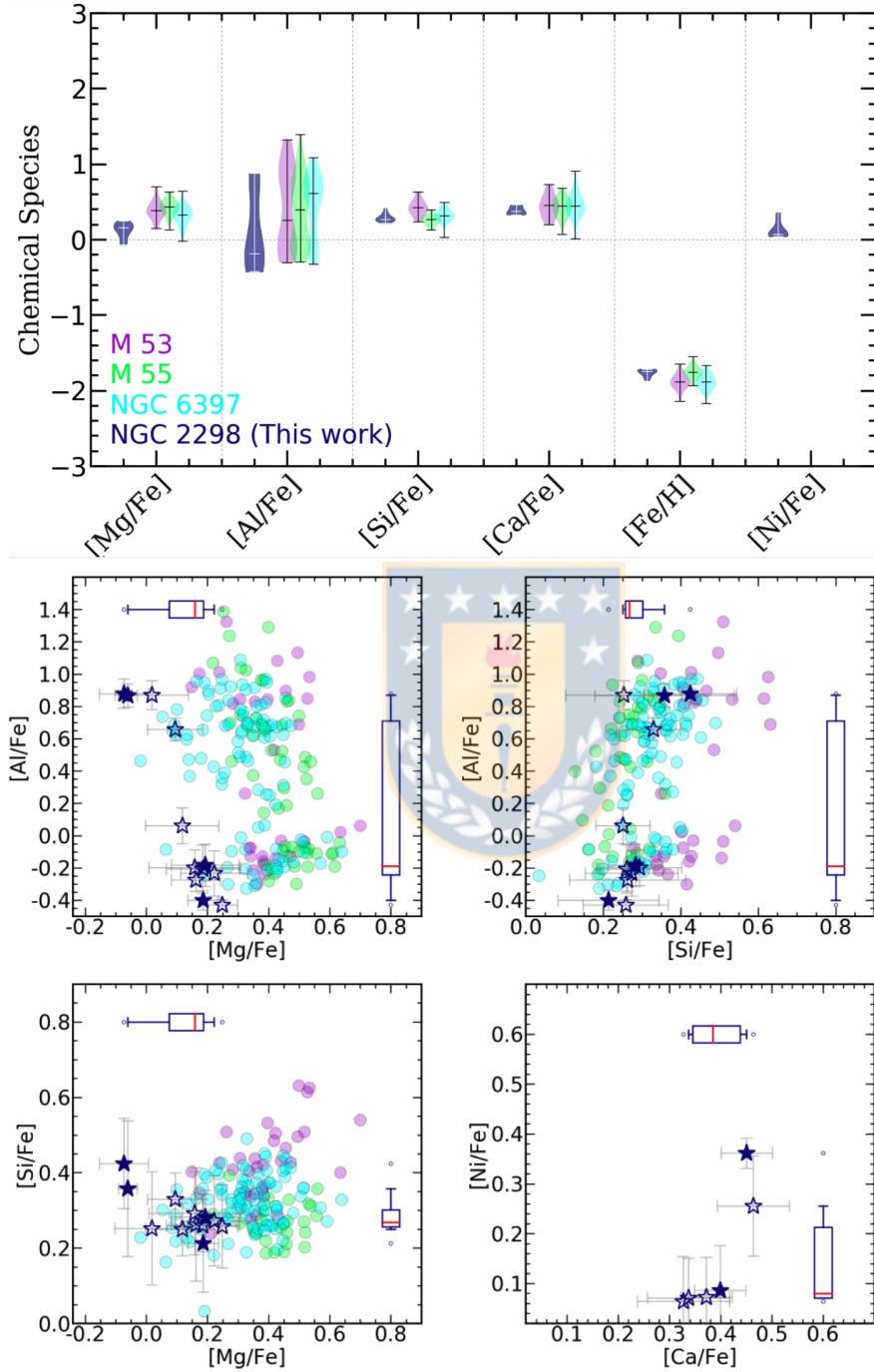


In the following section we show our results and estimations from the GC NGC 2298 as a system and individually for each of the twelve members that we used to perform the analysis.

#### 5.1.1 CNO

We remark that no conclusive answers can be drawn for C, N, and O from  $^{12}C^{14}N$ ,  $^{16}OH$ , and  $^{12}C^{16}O$ , as these lines become too weak to be detected or accurately measured at the metallicity and temperature range of our NGC 2298 stars. For this reason, we choose not to speculate on the interpretation of C, N, and O abundances for the present sample.

**Figure 5.1.1:** Summarized in this plot our findings and the final values report (Globally and deferentially respectively) [Baeza et al. \(2022\)](#)

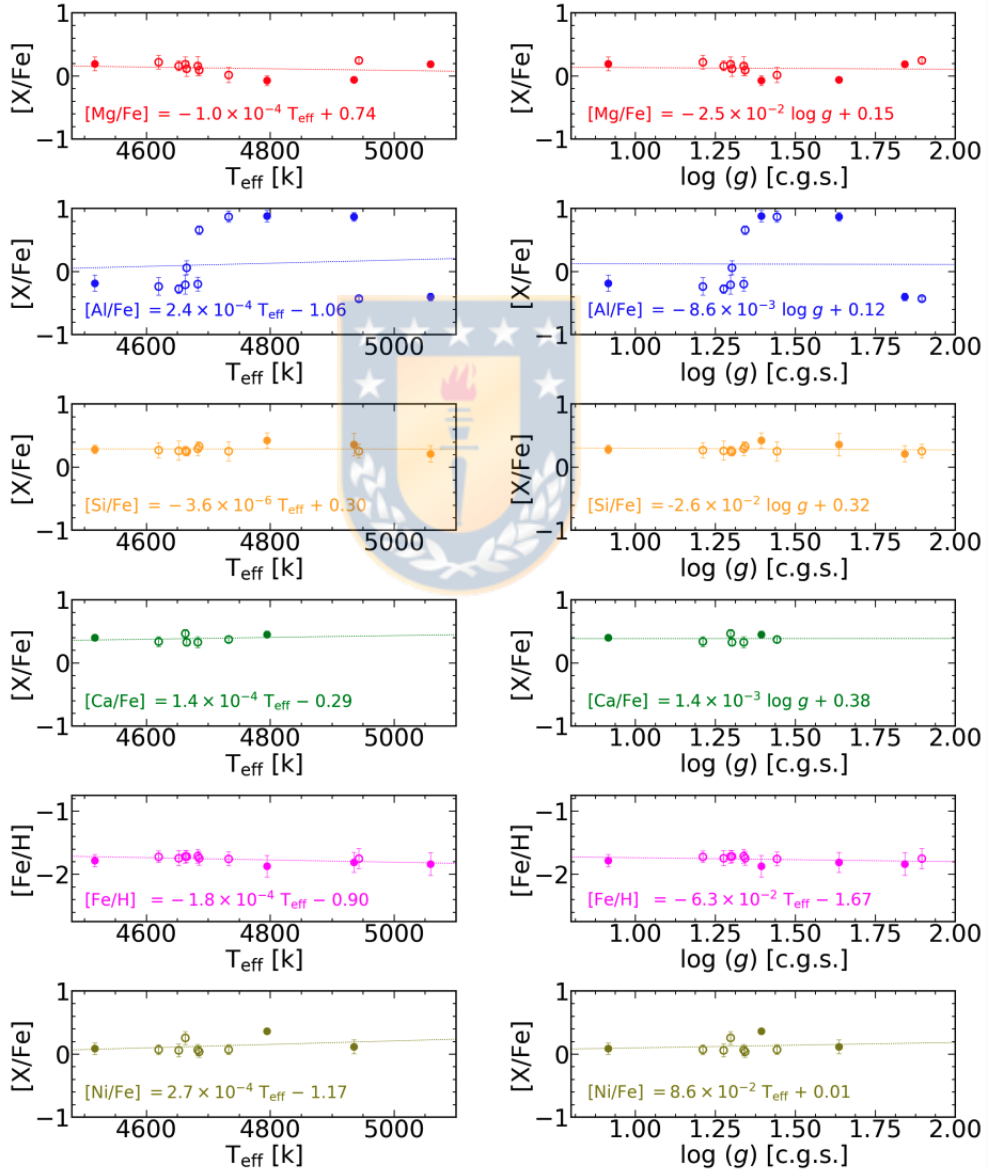


The filled star symbols correspond to AGB stars the empty stars corresponds to RGB star, the values from the other clusters were taken from [Mészáros et al. \(2020\)](#)

### 5.1.2 Independence of Parameters

In the fig (5.1.2) We demonstrates a lack of abundance dependence on the effective temperature or surface gravity, as well as on the evolutionary status (RGB or AGB) for Mg, Al, Si, Ca, Fe, or Ni at the metallicity of NGC 2298.

**Figure 5.1.2:** Linear Regression between stellar parameters and abundance estimation (Baeza et al. (2022))



The filled star symbols correspond to AGB stars the empty stars corresponds to RGB star, The dashed lines and inset notation represent the linear regression of the data

We also find that the RGB and AGB stars do not group separately in any of the

abundance-abundance planes presented in Fig (5.1.1). Therefore, the observed correlations anti-correlations in NGC 2298 does not depend on the evolutionary status of a star.

### 5.1.3 Multiple Stellar Population on NGC 2298

In the Fig (5.1.1) we show our final estimation globally and deferentially respectively , the values from other GC in the same range of metallicity were taken from Mészáros et al. (2020), the values present in this figure are shown in the table 5.1.1, we can see through values that this GC present a clear MP.

**Table 5.1.1:** Estimated abundances for the selected sources, also are shown the results from ASCAP

| Source ID          | [Fe/H]     | [Mg/Fe]      | [Al/Fe]      | [Si/Fe]      | [Ca/Fe]      | [Ni/Fe]      |
|--------------------|------------|--------------|--------------|--------------|--------------|--------------|
| 2M06485459-3559151 | -1.74±0.11 | +0.09 ± 0.09 | +0.65 ± 0.07 | +0.32 ± 0.07 | ...          | +0.03 ± 0.09 |
| 2M06485872-3600006 | -1.74±0.12 | +0.16 ± 0.08 | -0.27 ± 0.07 | +0.26 ± 0.15 | ...          | +0.05 ± 0.10 |
| 2M06485886-3558262 | -1.71±0.11 | +0.15 ± 0.15 | -0.19 ± 0.11 | +0.29 ± 0.11 | +0.32 ± 0.09 | +0.06 ± 0.09 |
| 2M06485916-3600503 | -1.72±0.10 | +0.18 ± 0.12 | -0.20 ± 0.15 | +0.25 ± 0.07 | +0.46 ± 0.07 | +0.25 ± 0.10 |
| 2M06490301-3559100 | -1.71±0.09 | +0.11 ± 0.12 | +0.06 ± 0.11 | +0.24 ± 0.07 | +0.32 ± 0.06 | ...          |
| 2M06490382-3600299 | -1.75±0.16 | +0.24 ± 0.05 | -0.42 ± 0.03 | +0.25 ± 0.11 | ...          | ...          |
| 2M06490734-3558013 | -1.72±0.09 | +0.22 ± 0.11 | -0.23 ± 0.14 | +0.27 ± 0.12 | +0.33 ± 0.08 | +0.07 ± 0.08 |
| 2M06491677-3557505 | -1.75±0.11 | +0.01 ± 0.12 | +0.87 ± 0.09 | +0.25 ± 0.15 | +0.37 ± 0.05 | +0.07 ± 0.08 |
| 2M06485140-3600380 | -1.87±0.17 | -0.07 ± 0.08 | +0.87 ± 0.09 | +0.42 ± 0.12 | +0.45 ± 0.05 | +0.36 ± 0.03 |
| 2M06485619-3602261 | -1.83±0.18 | +0.18 ± 0.05 | -0.40 ± 0.06 | +0.21 ± 0.13 | ...          | ...          |
| 2M06485888-3601165 | -1.78±0.10 | +0.19 ± 0.11 | -0.18 ± 0.13 | +0.28 ± 0.07 | +0.39 ± 0.05 | +0.08 ± 0.09 |
| 2M06485948-3559426 | -1.80±0.16 | -0.06 ± 0.03 | +0.86 ± 0.07 | +0.35 ± 0.18 | ...          | +0.09 ± 0.11 |

#### Statistics

|                  |       |       |       |       |       |       |
|------------------|-------|-------|-------|-------|-------|-------|
| median           | -1.75 | +0.16 | -0.19 | +0.27 | +0.37 | +0.07 |
| mean             | -1.76 | +0.12 | +0.12 | +0.29 | +0.38 | +0.12 |
| $1\sigma$        | 0.05  | 0.10  | 0.51  | 0.05  | 0.05  | 0.10  |
| Spread $\dagger$ | 0.14  | 0.30  | 1.29  | 0.15  | 0.13  | 0.27  |

#### ASPCAP DR17

|           |       |       |       |       |       |       |
|-----------|-------|-------|-------|-------|-------|-------|
| median    | -1.82 | +0.20 | -0.28 | +0.25 | +0.23 | -0.04 |
| mean      | -1.83 | +0.16 | +0.05 | +0.26 | +0.20 | -0.06 |
| $1\sigma$ | 0.08  | 0.14  | 0.55  | 0.04  | 0.14  | 0.05  |

the errors were estimated as is indicated in the section 4.3

### 5.1.3.1 The $\alpha$ elements Mg, Si, Ca

The  $\alpha$  element in NGC 2298 are overabundant ( $> +0.12$ ) compared to the Sun, supporting the idea that the main contributors to the chemistry of this cluster have likely been stars which go through the Alpha and Triple Alpha process and then pollutes the stars that we are studying, which it means SN progenitors (Tsujimoto and Bekki, 2012; Bekki et al., 2017; Bekki, 2017b,a; Jiang et al., 2017; Krause et al., 2013).

Our NGC 2298 sample has a star-to-star show a spread in [Si/Fe] and [Ca/Fe], which is slightly larger than the measurement uncertainties for each species, with the exception of [Mg/Fe]. There is a significant [Mg/Fe] spread of 0.3 dex, exceeding the observational uncertainties, which is anti-correlated with [Al/Fe] (see fig (5.1.1)). However, the [Mg/Fe] abundance ratio by itself exhibits a median value that is systematically offset by roughly 0.2 dex lower than M 53, M 55, and NGC 6397 stars from Mészáros et al. (2020).

The measures also reveals an apparent Mg-Si anti-correlation (not strong enough to asseverate but it could be interesting to look for further measures since the evidence for this Mg-Si anti-correlation does not exist for the other GCs at a similar metallicity as that of NGC 2298). The presence of a Mg-Si anti-correlation in NGC 2298 implies a leakage from the Mg-Al chain into Si production through the  $^{26}Al(p, \gamma) \rightarrow ^{27}Si(e^-, \nu) \rightarrow ^{28}Al(p, \gamma) \rightarrow ^{28}Si$  (see the last part of fig (2.1.2e)) reactions at a high temperature. In the absence of this leakage, we would expect a simple correlation between Mg and Si since they are both  $\alpha$  elements (see e.g. Yong et al., 2005; Carretta et al., 2009b; Mészáros et al., 2020). We find that some of the stars in NGC 2298 exhibit a higher Si abundance than their Mg-rich counterparts, confirming the likely occurrence of hot proton burning in the early populations of NGC 2298.

An Al-Si correlation is also observed in NGC 2298, as can be appreciated in Fig (5.1.1). Yong et al. (2005); Carretta et al. (2009b); Mészáros et al. (2015, 2020); Masseron et al. (2019) interpreted the Al-Si correlation as a signature of  $^{28}Si$  leakage from the Mg-Al chain (see fig (2.1.2e)). Interestingly, most of the Si-enriched stars in NGC 2298 also seem to correspond to the Mg-depleted and Al-enhanced cluster population, which are likely the result of Ne-Na and Mg-Al cycles occurring in the H-burning shell of a first-generation stars whose

nucleosynthetic products were later distributed through the cluster. We stress that, regarding any possible analysis bias, since we have not been able to find any dependence of the abundances with the evolutionary status (see fig (5.1.1,5.1.2)).

### 5.1.3.2 The odd-z element Al

Similar to the result reported 30 years ago by [McWilliam et al. \(1992\)](#), we confirm that this cluster also hosts a clear population of Al-enhanced stars with  $[Al/Fe] \gtrsim +0.5$ , which is significantly higher than typical Galactic abundances ( $[Al/Fe] < +0.5$  for the typical first-generation stars).

Fig (5.1.1) also clearly reveals two distinct groups in the Mg-Al plane, one of them lies in the region dominated by the lowest  $[Al/Fe]$  abundances with slightly super-Solar  $[Mg/Fe]$  abundance ratios rather than sub-Solar ones (often called first-generation stars or un-enriched stars), while the second group is governed by higher  $[Al/Fe]$  abundances with the lowest  $[Mg/Fe]$  abundances, containing a fraction of stars well below  $[Mg/Fe] \approx 0$  (called second-generation or enriched stars).

### 5.1.3.3 Iron peak elements Fe and Ni

We find a mean metallicity  $[Fe/H] = -1.76 \pm 0.01$  with a dispersion of  $\sigma_{[Fe/H]} = 0.048 \pm 0.009$  dex. Reported errors are errors on the mean. We also find an iron star-to-star spread of 0.14 dex, compatible with the measurement errors, so we have no evidence for an intrinsic Fe abundance spread in NGC 2298.

Our measured mean metallicity for this GC exhibits a deviation greater than the uncertainties in comparison to some previous works that employ a variety of methods reporting a wide range ( $\sim 0.25$  dex) of metallicity from  $[Fe/H]=-1.96$  to -1.71, but it is in reasonable agreement with a few of them. For instance, [Frogel et al. \(1983\)](#) transformed optical and NIR colors to Cohen's metallicity scale ([Cohen, 1983](#)), and they estimated a mean value of  $[Fe/H]=-1.76$ , which has been listed as  $[Fe/H]_{IR}$  in Table 5 of [Zinn and West \(1984\)](#), they found a mean metallicity of  $[Fe/H]=-1.85$ , in [Zinn \(1985\)](#) was found a  $[Fe/H]=-1.81$  on his metallicity scale, later [McWilliam et al. \(1992\)](#) found a metallicity of  $[Fe/H]=-1.89$ , then [Geisler et al. \(1995\)](#) estimated a metallicity of  $[Fe/H]=-1.82$ , the next year [Salaris and Cassisi \(1996\)](#) reported a metallicity of  $[Fe/H]=-1.91$  after [Carretta and Gratton \(1997\)](#) reported a metallicity of  $[Fe/H]=-1.71$  while [Kraft and Ivans](#)

(2003) listed a range of metallicity  $[\text{Fe}/\text{H}]$  between -1.93 to -1.83 also Pritzl et al. (2005) reported a metallicity of  $[\text{Fe}/\text{H}] = -1.90$ , the re-estimation carried out by Carretta et al. (2009a) provided a metallicity of  $[\text{Fe}/\text{H}] = -1.96$ , more recently Carrera et al. (2013) listed a  $[\text{Fe}/\text{H}] = -1.74$ , while Roediger et al. (2014) and Yong et al. (2014) have provided a metallicity estimation of  $[\text{Fe}/\text{H}] = -1.95$  and  $[\text{Fe}/\text{H}] = -1.96$ , respectively.

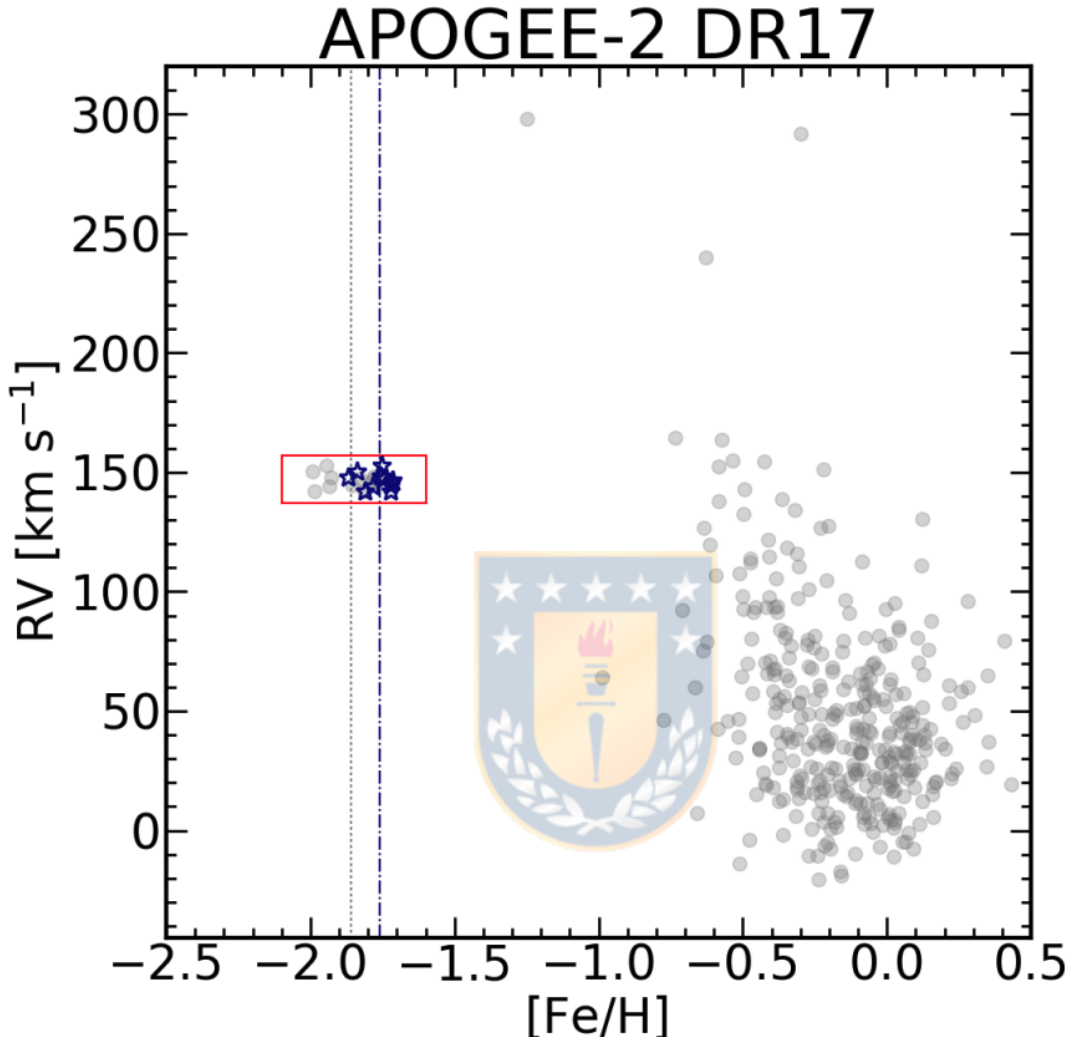
As far as other iron-peak elements are concerned, Ni is slightly overabundant relative to Solar (+0.12), with a star-to-star spread of 0.27 dex that is higher than the measurement uncertainties of  $[\text{Ni}/\text{Fe}]$  abundance ratios in NGC 2298, which strikingly appear to be weakly correlated with  $[\text{Ca}/\text{Fe}]$ , as can be appreciated in Fig (5.1.1). However, the observed star-to-star spread in the  $[\text{Ca}/\text{Fe}]$  abundance ratios is not statistically significant according to our error analysis, as has been observed in other GCs (Carretta and Bragaglia, 2021).

Our sample is tightly concentrated around the mean  $[\text{Ca}/\text{Fe}]$  of NGC 2298. Therefore, with the determinations of  $[\text{Ni}/\text{Fe}]$  and  $[\text{Ca}/\text{Fe}]$  for a limited sample of six cluster stars, we cannot draw firm conclusions about the apparent correlation between these two species. This possibility will have to be considered using larger samples in the future.

#### 5.1.4 Contrast whit the Pipeline of APOGEE

Finally we compare our measurements of  $[\text{Fe}/\text{H}]$  with the values of the pipeline ASCAP, in the fig (5.1.3) we overplot the different values that we estimate to the ASCAP results also we show the difference between the mean value for the cluster considering our estimation and the values of ASCAP, This figure reveals that BACCHUS-[ $\text{Fe}/\text{H}$ ] is systematically offset by roughly 0.1 dex to higher metallicity compared to the ASPCAP-[ $\text{Fe}/\text{H}$ ] abundance ratio, which is most likely due to systematics between BACCHUS and ASPCAP, similar to other studies of the APOGEE-2 spectra (see, e.g., Masseron et al. (2019); Fernández-Trincado et al. (2020c); Mészáros et al. (2020)).

**Figure 5.1.3:** Final values of  $[Fe/H]$  contrasted with the preliminary data of ASCAP



The gray dotted and navy blue dash-dotted lines mark the average  $[Fe/H]$  of the 12 NGC 2298 stars analyzed in this work , in gray the values of ASCAP and in navy our results ([Baeza et al. \(2022\)](#))

# Chapter 6

## Conclusion

During this Thesis we addressed the MP phenomena, review the past idea of GC and contrasted with the current state of the art, we start with a hypothesis which have been proven along this study, therefore our results indicates the prevalence of the MPs phenomenon at the low metallicity GC NGC 2298. It is important to note that RGB and AGB stars present in NGC 2298 do not appear to follow different paths or group separately in any of the abundance planes examined in this work, therefore, we conclude that the observed correlations anti-correlations does not depend on the evolutionary status of a star in NGC 2298.

In specific we have performed a high-resolution spectral analysis for 12 stars in the old GC NGC 2298. This cluster is located in a region of low interstellar reddening, and it has a halo orbit that crosses the Bulge, with an apocentric distance of  $\sim 16.44$  kpc (Massari et al., 2019). We found a mean and median metallicity of  $[Fe/H] = -1.76$  and  $-1.75$ , respectively, with a star-to-star spread of 0.14 dex that is compatible with the measurement errors, so we find no evidence for an intrinsic Fe abundance spread in NGC 2298. Our reported metallicity is  $\sim 0.2$  dex more metal-rich than previously thought, but it is in reasonable agreement with estimations provided by Kraft and Ivans (2003) and Carrera et al. (2013).

We confirm the existence of an Al-enriched population in NGC 2298, as was claimed three decades ago (McWilliam et al., 1992). We provide, for the first time, evidence for the standard anti-correlation between Mg and Al in our data.

We also detect an apparent Mg-Si anti-correlation (further studies will be needed) and an Al-Si correlation, which are likely signatures of  $^{28}Si$  leakage from the MgAl

chain (see fig (2.1.2e)), which is a feature common to other GCs (Masseron et al., 2019; Mészáros et al., 2020) at a similar metallicity range of NGC 2298.

Finally we report values of distance, reddening, metallicity and contrast with literature, these values can be found in the table 6.0.1

**Table 6.0.1:** Our findings Vs Literature Values

| Inferred                                   | in this work      | Literature      | Reference of literature     |
|--|-------------------|-----------------|-----------------------------|
| Distance<br>[kpc]                          | $10.28 \pm 0.05$  | 10.86           | Frogel et al. (1983)        |
|  |                   | 12.41           | Zinn (1985)                 |
|  |                   | 10.81           | Kraft and Ivans (2003)      |
|  |                   | 12.82           | Carrera et al. (2013)       |
|  |                   | $9.83 \pm 0.17$ | Baumgardt et al. (2019)     |
| Reddening<br>[E(B-V)*]                     | $0.182 \pm 0.057$ | 0.13            | Frogel et al. (1983)        |
|  |                   | 0.08            | Zinn (1985)                 |
|  |                   | 0.16            | Kraft and Ivans (2003)      |
|  |                   | 0.13            | Carrera et al. (2013)       |
|  |                   | 0.14            | Roediger et al. (2014)      |
|  |                   | 0.14            | Baumgardt et al. (2019)     |
| Radial Velocity<br>[km · s <sup>-1</sup> ] | $146 \pm 5$       | 165             | Zinn (1985)                 |
|  |                   | 150             | Geisler et al. (1995)       |
|  |                   | 147             | Baumgardt et al. (2019)     |
| [Fe/H]<br>[dex]                            | $1.76 \pm 0.14$   | -1.76           | Frogel et al. (1983)        |
|  |                   | -1.85           | Zinn and West (1984)        |
|  |                   | -1.81           | Zinn (1985)                 |
|  |                   | -1.89           | McWilliam et al. (1992)     |
|  |                   | -1.82           | Geisler et al. (1995)       |
|  |                   | -1.91           | Salaris and Cassisi (1996)  |
|  |                   | -1.71           | Carretta and Gratton (1997) |
|  |                   | -1.93 to -1.83  | Kraft and Ivans (2003)      |
|  |                   | -1.90           | Pritzl et al. (2005)        |
|  |                   | -1.96           | Carretta et al. (2009a)     |
|  |                   | -1.74           | Carrera et al. (2013)       |
|  |                   | -1.95           | Roediger et al. (2014)      |

\* this value was computed with the values of  $\frac{A_B}{A_V} = 1.32616$  and  $\frac{A_v}{A_V} = 1.00096$ , with a final value of  $A_v = 0.56 \pm 0.176$  which was obtained as the mean of the differential reddening in our best fit

# Bibliography

Ahumada, R., Allende Prieto, C., Almeida, A., Anders, F., Anderson, S. F., Andrews, B. H., Anguiano, B., Arcodia, R., Armengaud, E., Aubert, M., Avila, S., Avila-Reese, V., Badenes, C., Balland , C., Barger, K., Barrera-Ballesteros, J. K., Basu, S., Bautista, J., Beaton, R. L., Beers, T. C., Benavides, B. I. T., Bender, C. F., Bernardi, M., Bershadsky, M., Beutler, F., Bidin, C. M., Bird, J., Bizyaev, D., Blanc, G. A., Blanton, M. R., Boquien, M., Borissova, J., Bovy, J., Brand t, W. N., Brinkmann, J., Brownstein, J. R., Bundy, K., Bureau, M., Burgasser, A., Burtin, E., Cano-Díaz, M., Capasso, R., Cappellari, M., Carrera, R., Chabanier, S., Chaplin, W., Chapman, M., Cherinka, B., Chiappini, C., Doohyun Choi, P., Chojnowski, S. D., Chung, H., Clerc, N., Coffey, D., Comerford, J. M., Comparat, J., da Costa, L., Cousinou, M.-C., Covey, K., Crane, J. D., Cunha, K., da Silva Ilha, G., Dai, Y. S., Damsted, S. B., Darling, J., Davidson, James W., J., Davies, R., Dawson, K., De, N., de la Macorra, A., De Lee, N., de Andrade Queiroz, A. B., Deconto Machado, A., de la Torre, S., Dell'Agli, F., du Mas des Bourboux, H., Diamond-Stanic, A. M., Dillon, S., Donor, J., Drory, N., Duckworth, C., Dwelly, T., Ebelke, G., Eftekharzadeh, S., Eigenbrot, A. D., Elsworth, Y. P., Eracleous, M., Erfanianfar, G., Escoffier, S., Fan, X., Farr, E., Fernández-Trincado, J. G., Feuillet, D., Finoguenov, A., Fofie, P., Fraser-McKelvie, A., Frinchaboy, P. M., Fromenteau, S., Fu, H., Galbany, L., Garcia, R. A., García-Hernández, D. A., Garma Oehmichen, L. A., Ge, J., Geimba Maia, M. A., Geisler, D., Gelfand , J., Goddy, J., Gonzalez-Perez, V., Grabowski, K., Green, P., Grier, C. J., Guo, H., Guy, J., Harding, P., Hasselquist, S., Hawken, A. J., Hayes, C. R., Hearty, F., Hekker, S., Hogg, D. W., Holtzman, J. A., Horta, D., Hou, J., Hsieh, B.-C., Huber, D., Hunt, J. A. S., Ider Chitham, J., Imig, J., Jaber, M., Jimenez Angel, C. E., Johnson, J. A., Jones, A. M., Jönsson, H., Jullo, E., Kim, Y., Kinemuchi, K., Kirkpatrick, Charles C., I., Kite, G. W., Klaene, M., Kneib, J.-P., Kollmeier, J. A., Kong, H., Kounkel, M., Krishnarao, D., Lacerna, I., Lan, T.-W., Lane, R. R., Law, D. R., Le Goff, J.-M., Leung, H. W., Lewis, H., Li, C., Lian, J., Lin, L., Long, D., Longa-Peña, P., Lundgren, B., Lyke, B. W., Ted Mackereth, J., MacLeod, C. L., Majewski, S. R., Manchado, A., Maraston, C., Martini, P., Masseron, T., Masters, K. L., Mathur, S., McDermid, R. M., Merloni, A., Merrifield, M., Mészáros, S., Miglio, A., Minniti, D., Minsley, R., Miyaji, T., Mohammad, F. G., Mosser, B., Mueller, E.-M., Muna, D., Muñoz-Gutiérrez, A., Myers, A. D., Nadathur, S., Nair, P., Nandra, K., do Nascimento, J. C., Nevin, R. J.,

- Newman, J. A., Nidever, D. L., Nitschelm, C., Noterdaeme, P., O'Connell, J. E., Olmstead, M. D., Oravetz, D., Oravetz, A., Osorio, Y., Pace, Z. J., Padilla, N., Palanque-Delabrouille, N., Palicio, P. A., Pan, H.-A., Pan, K., Parker, J., Paviot, R., Peirani, S., Peña Ramírez, K., Penny, S., Percival, W. J., Perez-Fournon, I., Pérez-Ràfols, I., Petitjean, P., Pieri, M. M., Pinsonneault, M., Poovelil, V. J., Povick, J. T., Prakash, A., Price-Whelan, A. M., Raddick, M. J., Raichoor, A., Ray, A., Rembold, S. B., Rezaie, M., Riffel, R. A., Riffel, R., Rix, H.-W., Robin, A. C., Roman-Lopes, A., Román-Zúñiga, C., Rose, B., Ross, A. J., Rossi, G., Rowland s, K., Rubin, K. H. R., Salvato, M., Sánchez, A. G., Sánchez-Menguiano, L., Sánchez-Gallego, J. R., Sayres, C., Schaefer, A., Schiavon, R. P., Schimoia, J. S., Schlafly, E., Schlegel, D., Schneider, D. P., Schultheis, M., Schwone, A., Seo, H.-J., Serenelli, A., Shafieloo, A., Shamsi, S. J., Shao, Z., Shen, S., Shetrone, M., Shirley, R., Silva Aguirre, V., Simon, J. D., Skrutskie, M. F., Slosar, A., Smethurst, R., Sobeck, J., Sodi, B. C., Souto, D., Stark, D. V., Stassun, K. G., Steinmetz, M., Stello, D., Stermer, J., Storchi-Bergmann, T., Streblyanska, A., Stringfellow, G. S., Stutz, A., Suárez, G., Sun, J., Taghizadeh-Popp, M., Talbot, M. S., Tayar, J., Thakar, A. R., Theriault, R., Thomas, D., Thomas, Z. C., Tinker, J., Tojeiro, R., Toledo, H. H., Tremonti, C. A., Troup, N. W., Tuttle, S., Unda-Sanzana, E., Valentini, M., Vargas-González, J., Vargas-Magaña, M., Vázquez-Mata, J. A., Vivek, M., Wake, D., Wang, Y., Weaver, B. A., Weijmans, A.-M., Wild, V., Wilson, J. C., Wilson, R. F., Wolthuis, N., Wood-Vasey, W. M., Yan, R., Yang, M., Yèche, C., Zamora, O., Zarrouk, P., Zasowski, G., Zhang, K., Zhao, C., Zhao, G., Zheng, Z., Zheng, Z., Zhu, G., and Zou, H. (2020). The 16th Data Release of the Sloan Digital Sky Surveys: First Release from the APOGEE-2 Southern Survey and Full Release of eBOSS Spectra. *Astrophysical Journal, Supplement*, 249(1):3.
- Antoja, T., Ramos, P., Mateu, C., Helmi, A., Anders, F., Jordi, C., and Carballo-Bello, J. A. (2020). An all-sky proper-motion map of the Sagittarius stream using Gaia DR2. *Astronomy and Astrophysics*, 635:L3.
- Asplund, M., Amarsi, A. M., and Grevesse, N. (2021). The chemical make-up of the Sun: A 2020 vision. *Astronomy and Astrophysics*, 653:A141.
- Baeza, I., Fernández-Trincado, J. G., Villanova, S., Geisler, D., Minniti, D., Garro, E. R., Barbuy, B., Beers, T. C., and Lane, R. R. (2022). APOGEE-2S Mg-Al anti-correlation of the metal-poor globular cluster NGC 2298. *Astronomy and Astrophysics*, 662:A47.
- Balbinot, E., Santiago, B. X., da Costa, L. N., Makler, M., and Maia, M. A. G. (2011). The tidal tails of NGC 2298. *Monthly Notices of the Royal Astronomical Society*, 416(1):393–402.
- Baldry, I. K., Viskum, M., Bedding, T. R., Kjeldsen, H., and Frandsen, S. (1999). Spectroscopy of the roAp star alpha CIR – II. The bisector and equivalent width of the H $\alpha$  line. *Monthly Notices of the Royal Astronomical Society*, 302(2):381–390.

- Bastian, N., Covey, K. R., and Meyer, M. R. (2010). A Universal Stellar Initial Mass Function? A Critical Look at Variations. *Annual Review of Astronomy and Astrophysics*, 48:339–389.
- Bastian, N., Lamers, H. J. G. L. M., de Mink, S. E., Longmore, S. N., Goodwin, S. P., and Gieles, M. (2013). Early disc accretion as the origin of abundance anomalies in globular clusters. *Monthly Notices of the Royal Astronomical Society*, 436(3):2398–2411.
- Bastian, N. and Lardo, C. (2018). Multiple Stellar Populations in Globular Clusters. *Annual Review of Astronomy and Astrophysics*, 56:83–136.
- Baumgardt, H., Hilker, M., Sollima, A., and Bellini, A. (2019). Mean proper motions, space orbits, and velocity dispersion profiles of Galactic globular clusters derived from Gaia DR2 data. *Monthly Notices of the Royal Astronomical Society*, 482(4):5138–5155.
- Baumgardt, H. and Vasiliev, E. (2021). Accurate distances to Galactic globular clusters through a combination of Gaia EDR3, HST, and literature data. *Monthly Notices of the Royal Astronomical Society*, 505(4):5957–5977.
- Beaton, R. L., Oelkers, R. J., Hayes, C. R., Saito, R. K., Hempel, M., Pietrukowicz, P., Ahumada, A. V., Alonso, M. V., Alonso-Garcia, J., Arias, J. I., Bandyopadhyay, R. M., Barbá, R. H., Barbuy, B., Bedin, L. R., Bica, E., Borissova, J., Bronfman, L., Carraro, G., Catelan, M., Clariá, J. J., Cross, N., de Grijs, R., Dékány, I., Drew, J. E., Fariña, C., Feinstein, C., Fernández Lajús, E., Gamen, R. C., Geisler, D., Gieren, W., Goldman, B., Gonzalez, O. A., Gunthardt, G., Gurovich, S., Hambly, N. C., Irwin, M. J., Ivanov, V. D., Jordán, A., Kerins, E., Kinemuchi, K., Kurtev, R., López-Corredoira, M., Maccarone, T., Masetti, N., Merlo, D., Messineo, M., Mirabel, I. F., Monaco, L., Morelli, L., Padilla, N., Palma, T., Parisi, M. C., Pignata, G., Rejkuba, M., Roman-Lopes, A., Sale, S. E., Schreiber, M. R., Schröder, A. C., Smith, M., L. Sodré, J., Soto, M., Tamura, M., Tappert, C., Thompson, M. A., Toledo, I., Zoccali, M., and Pietrzynski, G. (2021). . *The Astrophysical Journal*, in preparation.
- Bekki, K. (2017a). Globular cluster formation with multiple stellar populations from hierarchical star cluster complexes. *Monthly Notices of the Royal Astronomical Society*, 467(2):1857–1873.
- Bekki, K. (2017b). Globular cluster formation with multiple stellar populations: self-enrichment in fractal massive molecular clouds. *Monthly Notices of the Royal Astronomical Society*, 469(3):2933–2951.
- Bekki, K., Jeřábková, T., and Kroupa, P. (2017). The origin of discrete multiple stellar populations in globular clusters. *Monthly Notices of the Royal Astronomical Society*, 471(2):2242–2253.
- Belokurov, V., Erkal, D., Evans, N. W., Koposov, S. E., and Deason, A. J. (2018). Co-formation of the disc and the stellar halo. *Monthly Notices of the Royal Astronomical Society*, 478(1):611–619.

- Blanton, M. R., Bershady, M. A., Abolfathi, B., Albareti, F. D., Allende Prieto, C., Almeida, A., Alonso-García, J., Anders, F., Anderson, S. F., Andrews, B., Aquino-Ortíz, E., Aragón-Salamanca, A., Argudo-Fernández, M., Armengaud, E., Aubourg, E., Avila-Reese, V., Badenes, C., Bailey, S., Barger, K. A., Barrera-Ballesteros, J., Bartosz, C., Bates, D., Baumgarten, F., Bautista, J., Beaton, R., Beers, T. C., Belfiore, F., Bender, C. F., Berlind, A. A., Bernardi, M., Beutler, F., Bird, J. C., Bizyaev, D., Blanc, G. A., Blomqvist, M., Bolton, A. S., Boquien, M., Borissova, J., van den Bosch, R., Bovy, J., Brandt, W. N., Brinkmann, J., Brownstein, J. R., Bundy, K., Burgasser, A. J., Burtin, E., Busca, N. G., Cappellari, M., Delgado Carigi, M. L., Carlberg, J. K., Carnero Rosell, A., Carrera, R., Chanover, N. J., Cherinka, B., Cheung, E., Gómez Maqueo Chew, Y., Chiappini, C., Choi, P. D., Chojnowski, D., Chuang, C.-H., Chung, H., Cirolini, R. F., Clerc, N., Cohen, R. E., Comparat, J., da Costa, L., Cousinou, M.-C., Covey, K., Crane, J. D., Croft, R. A. C., Cruz-Gonzalez, I., Garrido Cuadra, D., Cunha, K., Damke, G. J., Darling, J., Davies, R., Dawson, K., de la Macorra, A., Dell'Agli, F., De Lee, N., Delubac, T., Di Mille, F., Diamond-Stanic, A., Cano-Díaz, M., Donor, J., Downes, J. J., Drory, N., du Mas des Bourboux, H., Duckworth, C. J., Dwelly, T., Dyer, J., Ebelke, G., Eigenbrot, A. D., Eisenstein, D. J., Emsellem, E., Eracleous, M., Escoffier, S., Evans, M. L., Fan, X., Fernández-Alvar, E., Fernandez-Trincado, J. G., Feuillet, D. K., Finoguenov, A., Fleming, S. W., Font-Ribera, A., Fredrickson, A., Freischlad, G., Frinchaboy, P. M., Fuentes, C. E., Galbany, L., Garcia-Dias, R., García-Hernández, D. A., Gaulme, P., Geisler, D., Gelfand, J. D., Gil-Marín, H., Gillespie, B. A., Goddard, D., Gonzalez-Perez, V., Grabowski, K., Green, P. J., Grier, C. J., Gunn, J. E., Guo, H., Guy, J., Hagen, A., Hahn, C., Hall, M., Harding, P., Hasselquist, S., Hawley, S. L., Hearty, F., Gonzalez Hernández, J. I., Ho, S., Hogg, D. W., Holley-Bockelmann, K., Holtzman, J. A., Holzer, P. H., Huehnerhoff, J., Hutchinson, T. A., Hwang, H. S., Ibarra-Medel, H. J., da Silva Ilha, G., Ivans, I. I., Ivory, K., Jackson, K., Jensen, T. W., Johnson, J. A., Jones, A., Jönsson, H., Jullo, E., Kamble, V., Kinemuchi, K., Kirkby, D., Kitaura, F.-S., Klaene, M., Knapp, G. R., Kneib, J.-P., Kollmeier, J. A., Lacerna, I., Lane, R. R., Lang, D., Law, D. R., Lazarz, D., Lee, Y., Le Goff, J.-M., Liang, F.-H., Li, C., Li, H., Lian, J., Lima, M., Lin, L., Lin, Y.-T., Bertran de Lis, S., Liu, C., de Icaza Lizaola, M. A. C., Long, D., Lucatello, S., Lundgren, B., MacDonald, N. K., Deconto Machado, A., MacLeod, C. L., Mahadevan, S., Geimba Maia, M. A., Maiolino, R., Majewski, S. R., Malanushenko, E., Malanushenko, V., Manchado, A., Mao, S., Maraston, C., Marques-Chaves, R., Masseron, T., Masters, K. L., McBride, C. K., McDermid, R. M., McGrath, B., McGreer, I. D., Medina Peña, N., Melendez, M., Merloni, A., Merrifield, M. R., Meszaros, S., Meza, A., Minchev, I., Minniti, D., Miyaji, T., More, S., Mulchaey, J., Müller-Sánchez, F., Muna, D., Munoz, R. R., Myers, A. D., Nair, P., Nandra, K., Correa do Nascimento, J., Negrete, A., Ness, M., Newman, J. A., Nichol, R. C., Nidever, D. L., Nitschelm, C., Ntelis, P., O'Connell, J. E., Oelkers, R. J., Oravetz, A., Oravetz, D., Pace, Z., Padilla, N., Palanque-Delabrouille, N., Alonso Palicio, P., Pan, K., Parejko, J. K., Parikh, T., Pâris, I., Park, C.,

- Patten, A. Y., Peirani, S., Pellejero-Ibanez, M., Penny, S., Percival, W. J., Perez-Fournon, I., Petitjean, P., Pieri, M. M., Pinsonneault, M., Pisani, A., Poleski, R., Prada, F., Prakash, A., Queiroz, A. B. d. A., Raddick, M. J., Raichoor, A., Barboza Rembold, S. r., Richstein, H., Riffel, R. A., Riffel, R., Rix, H.-W., Robin, A. C., Rockosi, C. M., Rodríguez-Torres, S., Roman-Lopes, A., Román-Zúñiga, C., Rosado, M., Ross, A. J., Rossi, G., Ruan, J., Ruggeri, R., Rykoff, E. S., Salazar-Albornoz, S., Salvato, M., Sánchez, A. G., Aguado, D. S., Sánchez-Gallego, J. R., Santana, F. A., Santiago, B. X., Sayres, C., Schiavon, R. P., da Silva Schimoia, J., Schlafly, E. F., Schlegel, D. J., Schneider, D. P., Schultheis, M., Schuster, W. J., Schwone, A., Seo, H.-J., Shao, Z., Shen, S., Shetrone, M., Shull, M., Simon, J. D., Skinner, D., Skrutskie, M. F., Slosar, A., Smith, V. V., Sobeck, J. S., Sobreira, F., Somers, G., Souto, D., Stark, D. V., Stassun, K., Stauffer, F., Steinmetz, M., Storchi-Bergmann, T., Streblyanska, A., Stringfellow, G. S., Suárez, G., Sun, J., Suzuki, N., Szigeti, L., Taghizadeh-Popp, M., Tang, B., Tao, C., Tayar, J., Tembe, M., Teske, J., Thakar, A. R., Thomas, D., Thompson, B. A., Tinker, J. L., Tissera, P., Tojeiro, R., Hernandez Toledo, H., de la Torre, S., Tremonti, C., Troup, N. W., Valenzuela, O., Martinez Valpuesta, I., Vargas-González, J., Vargas-Magaña, M., Vazquez, J. A., Villanova, S., Vivek, M., Vogt, N., Wake, D., Walterbos, R., Wang, Y., Weaver, B. A., Weijmans, A.-M., Weinberg, D. H., Westfall, K. B., Whelan, D. G., Wild, V., Wilson, J., Wood-Vasey, W. M., Wylezalek, D., Xiao, T., Yan, R., Yang, M., Ybarra, J. E., Yèche, C., Zakamska, N., Zamora, O., Zarrouk, P., Zasowski, G., Zhang, K., Zhao, G.-B., Zheng, Z., Zheng, Z., Zhou, X., Zhou, Z.-M., Zhu, G. B., Zoccali, M., and Zou, H. (2017). Sloan Digital Sky Survey IV: Mapping the Milky Way, Nearby Galaxies, and the Distant Universe. *Astronomical Journal*, 154(1):28.
- Boeltzig, A., Bruno, C. G., Cavanna, F., Cristallo, S., Davinson, T., Depalo, R., deBoer, R. J., Di Leva, A., Ferraro, F., Imbriani, G., Marigo, P., Terrasi, F., and Wiescher, M. (2016). Shell and explosive hydrogen burning. Nuclear reaction rates for hydrogen burning in RGB, AGB and Novae. *European Physical Journal A*, 52(4):75.
- Borb, C. B.-S. . (Retrieved 11 Apr 2006). *Triple-Alpha\_Process.svg*, via Wikimedia Commons. [https://commons.wikimedia.org/wiki/File:Triple-Alpha\\_Process.svg](https://commons.wikimedia.org/wiki/File:Triple-Alpha_Process.svg), No machine-readable author provided. Borb assumed (based on copyright claims).
- Bowen, I. S. and Vaughan, A. H., J. (1973). The optical design of the 40-in. telescope and of the Irénée DuPont telescope at Las Campanas Observatory, Chile. *Applied Optics*, 12:1430–1434.
- Bressan, A., Marigo, P., Girardi, L., Salasnich, B., Dal Cero, C., Rubele, S., and Nanni, A. (2012). PARSEC: stellar tracks and isochrones with the PAdova and TRieste Stellar Evolution Code. *Monthly Notices of the Royal Astronomical Society*, 427:127–145.
- Britannica, T. E. o. E. (2014). *globular cluster*. Encyclopedia Britannica.

- Bruzual A., G. (2010). Star clusters as simple stellar populations. *Philosophical Transactions of the Royal Society of London Series A*, 368(1913):783–799.
- Carballo-Bello, J. A., Martínez-Delgado, D., Navarrete, C., Catelan, M., Muñoz, R. R., Antoja, T., and Sollima, A. (2018). Tails and streams around the Galactic globular clusters NGC 1851, NGC 1904, NGC 2298 and NGC 2808. *Monthly Notices of the Royal Astronomical Society*, 474(1):683–695.
- Carrera, R., Pancino, E., Gallart, C., and del Pino, A. (2013). The near-infrared Ca II triplet as a metallicity indicator - II. Extension to extremely metal-poor metallicity regimes. *Monthly Notices of the Royal Astronomical Society*, 434(2):1681–1691.
- Carretta, E. and Bragaglia, A. (2021). Excess of Ca (and Sc) produced in globular cluster multiple populations: a first census in 77 Galactic globular clusters. *Astronomy and Astrophysics*, 646:A9.
- Carretta, E., Bragaglia, A., Gratton, R., D’Orazi, V., and Lucatello, S. (2009a). Intrinsic iron spread and a new metallicity scale for globular clusters. *Astronomy and Astrophysics*, 508(2):695–706.
- Carretta, E., Bragaglia, A., Gratton, R., and Lucatello, S. (2009b). Na-O anticorrelation and HB. VIII. Proton-capture elements and metallicities in 17 globular clusters from UVES spectra. *Astronomy and Astrophysics*, 505(1):139–155.
- Carretta, E., Bragaglia, A., Gratton, R. G., Recio-Blanco, A., Lucatello, S., D’Orazi, V., and Cassisi, S. (2010). Properties of stellar generations in globular clusters and relations with global parameters. *Astronomy and Astrophysics*, 516:A55.
- Carretta, E. and Gratton, R. G. (1997). Abundances for globular cluster giants. I. Homogeneous metallicities for 24 clusters. *Astronomy and Astrophysics, Supplement*, 121:95–112.
- Carroll, B. W. and Ostlie, D. A. (2006). *An introduction to modern astrophysics and cosmology*. Pearson Education Limited 2014.
- Cassisi, S. and Salaris, M. (2014). The main sequences of NGC 2808: constraints on the early disc accretion scenario. *Astronomy and Astrophysics*, 563:A10.
- Çakmak, H. and Karataş, Y. (2022). A dynamical evolution study of the open clusters: Berkeley 10, Berkeley 81, Berkeley 89 and Ruprecht 135. *na*, 96:101833.
- Chantereau, W., Charbonnel, C., and Meynet, G. (2016). Evolution of long-lived globular cluster stars. III. Effect of the initial helium spread on the position of stars in a synthetic Hertzsprung-Russell diagram. *Astronomy and Astrophysics*, 592:A111.
- Cohen, J. G. (1983). Abundances in globular cluster red giants. V. The metal-rich globular clusters. *The Astrophysical Journal*, 270:654–665.

- COSMOS (retrieved 2022). *Thermal Doppler Broadening* , *thermalbroadening.jpg*. Swinburne University of Technology <https://astronomy.swin.edu.au/cosmos/T/Thermal+Doppler+Broadening>.
- Crane, J. D., Majewski, S. R., Rocha-Pinto, H. J., Frinchaboy, P. M., Skrutskie, M. F., and Law, D. R. (2003). Exploring Halo Substructure with Giant Stars: Spectroscopy of Stars in the Galactic Anticenter Stellar Structure. *Astrophysical Journal, Letters*, 594(2):L119–L122.
- Cunha, K., Smith, V. V., Hasselquist, S., Souto, D., Shetrone, M. D., Allende Prieto, C., Bizyaev, D., Frinchaboy, P., García-Hernández, D. A., Holtzman, J., Johnson, J. A., Jónsson, H., Majewski, S. R., Mészáros, S., Nidever, D., Pinsonneault, M., Schiavon, R. P., Sobeck, J., Skrutskie, M. F., Zamora, O., Zasowski, G., and Fernández-Trincado, J. G. (2017). Adding the s-Process Element Cerium to the APOGEE Survey: Identification and Characterization of Ce II Lines in the H-band Spectral Window. *The Astrophysical Journal*, 844(2):145.
- Dalessandro, E., Schiavon, R. P., Rood, R. T., Ferraro, F. R., Sohn, S. T., Lanzoni, B., and O’Connell, R. W. (2012). Ultraviolet Properties of Galactic Globular Clusters with Galex. II. Integrated Colors. *Astronomical Journal*, 144(5):126.
- Dall, T. H., Santos, N. C., Arentoft, T., Bedding, T. R., and Kjeldsen, H. (2006). Bisectors of the cross-correlation function applied to stellar spectra. Discriminating stellar activity, oscillations and planets. *Astronomy and Astrophysics*, 454(1):341–348.
- de Mink, S. E., Pols, O. R., Langer, N., and Izzard, R. G. (2009). Massive binaries as the source of abundance anomalies in globular clusters. *Astronomy and Astrophysics*, 507(1):L1–L4.
- Decressin, T., Charbonnel, C., and Meynet, G. (2007a). Origin of the abundance patterns in Galactic globular clusters: constraints on dynamical and chemical properties of globular clusters. *Astronomy and Astrophysics*, 475(3):859–873.
- Decressin, T., Meynet, G., Charbonnel, C., Prantzos, N., and Ekström, S. (2007b). Fast rotating massive stars and the origin of the abundance patterns in galactic globular clusters. *Astronomy and Astrophysics*, 464(3):1029–1044.
- D’Ercole, A., D’Antona, F., and Vesperini, E. (2016). Accretion of pristine gas and dilution during the formation of multiple-population globular clusters. *Monthly Notices of the Royal Astronomical Society*, 461(4):4088–4098.
- D’Ercole, A., Vesperini, E., D’Antona, F., McMillan, S. L. W., and Recchi, S. (2008). Formation and dynamical evolution of multiple stellar generations in globular clusters. *Monthly Notices of the Royal Astronomical Society*, 391(2):825–843.
- Doctor C, C. B.-S. . (Retrieved 22 May 2016). *Proton-proton\_reaction\_chain.svg*

- , via Wikimedia Commons. [https://commons.wikimedia.org/wiki/File:Proton-proton\\_reaction\\_chain.svg](https://commons.wikimedia.org/wiki/File:Proton-proton_reaction_chain.svg).
- Dondoglio, E., Milone, A. P., Renzini, A., Vesperini, E., Lagioia, E. P., Marino, A. F., Bellini, A., Carlos, M., Cordoni, G., Jang, S., Legnardi, M. V., Libralato, M., Mohandasan, A., D'Antona, F., Martorano, M., Muratore, F., and Tailo, M. (2022). Survey of Multiple Populations in Globular Clusters among Very-low-mass Stars. *The Astrophysical Journal*, 927(2):207.
- Edlen, B. (1953). The dispersion of standard air. *Journal of the Optical Society of America (1917-1983)*, 43(5):339.
- Eldridge, J. J. (2008). Massive stars in their death throes. *Philosophical Transactions of the Royal Society of London Series A*, 366(1884):4441–4452.
- Fastfission, W. C. (2022). *Binding\_energy\_curve\_-\_common\_isotopes.svg*. [https://commons.wikimedia.org/wiki/File:Binding\\_energy\\_curve\\_-\\_common\\_isotopes.svg#file](https://commons.wikimedia.org/wiki/File:Binding_energy_curve_-_common_isotopes.svg#file).
- Fernández-Trincado, J. G., Beers, T. C., and Minniti, D. (2020a). Jurassic: A chemically anomalous structure in the Galactic halo. *Astronomy and Astrophysics*, 644:A83.
- Fernández-Trincado, J. G., Beers, T. C., Minniti, D., Carigi, L., Barbuy, B., Placco, V. M., Moni Bidin, C., Villanova, S., Roman-Lopes, A., and Nitschelm, C. (2020b). Discovery of a Large Population of Nitrogen-enhanced Stars in the Magellanic Clouds. *Astrophysical Journal, Letters*, 903(1):L17.
- Fernández-Trincado, J. G., Beers, T. C., Minniti, D., Carigi, L., Placco, V. M., Chun, S.-H., Lane, R. R., Geisler, D., Villanova, S., Souza, S. O., Barbuy, B., Pérez-Villegas, A., Chiappini, C., Queiroz, A. B. A., Tang, B., Alonso-García, J., Piatti, A. E., Palma, T., Alves-Brito, A., Moni Bidin, C., Roman-Lopes, A., Muñoz, R. R., Singh, H. P., Kundu, R., Chaves-Velasquez, L., Romero-Colmenares, M., Longa-Peña, P., Soto, M., and Vieira, K. (2021a). APOGEE discovery of a chemically atypical star disrupted from NGC 6723 and captured by the Milky Way bulge. *Astronomy and Astrophysics*, 647:A64.
- Fernández-Trincado, J. G., Beers, T. C., Minniti, D., Moni Bidin, C., Barbuy, B., Villanova, S., Geisler, D., Lane, R. R., Roman-Lopes, A., and Bizyaev, D. (2021b). APOGEE spectroscopic evidence for chemical anomalies in dwarf galaxies: The case of M 54 and Sagittarius. *Astronomy and Astrophysics*, 648:A70.
- Fernández-Trincado, J. G., Beers, T. C., Minniti, D., Tang, B., Villanova, S., Geisler, D., Pérez-Villegas, A., and Vieira, K. (2020c). Aluminium-enriched metal-poor stars buried in the inner Galaxy. *Astronomy and Astrophysics*, 643:L4.
- Fernández-Trincado, J. G., Beers, T. C., Minniti, D., Tang, B., Villanova, S., Geisler, D., Pérez-Villegas, A., and Vieira, K. (2020d). Aluminium-enriched

- metal-poor stars buried in the inner Galaxy. *Astronomy and Astrophysics*, 643:L4.
- Fernández-Trincado, J. G., Beers, T. C., Placco, V. M., Moreno, E., Alves-Brito, A., Minniti, D., Tang, B., Pérez-Villegas, A., Reylé, C., Robin, A. C., and Villanova, S. (2019a). Discovery of a New Stellar Subpopulation Residing in the (Inner) Stellar Halo of the Milky Way. *Astrophysical Journal Letters*, 886(1):L8.
- Fernández-Trincado, J. G., Beers, T. C., Tang, B., Moreno, E., Pérez-Villegas, A., and Ortigoza-Urdaneta, M. (2019b). Chemodynamics of newly identified giants with a globular cluster like abundance patterns in the bulge, disc, and halo of the Milky Way. *Monthly Notices of the Royal Astronomical Society*, 488(2):2864–2880.
- Fernández-Trincado, J. G., Chaves-Velasquez, L., Pérez-Villegas, A., Vieira, K., Moreno, E., Ortigoza-Urdaneta, M., and Vega-Neme, L. (2020e). Dynamical orbital classification of selected N-rich stars with Gaia Data Release 2 astrometry. *Monthly Notices of the Royal Astronomical Society*, 495(4):4113–4123.
- Fernández-Trincado, J. G., Robin, A. C., Moreno, E., Schiavon, R. P., García Pérez, A. E., Vieira, K., Cunha, K., Zamora, O., Sneden, C., Souto, D., Carrera, R., Johnson, J. A., Shetrone, M., Zasowski, G., García-Hernández, D. A., Majewski, S. R., Reylé, C., Blanco-Cuaresma, S., Martinez-Medina, L. A., Pérez-Villegas, A., Valenzuela, O., Pichardo, B., Meza, A., Mészáros, S., Sobeck, J., Geisler, D., Anders, F., Schultheis, M., Tang, B., Roman-Lopes, A., Mennickent, R. E., Pan, K., Nitschelm, C., and Allard, F. (2016). Discovery of a Metal-poor Field Giant with a Globular Cluster Second-generation Abundance Pattern. *The Astrophysical Journal*, 833(2):132.
- Fernández-Trincado, J. G., Zamora, O., García-Hernández, D. A., Souto, D., Dell’Agli, F., Schiavon, R. P., Geisler, D., Tang, B., Villanova, S., Hasselquist, S., Mennickent, R. E., Cunha, K., Shetrone, M., Allende Prieto, C., Vieira, K., Zasowski, G., Sobeck, J., Hayes, C. R., Majewski, S. R., Placco, V. M., Beers, T. C., Schleicher, D. R. G., Robin, A. C., Mészáros, S., Masseron, T., García Pérez, A. E., Anders, F., Meza, A., Alves-Brito, A., Carrera, R., Minniti, D., Lane, R. R., Fernández-Alvar, E., Moreno, E., Pichardo, B., Pérez-Villegas, A., Schultheis, M., Roman-Lopes, A., Fuentes, C. E., Nitschelm, C., Harding, P., Bizyaev, D., Pan, K., Oravetz, D., Simmons, A., Ivans, I. I., Blanco-Cuaresma, S., Hernández, J., Alonso-García, J., Valenzuela, O., and Chanamé, J. (2017). Atypical Mg-poor Milky Way Field Stars with Globular Cluster Second-generation-like Chemical Patterns. *Astrophysical Journal Letters*, 846(1):L2.
- Fernández-Trincado, J. G., Zamora, O., Souto, D., Cohen, R. E., Dell’Agli, F., García-Hernández, D. A., Masseron, T., Schiavon, R. P., Mészáros, S., Cunha, K., Hasselquist, S., Shetrone, M., Schiappacasse Ulloa, J., Tang, B., Geisler, D., Schleicher, D. R. G., Villanova, S., Mennickent, R. E., Minniti, D., Alonso-García, J., Manchado, A., Beers, T. C., Sobeck, J., Zasowski, G., Schultheis, M., Majewski, S. R., Rojas-Arriagada, A., Almeida, A., Santana, F., Oelkers,

- R. J., Longa-Peña, P., Carrera, R., Burgasser, A. J., Lane, R. R., Roman-Lopes, A., Ivans, I. I., and Hearty, F. R. (2019c). H-band discovery of additional second-generation stars in the Galactic bulge globular cluster NGC 6522 as observed by APOGEE and Gaia. *Astronomy and Astrophysics*, 627:A178.
- Forbes, D. A. and Bridges, T. (2010). Accreted versus in situ Milky Way globular clusters. *Monthly Notices of the Royal Astronomical Society*, 404(3):1203–1214.
- Frelijj Rubilar, H. E. (2017). *Searching for multiple populations in NGC 7099 using Washington Photometry*. PhD thesis, Universidad de Concepción.
- Frogel, J. A., Cohen, J. G., and Persson, S. E. (1983). Globular cluster giant branches and the metallicity scale. *The Astrophysical Journal*, 275:773–789.
- Gaia Collaboration, Brown, A. G. A., Vallenari, A., Prusti, T., de Bruijne, J. H. J., Babusiaux, C., Bailer-Jones, C. A. L., Biermann, M., Evans, D. W., Eyer, L., Jansen, F., Jordi, C., Klioner, S. A., Lammers, U., Lindegren, L., Luri, X., Mignard, F., Panem, C., Pourbaix, D., Randich, S., Sartoretti, P., Siddiqui, H. I., Soubiran, C., van Leeuwen, F., Walton, N. A., Arenou, F., Bastian, U., Cropper, M., Drimmel, R., Katz, D., Lattanzi, M. G., Bakker, J., Cacciari, C., Castañeda, J., Chaoul, L., Cheek, N., De Angeli, F., Fabricius, C., Guerra, R., Holl, B., Masana, E., Messineo, R., Mowlavi, N., Nienartowicz, K., Panuzzo, P., Portell, J., Riello, M., Seabroke, G. M., Tanga, P., Thévenin, F., Gracia-Abril, G., Comoretto, G., Garcia-Reinaldos, M., Teyssier, D., Altmann, M., Andrae, R., Audard, M., Bellas-Velidis, I., Benson, K., Berthier, J., Blomme, R., Burgess, P., Busso, G., Carry, B., Cellino, A., Clementini, G., Clotet, M., Creevey, O., Davidson, M., De Ridder, J., Delchambre, L., Dell’Oro, A., Ducourant, C., Fernández-Hernández, J., Fouesneau, M., Frémat, Y., Galluccio, L., García-Torres, M., González-Núñez, J., González-Vidal, J. J., Gosset, E., Guy, L. P., Halbwachs, J. L., Hambly, N. C., Harrison, D. L., Hernández, J., Hestroffer, D., Hodgkin, S. T., Hutton, A., Jasniewicz, G., Jean-Antoine-Piccolo, A., Jordan, S., Korn, A. J., Krone-Martins, A., Lanzafame, A. C., Lebzelter, T., Löffler, W., Manteiga, M., Marrese, P. M., Martín-Fleitas, J. M., Moitinho, A., Mora, A., Muinonen, K., Osinde, J., Pancino, E., Pauwels, T., Petit, J. M., Recio-Blanco, A., Richards, P. J., Rimoldini, L., Robin, A. C., Sarro, L. M., Siopis, C., Smith, M., Sozzetti, A., Süveges, M., Torra, J., van Reeven, W., Abbas, U., Abreu Aramburu, A., Accart, S., Aerts, C., Altavilla, G., Álvarez, M. A., Alvarez, R., Alves, J., Anderson, R. I., Andrei, A. H., Anglada Varela, E., Antiche, E., Antoja, T., Arcay, B., Astraatmadja, T. L., Bach, N., Baker, S. G., Balaguer-Núñez, L., Balm, P., Barache, C., Barata, C., Barbato, D., Barblan, F., Barklem, P. S., Barrado, D., Barros, M., Barstow, M. A., Bartholomé Muñoz, S., Bassilana, J. L., Becciani, U., Bellazzini, M., Berihuete, A., Bertone, S., Bianchi, L., Bienaymé, O., Blanco-Cuaresma, S., Boch, T., Boeche, C., Bombrun, A., Borrachero, R., Bossini, D., Bouquillon, S., Bourda, G., Bragaglia, A., Bramante, L., Breddels, M. A., Bressan, A., Brouillet, N., Brüsemeister, T., Brugaletta, E., Bucciarelli, B., Burlacu, A., Busonero, D., Butkevich, A. G., Buzzi, R., Caffau, E., Cancelliere, R., Cannizzaro, G., Cantat-Gaudin, T., Carballo, R.,

Carlucci, T., Carrasco, J. M., Casamiquela, L., Castellani, M., Castro-Ginard, A., Charlot, P., Chemin, L., Chiavassa, A., Cocozza, G., Costigan, G., Cowell, S., Crifo, F., Crosta, M., Crowley, C., Cuypers, J., Dafonte, C., Damerdji, Y., Dapergolas, A., David, P., David, M., de Laverny, P., De Luise, F., De March, R., de Martino, D., de Souza, R., de Torres, A., Debosscher, J., del Pozo, E., Delbo, M., Delgado, A., Delgado, H. E., Di Matteo, P., Diakite, S., Diener, C., Distefano, E., Dolding, C., Drazinos, P., Durán, J., Edvardsson, B., Enke, H., Eriksson, K., Esquej, P., Eynard Bontemps, G., Fabre, C., Fabrizio, M., Faigler, S., Falcão, A. J., Farràs Casas, M., Federici, L., Fedorets, G., Fernique, P., Figueras, F., Filippi, F., Findeisen, K., Fonti, A., Fraile, E., Fraser, M., Frézouls, B., Gai, M., Galleti, S., Garabato, D., García-Sedano, F., Garofalo, A., Garralda, N., Gavel, A., Gavras, P., Gerssen, J., Geyer, R., Giacobbe, P., Gilmore, G., Girona, S., Giuffrida, G., Glass, F., Gomes, M., Granvik, M., Gueguen, A., Guerrier, A., Guiraud, J., Gutiérrez-Sánchez, R., Haigron, R., Hatzidimitriou, D., Hauser, M., Haywood, M., Heiter, U., Helmi, A., Heu, J., Hilger, T., Hobbs, D., Hofmann, W., Holland, G., Huckle, H. E., Hypki, A., Icardi, V., Janßen, K., Jevardat de Fombelle, G., Jonker, P. G., Juhász, Á. L., Julbe, F., Karampelas, A., Kewley, A., Klar, J., Kochoska, A., Kohley, R., Kolenberg, K., Kontizas, M., Kontizas, E., Koposov, S. E., Kordopatis, G., Kostrzewa-Rutkowska, Z., Koubsky, P., Lambert, S., Lanza, A. F., Lasne, Y., Lavigne, J. B., Le Fustec, Y., Le Poncin-Lafitte, C., Lebreton, Y., Leccia, S., Leclerc, N., Lecoeur-Taibi, I., Lenhardt, H., Leroux, F., Liao, S., Licata, E., Lindstrøm, H. E. P., Lister, T. A., Livanou, E., Lobel, A., López, M., Managau, S., Mann, R. G., Mantelet, G., Marchal, O., Marchant, J. M., Marconi, M., Marinoni, S., Marschalkó, G., Marshall, D. J., Martino, M., Marton, G., Mary, N., Massari, D., Matijević, G., Mazeh, T., McMillan, P. J., Messina, S., Michalik, D., Millar, N. R., Molina, D., Molinaro, R., Molnár, L., Montegriffo, P., Mor, R., Morbidelli, R., Morel, T., Morris, D., Mulone, A. F., Muraveva, T., Musella, I., Nelemans, G., Nicastro, L., Noval, L., O'Mullane, W., Ordénovic, C., Ordóñez-Blanco, D., Osborne, P., Pagani, C., Pagano, I., Pailler, F., Palacin, H., Palaversa, L., Panahi, A., Pawlak, M., Piersimoni, A. M., Pineau, F. X., Plachy, E., Plum, G., Poggio, E., Poujoulet, E., Prša, A., Pulone, L., Racero, E., Ragaini, S., Rambaux, N., Ramos-Lerate, M., Regibo, S., Reylé, C., Riclet, F., Ripepi, V., Riva, A., Rivard, A., Rixon, G., Roegiers, T., Roelens, M., Romero-Gómez, M., Rowell, N., Royer, F., Ruiz-Dern, L., Sadowski, G., Sagristà Sellés, T., Sahlmann, J., Salgado, J., Salguero, E., Sanna, N., Santana-Ros, T., Sarasso, M., Savietto, H., Schultheis, M., Sciacca, E., Segol, M., Segovia, J. C., Ségransan, D., Shih, I. C., Siltala, L., Silva, A. F., Smart, R. L., Smith, K. W., Solano, E., Solitro, F., Sordo, R., Soria Nieto, S., Souchay, J., Spagna, A., Spoto, F., Stampa, U., Steele, I. A., Steidelmüller, H., Stephenson, C. A., Stoev, H., Suess, F. F., Surdej, J., Szabadoss, L., Szegedi-Elek, E., Tapiador, D., Taris, F., Tauran, G., Taylor, M. B., Teixeira, R., Terrett, D., Teyssandier, P., Thuillot, W., Titarenko, A., Torra Clotet, F., Turon, C., Ulla, A., Utrilla, E., Uzzi, S., Vaillant, M., Valentini, G., Valette, V., van Elteren, A., Van Hemelryck, E., van Leeuwen, M., Vaschetto, M., Vecchiato, A., Veljanoski, J., Viala, Y., Vicente, D., Vogt, S.,

- von Essen, C., Voss, H., Votruba, V., Voutsinas, S., Walmsley, G., Weiler, M., Wertz, O., Wevers, T., Wyrzykowski, Ł., Yoldas, A., Žerjal, M., Ziaeepour, H., Zorec, J., Zschocke, S., Zucker, S., Zurbach, C., and Zwitter, T. (2018). Gaia Data Release 2. Summary of the contents and survey properties. *Astronomy and Astrophysics*, 616:A1.
- Gaia Collaboration, Brown, A. G. A., Vallenari, A., Prusti, T., de Bruijne, J. H. J., Babusiaux, C., Biermann, M., Creevey, O. L., Evans, D. W., Eyer, L., Hutton, A., Jansen, F., Jordi, C., Klioner, S. A., Lammers, U., Lindegren, L., Luri, X., Mignard, F., Panem, C., Pourbaix, D., Randich, S., Sartoretti, P., Soubiran, C., Walton, N. A., Arenou, F., Bailer-Jones, C. A. L., Bastian, U., Cropper, M., Drimmel, R., Katz, D., Lattanzi, M. G., van Leeuwen, F., Bakker, J., Cacciari, C., Castañeda, J., De Angeli, F., Ducourant, C., Fabricius, C., Fouesneau, M., Frémat, Y., Guerra, R., Guerrier, A., Guiraud, J., Jean-Antoine Piccolo, A., Masana, E., Messineo, R., Mowlavi, N., Nicolas, C., Nienartowicz, K., Pailler, F., Panuzzo, P., Riclet, F., Roux, W., Seabroke, G. M., Sordo, R., Tanga, P., Thévenin, F., Gracia-Abril, G., Portell, J., Teyssier, D., Altmann, M., Andrae, R., Bellas-Velidis, I., Benson, K., Berthier, J., Blomme, R., Brugaletta, E., Burgess, P. W., Busso, G., Carry, B., Cellino, A., Cheek, N., Clementini, G., Damerdji, Y., Davidson, M., Delchambre, L., Dell’Oro, A., Fernández-Hernández, J., Galluccio, L., García-Lario, P., Garcia-Reinaldos, M., González-Núñez, J., Gosset, E., Haigron, R., Halbwachs, J. L., Hambly, N. C., Harrison, D. L., Hatzidimitriou, D., Heiter, U., Hernández, J., Hestroffer, D., Hodgkin, S. T., Holl, B., Janßen, K., Jevardat de Fombelle, G., Jordan, S., Krone-Martins, A., Lanzafame, A. C., Löffler, W., Lorca, A., Manteiga, M., Marchal, O., Marrese, P. M., Moitinho, A., Mora, A., Muinonen, K., Osborne, P., Pancino, E., Pauwels, T., Petit, J. M., Recio-Blanco, A., Richards, P. J., Riello, M., Rimoldini, L., Robin, A. C., Roegiers, T., Rybizki, J., Sarro, L. M., Siopis, C., Smith, M., Sozzetti, A., Ulla, A., Utrilla, E., van Leeuwen, M., van Reeven, W., Abbas, U., Abreu Aramburu, A., Accart, S., Aerts, C., Aguado, J. J., Ajaj, M., Altavilla, G., Álvarez, M. A., Álvarez Cid-Fuentes, J., Alves, J., Anderson, R. I., Anglada Varela, E., Antoja, T., Audard, M., Baines, D., Baker, S. G., Balaguer-Núñez, L., Balbinot, E., Balog, Z., Barache, C., Barbato, D., Barros, M., Barstow, M. A., Bartolomé, S., Bassilana, J. L., Bauchet, N., Baudesson-Stella, A., Becciani, U., Bellazzini, M., Bernet, M., Bertone, S., Bianchi, L., Blanco-Cuaresma, S., Boch, T., Bombrun, A., Bossini, D., Bouquillon, S., Bragaglia, A., Bramante, L., Breedt, E., Bressan, A., Brouillet, N., Bucciarelli, B., Burlacu, A., Busonero, D., Butkevich, A. G., Buzzi, R., Caffau, E., Cancelliere, R., Cánovas, H., Cantat-Gaudin, T., Carballo, R., Carlucci, T., Carnerero, M. I., Carrasco, J. M., Casamiquela, L., Castellani, M., Castro-Ginard, A., Castro Sampol, P., Chaoul, L., Charlot, P., Chemin, L., Chiavassa, A., Cioni, M. R. L., Comoretto, G., Cooper, W. J., Cornez, T., Cowell, S., Crifo, F., Crosta, M., Crowley, C., Dafonte, C., Dapergolas, A., David, M., David, P., de Laverny, P., De Luise, F., De March, R., De Ridder, J., de Souza, R., de Teodoro, P., de Torres, A., del Peloso, E. F., del Pozo, E., Delbo, M., Delgado, A., Delgado, H. E., Delisle, J. B., Di Matteo, P., Diakite,

S., Diener, C., Distefano, E., Dolding, C., Eappachen, D., Edvardsson, B., Enke, H., Esquej, P., Fabre, C., Fabrizio, M., Faigler, S., Fedorets, G., Fernique, P., Fienga, A., Figueras, F., Fouron, C., Fragkoudi, F., Fraile, E., Franke, F., Gai, M., Garabato, D., Garcia-Gutierrez, A., García-Torres, M., Garofalo, A., Gavras, P., Gerlach, E., Geyer, R., Giacobbe, P., Gilmore, G., Girona, S., Giuffrida, G., Gomel, R., Gomez, A., Gonzalez-Santamaria, I., González-Vidal, J. J., Granvik, M., Gutiérrez-Sánchez, R., Guy, L. P., Hauser, M., Haywood, M., Helmi, A., Hidalgo, S. L., Hilger, T., Hładczuk, N., Hobbs, D., Holland, G., Huckle, H. E., Jasniewicz, G., Jonker, P. G., Juaristi Campillo, J., Julbe, F., Karbevska, L., Kervella, P., Khanna, S., Kochoska, A., Kontizas, M., Kordopatis, G., Korn, A. J., Kostrzewa-Rutkowska, Z., Kruszyńska, K., Lambert, S., Lanza, A. F., Lasne, Y., Le Campion, J. F., Le Fustec, Y., Lebreton, Y., Lebzelter, T., Leccia, S., Leclerc, N., Lecoeur-Taibi, I., Liao, S., Licata, E., Lindstrøm, E. P., Lister, T. A., Livanou, E., Lobel, A., Madrero Pardo, P., Managau, S., Mann, R. G., Marchant, J. M., Marconi, M., Marcos Santos, M. M. S., Marinoni, S., Marocco, F., Marshall, D. J., Martin Polo, L., Martín-Fleitas, J. M., Masip, A., Massari, D., Mastrobuono-Battisti, A., Mazeh, T., McMillan, P. J., Messina, S., Michalik, D., Millar, N. R., Mints, A., Molina, D., Molinaro, R., Molnár, L., Montegriffo, P., Mor, R., Morbidelli, R., Morel, T., Morris, D., Mulone, A. F., Munoz, D., Muraveva, T., Murphy, C. P., Musella, I., Noval, L., Ordénovic, C., Orrù, G., Osinde, J., Pagani, C., Pagano, I., Palaversa, L., Palicio, P. A., Panahi, A., Pawlak, M., Peñalosa Esteller, X., Penttilä, A., Piersimoni, A. M., Pineau, F. X., Plachy, E., Plum, G., Poggio, E., Poretti, E., Poujoulet, E., Prša, A., Pulone, L., Racero, E., Ragaini, S., Rainer, M., Raiteri, C. M., Rambaux, N., Ramos, P., Ramos-Lerate, M., Re Fiorentin, P., Regibo, S., Reylé, C., Ripepi, V., Riva, A., Rixon, G., Robichon, N., Robin, C., Roelens, M., Rohrbasser, L., Romero-Gómez, M., Rowell, N., Royer, F., Rybicki, K. A., Sadowski, G., Sagristà Sellés, A., Sahlmann, J., Salgado, J., Salguero, E., Samaras, N., Sanchez Gimenez, V., Sanna, N., Santoveña, R., Sarasso, M., Schultheis, M., Sciacca, E., Segol, M., Segovia, J. C., Ségransan, D., Semeux, D., Shahaf, S., Siddiqui, H. I., Siebert, A., Siltala, L., Slezak, E., Smart, R. L., Solano, E., Solitro, F., Souami, D., Souchay, J., Spagna, A., Spoto, F., Steele, I. A., Steidelmüller, H., Stephenson, C. A., Süveges, M., Szabados, L., Szegedi-Elek, E., Taris, F., Tauran, G., Taylor, M. B., Teixeira, R., Thuillot, W., Tonello, N., Torra, F., Torra, J., Turon, C., Unger, N., Vaillant, M., van Dillen, E., Vanel, O., Vecchiato, A., Viala, Y., Vicente, D., Voutsinas, S., Weiler, M., Wevers, T., Wyrzykowski, Ł., Yoldas, A., Yvard, P., Zhao, H., Zorec, J., Zucker, S., Zurbach, C., and Zwitter, T. (2021). Gaia Early Data Release 3. Summary of the contents and survey properties. *Astronomy and Astrophysics*, 649:A1.

Gaia Collaboration, Brown, A. G. A., Vallenari, A., Prusti, T., de Bruijne, J. H. J., Mignard, F., Drimmel, R., Babusiaux, C., Bailer-Jones, C. A. L., Bastian, U., Biermann, M., Evans, D. W., Eyer, L., Jansen, F., Jordi, C., Katz, D., Klioner, S. A., Lammers, U., Lindegren, L., Luri, X., O'Mullane, W., Panem, C., Pourbaix, D., Randich, S., Sartoretti, P., Siddiqui, H. I., Soubiran, C., Valette, V., van Leeuwen, F., Walton, N. A., Aerts, C., Arenou, F., Cropper, M., Høg, E.,

Lattanzi, M. G., Grebel, E. K., Holland, A. D., Huc, C., Passot, X., Perryman, M., Bramante, L., Cacciari, C., Castañeda, J., Chaoul, L., Cheek, N., De Angeli, F., Fabricius, C., Guerra, R., Hernández, J., Jean-Antoine-Piccolo, A., Masana, E., Messineo, R., Mowlavi, N., Nienartowicz, K., Ordóñez-Blanco, D., Panuzzo, P., Portell, J., Richards, P. J., Riello, M., Seabroke, G. M., Tanga, P., Thévenin, F., Torra, J., Els, S. G., Gracia-Abril, G., Comoretto, G., Garcia-Reinaldos, M., Lock, T., Mercier, E., Altmann, M., Andrae, R., Astraatmadja, T. L., Bellas-Velidis, I., Benson, K., Berthier, J., Blomme, R., Busso, G., Carry, B., Cellino, A., Clementini, G., Cowell, S., Creevey, O., Cuypers, J., Davidson, M., De Ridder, J., de Torres, A., Delchambre, L., Dell’Oro, A., Ducourant, C., Frémat, Y., García-Torres, M., Gosset, E., Halbwachs, J. L., Hambly, N. C., Harrison, D. L., Hauser, M., Hestroffer, D., Hodgkin, S. T., Huckle, H. E., Hutton, A., Jasniewicz, G., Jordan, S., Kontizas, M., Korn, A. J., Lanzafame, A. C., Manteiga, M., Moitinho, A., Muinonen, K., Osinde, J., Pancino, E., Pauwels, T., Petit, J. M., Recio-Blanco, A., Robin, A. C., Sarro, L. M., Siopis, C., Smith, M., Smith, K. W., Sozzetti, A., Thuillot, W., van Reeven, W., Viala, Y., Abbas, U., Abreu Aramburu, A., Accart, S., Aguado, J. J., Allan, P. M., Allasia, W., Altavilla, G., Álvarez, M. A., Alves, J., Anderson, R. I., Andrei, A. H., Anglada Varela, E., Antiche, E., Antoja, T., Antón, S., Arcay, B., Bach, N., Baker, S. G., Balaguer-Núñez, L., Barache, C., Barata, C., Barbier, A., Barblan, F., Barrado y Navascués, D., Barros, M., Barstow, M. A., Becciani, U., Bellazzini, M., Bello García, A., Belokurov, V., Bendjoya, P., Berihuete, A., Bianchi, L., Bienaymé, O., Billebaud, F., Blagorodnova, N., Blanco-Cuaresma, S., Boch, T., Bombrun, A., Borrachero, R., Bouquillon, S., Bourda, G., Bouy, H., Bragaglia, A., Breddels, M. A., Brouillet, N., Brüsemeister, T., Bucciarelli, B., Burgess, P., Burgon, R., Burlacu, A., Busonero, D., Buzzi, R., Caffau, E., Cambras, J., Campbell, H., Cancelliere, R., Cantat-Gaudin, T., Carlucci, T., Carrasco, J. M., Castellani, M., Charlot, P., Charnas, J., Chiavassa, A., Clotet, M., Cocozza, G., Collins, R. S., Costigan, G., Crifo, F., Cross, N. J. G., Crosta, M., Crowley, C., Dafonte, C., Damerdji, Y., Dapergolas, A., David, P., David, M., De Cat, P., de Felice, F., de Laverny, P., De Luise, F., De March, R., de Martino, D., de Souza, R., Debosscher, J., del Pozo, E., Delbo, M., Delgado, A., Delgado, H. E., Di Matteo, P., Diakite, S., Distefano, E., Dolding, C., Dos Anjos, S., Drazinos, P., Duran, J., Dzigan, Y., Edvardsson, B., Enke, H., Evans, N. W., Eynard Bontemps, G., Fabre, C., Fabrizio, M., Faigler, S., Falcão, A. J., Farràs Casas, M., Federici, L., Fedorets, G., Fernández-Hernández, J., Fernique, P., Fienga, A., Figueras, F., Filippi, F., Findeisen, K., Fonti, A., Fouesneau, M., Fraile, E., Fraser, M., Fuchs, J., Gai, M., Galleti, S., Galluccio, L., Garabato, D., García-Sedano, F., Garofalo, A., Garralda, N., Gavras, P., Gerssen, J., Geyer, R., Gilmore, G., Girona, S., Giuffrida, G., Gomes, M., González-Marcos, A., González-Núñez, J., González-Vidal, J. J., Granvik, M., Guerrier, A., Guillout, P., Guiraud, J., Gúrpide, A., Gutiérrez-Sánchez, R., Guy, L. P., Haigron, R., Hatzidimitriou, D., Haywood, M., Heiter, U., Helmi, A., Hobbs, D., Hofmann, W., Holl, B., Holland, G., Hunt, J. A. S., Hypki, A., Icardi, V., Irwin, M., Jevardat de Fombelle, G., Jofré, P., Jonker, P. G.,

Jorissen, A., Julbe, F., Karampelas, A., Kochoska, A., Kohley, R., Kolenberg, K., Kontizas, E., Koposov, S. E., Kordopatis, G., Koubsky, P., Krone-Martins, A., Kudryashova, M., Kull, I., Bachchan, R. K., Lacoste-Seris, F., Lanza, A. F., Lavigne, J. B., Le Poncin-Lafitte, C., Lebreton, Y., Lebzelter, T., Leccia, S., Leclerc, N., Lecoeur-Taibi, I., Lemaitre, V., Lenhardt, H., Leroux, F., Liao, S., Licata, E., Lindstrøm, H. E. P., Lister, T. A., Livanou, E., Lobel, A., Löffler, W., López, M., Lorenz, D., MacDonald, I., Magalhães Fernandes, T., Managau, S., Mann, R. G., Mantelet, G., Marchal, O., Marchant, J. M., Marconi, M., Marinoni, S., Marrese, P. M., Marschalkó, G., Marshall, D. J., Martín-Fleitas, J. M., Martino, M., Mary, N., Matijević, G., Mazeh, T., McMillan, P. J., Messina, S., Michalik, D., Millar, N. R., Miranda, B. M. H., Molina, D., Molinaro, R., Molinaro, M., Mohnár, L., Moniez, M., Montegriffo, P., Mor, R., Mora, A., Morbidelli, R., Morel, T., Morgenthaler, S., Morris, D., Mulone, A. F., Muraveva, T., Musella, I., Narbonne, J., Nelemans, G., Nicastro, L., Noval, L., Ordénovic, C., Ordieres-Meré, J., Osborne, P., Pagani, C., Pagano, I., Pailler, F., Palacin, H., Palaversa, L., Parsons, P., Pecoraro, M., Pedrosa, R., Pentikäinen, H., Pichon, B., Piersimoni, A. M., Pineau, F. X., Plachy, E., Plum, G., Poujoulet, E., Prša, A., Pulone, L., Ragaini, S., Rago, S., Rambaux, N., Ramos-Lerate, M., Ranalli, P., Rauw, G., Read, A., Regibo, S., Reylé, C., Ribeiro, R. A., Rimoldini, L., Ripepi, V., Riva, A., Rixon, G., Roelens, M., Romero-Gómez, M., Rowell, N., Royer, F., Ruiz-Dern, L., Sadowski, G., Sagristà Sellés, T., Sahlmann, J., Salgado, J., Salguero, E., Sarasso, M., Savietto, H., Schultheis, M., Sciacca, E., Segol, M., Segovia, J. C., Segransan, D., Shih, I. C., Smareglia, R., Smart, R. L., Solano, E., Solitro, F., Sordo, R., Soria Nieto, S., Souchay, J., Spagna, A., Spoto, F., Stampa, U., Steele, I. A., Steidelmüller, H., Stephenson, C. A., Stoev, H., Suess, F. F., Süveges, M., Surdej, J., Szabados, L., Szegedi-Elek, E., Tapiador, D., Taris, F., Tauran, G., Taylor, M. B., Teixeira, R., Terrett, D., Tingley, B., Trager, S. C., Turon, C., Ulla, A., Utrilla, E., Valentini, G., van Elteren, A., Van Hemelryck, E., van Leeuwen, M., Varadi, M., Vecchiato, A., Veljanoski, J., Via, T., Vicente, D., Vogt, S., Voss, H., Votruba, V., Voutsinas, S., Walmsley, G., Weiler, M., Weingrill, K., Wevers, T., Wyrzykowski, Ł., Yoldas, A., Žerjal, M., Zucker, S., Zurbach, C., Zwitter, T., Alecu, A., Allen, M., Allende Prieto, C., Amorim, A., Anglada-Escudé, G., Arsenijevic, V., Azaz, S., Balm, P., Beck, M., Bernstein, H. H., Bigot, L., Bijaoui, A., Blasco, C., Bonfigli, M., Bono, G., Boudreault, S., Bressan, A., Brown, S., Brunet, P. M., Bunclark, P., Buonanno, R., Butkevich, A. G., Carret, C., Carrion, C., Chemin, L., Chéreau, F., Corcione, L., Darmigny, E., de Boer, K. S., de Teodoro, P., de Zeeuw, P. T., Delle Luche, C., Domingues, C. D., Dubath, P., Fodor, F., Frézouls, B., Fries, A., Fustes, D., Fyfe, D., Gallardo, E., Gallegos, J., Gardiol, D., Gebran, M., Gomboc, A., Gómez, A., Grux, E., Gueguen, A., Heyrovsky, A., Hoar, J., Iannicola, G., Isasi Parache, Y., Janotto, A. M., Joliet, E., Jonckheere, A., Keil, R., Kim, D. W., Klagyivik, P., Klar, J., Knude, J., Kochukhov, O., Kolka, I., Kos, J., Kutka, A., Lainey, V., LeBouquin, D., Liu, C., Loreggia, D., Makarov, V. V., Marseille, M. G., Martayan, C., Martinez-Rubi, O., Massart, B., Meynadier, F., Mignot, S.,

Munari, U., Nguyen, A. T., Nordlander, T., Ocvirk, P., O'Flaherty, K. S., Olias Sanz, A., Ortiz, P., Osorio, J., Oszkiewicz, D., Ouzounis, A., Palmer, M., Park, P., Pasquato, E., Peltzer, C., Peralta, J., Péturaud, F., Pieniluoma, T., Pigozzi, E., Poels, J., Prat, G., Prod'homme, T., Raison, F., Rebordao, J. M., Risquez, D., Rocca-Volmerange, B., Rosen, S., Ruiz-Fuertes, M. I., Russo, F., Sembay, S., Serraller Vizcaino, I., Short, A., Siebert, A., Silva, H., Sinachopoulos, D., Slezak, E., Soffel, M., Sosnowska, D., Straižys, V., ter Linden, M., Terrell, D., Theil, S., Tiede, C., Troisi, L., Tsalmantza, P., Tur, D., Vaccari, M., Vachier, F., Valles, P., Van Hamme, W., Veltz, L., Virtanen, J., Wallut, J. M., Wichmann, R., Wilkinson, M. I., Ziaeepour, H., and Zschocke, S. (2016). Gaia Data Release 1. Summary of the astrometric, photometric, and survey properties. *Astronomy and Astrophysics*, 595:A2.

Gaia Collaboration, Vallenari, A., Brown, A. G. A., Prusti, T., de Bruijne, J. H. J., Arenou, F., Babusiaux, C., Biermann, M., Creevey, O. L., Ducourant, C., Evans, D. W., Eyer, L., Guerra, R., Hutton, A., Jordi, C., Klioner, S. A., Lammers, U. L., Lindegren, L., Luri, X., Mignard, F., Panem, C., Pourbaix, D., Randich, S., Sartoretti, P., Soubiran, C., Tanga, P., Walton, N. A., Bailer-Jones, C. A. L., Bastian, U., Drimmel, R., Jansen, F., Katz, D., Lattanzi, M. G., van Leeuwen, F., Bakker, J., Cacciari, C., Castañeda, J., De Angeli, F., Fabricius, C., Fouesneau, M., Frémat, Y., Galluccio, L., Guerrier, A., Heiter, U., Masana, E., Messineo, R., Mowlavi, N., Nicolas, C., Nienartowicz, K., Pailler, F., Panuzzo, P., Riclet, F., Roux, W., Seabroke, G. M., Sordoørcit, R., Thévenin, F., Gracia-Abril, G., Portell, J., Teyssier, D., Altmann, M., Andrae, R., Audard, M., Bellas-Velidis, I., Benson, K., Berthier, J., Blomme, R., Burgess, P. W., Busonero, D., Busso, G., Cánovas, H., Carry, B., Cellino, A., Cheek, N., Clementini, G., Damerdji, Y., Davidson, M., de Teodoro, P., Nuñez Campos, M., Delchambre, L., Dell'Oro, A., Esquej, P., Fernández-Hernández, J., Fraile, E., Garabato, D., García-Lario, P., Gosset, E., Haigron, R., Halbwachs, J. L., Hambly, N. C., Harrison, D. L., Hernández, J., Hestroffer, D., Hodgkin, S. T., Holl, B., Janßen, K., Jevardat de Fombelle, G., Jordan, S., Krone-Martins, A., Lanzafame, A. C., Löffler, W., Marchal, O., Marrese, P. M., Moitinho, A., Muinonen, K., Osborne, P., Pancino, E., Pauwels, T., Recio-Blanco, A., Reylé, C., Riello, M., Rimoldini, L., Roegiers, T., Rybizki, J., Sarro, L. M., Siopis, C., Smith, M., Sozzetti, A., Utrilla, E., van Leeuwen, M., Abbas, U., Ábrahám, P., Abreu Aramburu, A., Aerts, C., Aguado, J. J., Ajaj, M., Aldea-Montero, F., Altavilla, G., Álvarez, M. A., Alves, J., Anders, F., Anderson, R. I., Anglada Varela, E., Antoja, T., Baines, D., Baker, S. G., Balaguer-Núñez, L., Balbinot, E., Balog, Z., Barache, C., Barbato, D., Barros, M., Barstow, M. A., Bartolomé, S., Bassilana, J. L., Bauchet, N., Becciani, U., Bellazzini, M., Berihuete, A., Bernet, M., Bertone, S., Bianchi, L., Binnenfeld, A., Blanco-Cuaresma, S., Blazere, A., Boch, T., Bombrun, A., Bossini, D., Bouquillon, S., Bragaglia, A., Bramante, L., Breedt, E., Bressan, A., Brouillet, N., Brugaletta, E., Bucciarelli, B., Burlacu, A., Butkevich, A. G., Buzzi, R., Caffau, E., Cancelliere, R., Cantat-Gaudin, T., Carballo, R., Carlucci, T., Carnerero, M. I., Carrasco, J. M., Casamiquela, L., Castellani, M., Castro-Ginard, A., Chaoul, L., Charlot, P., Chemin, L., Chiaramida, V., Chiavassa, A.,

Chornay, N., Comoretto, G., Contursi, G., Cooper, W. J., Cornez, T., Cowell, S., Crifo, F., Cropper, M., Crosta, M., Crowley, C., Dafonte, C., Dapergolas, A., David, M., David, P., de Laverny, P., De Luise, F., De March, R., De Ridder, J., de Souza, R., de Torres, A., del Peloso, E. F., del Pozo, E., Delbo, M., Delgado, A., Delisle, J. B., Demouchy, C., Dharmawardena, T. E., Di Matteo, P., Diakite, S., Diener, C., Distefano, E., Dolding, C., Edvardsson, B., Enke, H., Fabre, C., Fabrizio, M., Faigler, S., Fedorets, G., Fernique, P., Fienga, A., Figueras, F., Fournier, Y., Fouron, C., Frakoudi, F., Gai, M., Garcia-Gutierrez, A., Garcia-Reinaldos, M., García-Torres, M., Garofalo, A., Gavel, A., Gavras, P., Gerlach, E., Geyer, R., Giacobbe, P., Gilmore, G., Girona, S., Giuffrida, G., Gomel, R., Gomez, A., González-Núñez, J., González-Santamaría, I., González-Vidal, J. J., Granvik, M., Guillout, P., Guiraud, J., Gutiérrez-Sánchez, R., Guy, L. P., Hatzidimitriou, D., Hauser, M., Haywood, M., Helmer, A., Helmi, A., Sarmiento, M. H., Hidalgo, S. L., Hilger, T., Hładczuk, N., Hobbs, D., Holland, G., Huckle, H. E., Jardine, K., Jasniewicz, G., Jean-Antoine Piccolo, A., Jiménez-Arranz, Ó., Jorissen, A., Juaristi Campillo, J., Julbe, F., Karbevska, L., Kervella, P., Khanna, S., Kontizas, M., Kordopatis, G., Korn, A. J., Kóspál, Á., Kostrzewska-Rutkowska, Z., Kruszyńska, K., Kun, M., Laizeau, P., Lambert, S., Lanza, A. F., Lasne, Y., Le Campion, J. F., Lebreton, Y., Lebzelter, T., Leccia, S., Leclerc, N., Lecoeur-Taibi, I., Liao, S., Licata, E. L., Lindstrøm, H. E. P., Lister, T. A., Livanou, E., Lobel, A., Lorca, A., Loup, C., Madrero Pardo, P., Magdaleno Romeo, A., Managau, S., Mann, R. G., Manteiga, M., Marchant, J. M., Marconi, M., Marcos, J., Marcos Santos, M. M. S., Marín Pina, D., Marinoni, S., Marocco, F., Marshall, D. J., Polo, L. M., Martín-Fleitas, J. M., Marton, G., Mary, N., Masip, A., Massari, D., Mastrobuono-Battisti, A., Mazeh, T., McMillan, P. J., Messina, S., Michalik, D., Millar, N. R., Mints, A., Molina, D., Molinaro, R., Molnár, L., Monari, G., Monguió, M., Montegriffo, P., Montero, A., Mor, R., Mora, A., Morbidelli, R., Morel, T., Morris, D., Muraveva, T., Murphy, C. P., Musella, I., Nagy, Z., Noval, L., Ocaña, F., Ogden, A., Ordenovic, C., Osinde, J. O., Pagani, C., Pagano, I., Palaversa, L., Palicio, P. A., Pallas-Quintela, L., Panahi, A., Payne-Wardenaar, S., Peñalosa Esteller, X., Penttilä, A., Pichon, B., Piersimoni, A. M., Pineau, F. X., Plachy, E., Plum, G., Poggio, E., Prša, A., Pulone, L., Racero, E., Ragaini, S., Rainer, M., Raiteri, C. M., Rambaux, N., Ramos, P., Ramos-Lerate, M., Re Fiorentin, P., Regibo, S., Richards, P. J., Rios Diaz, C., Ripepi, V., Riva, A., Rix, H. W., Rixon, G., Robichon, N., Robin, A. C., Robin, C., Roelens, M., Rogues, H. R. O., Rohrbasser, L., Romero-Gómez, M., Rowell, N., Royer, F., Ruz Mieres, D., Rybicki, K. A., Sadowski, G., Sáez Núñez, A., Sagristà Sellés, A., Sahlmann, J., Salguero, E., Samaras, N., Sanchez Gimenez, V., Sanna, N., Santoveña, R., Sarasso, M., Schultheis, M., Sciacca, E., Segol, M., Segovia, J. C., Ségransan, D., Semeux, D., Shahaf, S., Siddiqui, H. I., Siebert, A., Siltala, L., Silvelo, A., Slezak, E., Slezak, I., Smart, R. L., Snaith, O. N., Solano, E., Solitro, F., Souami, D., Souchay, J., Spagna, A., Spina, L., Spoto, F., Steele, I. A., Steidelmüller, H., Stephenson, C. A., Süveges, M., Surdej, J., Szabados, L., Szegedi-Elek, E., Taris, F., Taylo, M. B., Teixeira, R., Tolomei, L., Tonello, N., Torra, F., Torra,

- J., Torralba Elipe, G., Trabucchi, M., Tsounis, A. T., Turon, C., Ulla, A., Unger, N., Vaillant, M. V., van Dillen, E., van Reeven, W., Vanel, O., Vecchiato, A., Viala, Y., Vicente, D., Voutsinas, S., Weiler, M., Wevers, T., Wyrzykowski, L., Yoldas, A., Yvard, P., Zhao, H., Zorec, J., Zucker, S., and Zwitter, T. (2022). Gaia Data Release 3: Summary of the content and survey properties. *arXiv e-prints*, page arXiv:2208.00211.
- García Pérez, A. E., Allende Prieto, C., Holtzman, J. A., Shetrone, M., Mészáros, S., Bizyaev, D., Carrera, R., Cunha, K., García-Hernández, D. A., Johnson, J. A., Majewski, S. R., Nidever, D. L., Schiavon, R. P., Shane, N., Smith, V. V., Sobeck, J., Troup, N., Zamora, O., Weinberg, D. H., Bovy, J., Eisenstein, D. J., Feuillet, D., Frinchaboy, P. M., Hayden, M. R., Hearty, F. R., Nguyen, D. C., O'Connell, R. W., Pinsonneault, M. H., Wilson, J. C., and Zasowski, G. (2016). ASPCAP: The APOGEE Stellar Parameter and Chemical Abundances Pipeline. *Astronomical Journal*, 151(6):144.
- Geisler, D. (2018). CAPOS: bulge Cluster APOGee Survey. In *The Galactic Bulge at the Crossroads*, page 12.
- Geisler, D., Piatti, A. E., Claria, J. J., and Minniti, D. (1995). Lower Metallicity Limit of the Galactic Globular Cluster System: Calcium Triplet Spectroscopy of Metal-Poor Cluster Giants. *Astronomical Journal*, 109:605.
- Geisler, D., Villanova, S., O'Connell, J. E., Cohen, R. E., Moni Bidin, C., Fernández-Trincado, J. G., Muñoz, C., Minniti, D., Zoccali, M., Rojas-Arriagada, A., Contreras Ramos, R., Catelan, M., Mauro, F., Cortés, C., Ferreira Lopes, C. E., Arentsen, A., Starkenburg, E., Martin, N. F., Tang, B., Parisi, C., Alonso-García, J., Gran, F., Cunha, K., Smith, V., Majewski, S. R., Jönsson, H., García-Hernández, D. A., Horta, D., Mészáros, S., Monaco, L., Monachesi, A., Muñoz, R. R., Brownstein, J., Beers, T. C., Lane, R. R., Barbuy, B., Sobeck, J., Henao, L., González-Díaz, D., Miranda, R. E., Reinarz, Y., and Santander, T. A. (2021a). CAPOS: The bulge Cluster APOGee Survey. I. Overview and initial ASPCAP results. *Astronomy and Astrophysics*, 652:A157.
- Geisler, D., Villanova, S., O'Connell, J. E., Saito, R. K., Hempel, M., Pietrukowicz, P., Ahumada, A. V., Alonso, M. V., Alonso-Garcia, J., Arias, J. I., Bandyopadhyay, R. M., Barbá, R. H., Barbuy, B., Bedin, L. R., Bica, E., Borissova, J., Bronfman, L., Carraro, G., Catelan, M., Clariá, J. J., Cross, N., de Grijs, R., Dékány, I., Drew, J. E., Fariña, C., Feinstein, C., Fernández Lajús, E., Gamen, R. C., Geisler, D., Gieren, W., Goldman, B., Gonzalez, O. A., Gunthardt, G., Gurovich, S., Hambley, N. C., Irwin, M. J., Ivanov, V. D., Jordán, A., Kerins, E., Kinemuchi, K., Kurtev, R., López-Corredoira, M., Maccarone, T., Masetti, N., Merlo, D., Messineo, M., Mirabel, I. F., Monaco, L., Morelli, L., Padilla, N., Palma, T., Parisi, M. C., Pignata, G., Rejkuba, M., Roman-Lopes, A., Sale, S. E., Schreiber, M. R., Schröder, A. C., Smith, M., L. Sodré, J., Soto, M., Tamura, M., Tappert, C., Thompson, M. A., Toledo, I., Zoccali, M., and Pietrzynski, G. (2021b). CAPOS: the bulge Cluster APOGee Survey I. Overview and Initial ASPCAP Results. *Astronomy and Astrophysics*, submitted.

- Gieles, M., Charbonnel, C., Krause, M. G. H., Hénault-Brunet, V., Agertz, O., Lamers, H. J. G. L. M., Bastian, N., Gualandris, A., Zocchi, A., and Petts, J. A. (2018). Concurrent formation of supermassive stars and globular clusters: implications for early self-enrichment. *Monthly Notices of the Royal Astronomical Society*, 478(2):2461–2479.
- Goldsbury, R., Richer, H. B., Anderson, J., Dotter, A., Sarajedini, A., and Woodley, K. (2010). The ACS Survey of Galactic Globular Clusters. X. New Determinations of Centers for 65 Clusters. *Astronomical Journal*, 140(6):1830–1837.
- González Manrique, S. J., Quintero Noda, C., Kuckein, C., Ruiz Cobo, B., and Carlsson, M. (2020). Capabilities of bisector analysis of the Si I 10 827 Å line for estimating line-of-sight velocities in the quiet Sun. *Astronomy and Astrophysics*, 634:A19.
- Gratton, R., Bragaglia, A., Carretta, E., D’Orazi, V., Lucatello, S., and Sollima, A. (2019). What is a globular cluster? An observational perspective. *Astronomy and Astrophysics Reviews*, 27(1):8.
- Gray, D. F. (1988). *Lectures on spectral-line analysis: F, G, and K stars*. Ontario.
- Gray, D. F. (2005). *The Observation and Analysis of Stellar Photospheres*. Cambridge University Press.
- Gray, D. F. (2010). Empirical Decoding of the Shapes of Spectral-Line Bisectors. *The Astrophysical Journal*, 710(2):1003–1008.
- Griggio, M. and Bedin, L. R. (2022). Astrometric star-cluster membership probability: application to the case of M 37 with Gaia EDR3. *mnras*, 511(4):4702–4709.
- Gunn, J. E., Siegmund, W. A., Mannery, E. J., Owen, R. E., Hull, C. L., Leger, R. F., Carey, L. N., Knapp, G. R., York, D. G., Boroski, W. N., Kent, S. M., Lupton, R. H., Rockosi, C. M., Evans, M. L., Waddell, P., Anderson, J. E., Annis, J., Barentine, J. C., Bartoszek, L. M., Bastian, S., Bracker, S. B., Brewington, H. J., Briegel, C. I., Brinkmann, J., Brown, Y. J., Carr, M. A., Czarapata, P. C., Drennan, C. C., Dombeck, T., Federwitz, G. R., Gillespie, B. A., Gonzales, C., Hansen, S. U., Harvanek, M., Hayes, J., Jordan, W., Kinney, E., Klaene, M., Kleinman, S. J., Kron, R. G., Kresinski, J., Lee, G., Limmongkol, S., Lindenmeyer, C. W., Long, D. C., Loomis, C. L., McGehee, P. M., Mantsch, P. M., Neilsen, Eric H., J., Neswold, R. M., Newman, P. R., Nitta, A., Peoples, John, J., Pier, J. R., Prieto, P. S., Prosapio, A., Rivetta, C., Schneider, D. P., Snedden, S., and Wang, S.-i. (2006). The 2.5 m Telescope of the Sloan Digital Sky Survey. *Astronomical Journal*, 131(4):2332–2359.
- Gustafsson, B., Edvardsson, B., Eriksson, K., Jørgensen, U. G., Nordlund, Å., and Plez, B. (2008). A grid of MARCS model atmospheres for late-type stars. I. Methods and general properties. *Astronomy and Astrophysics*, 486:951–970.

- Hanke, M., Koch, A., Prudil, Z., Grebel, E. K., and Bastian, U. (2020). Purveyors of fine halos. II. Chemodynamical association of halo stars with Milky Way globular clusters. *Astronomy and Astrophysics*, 637:A98.
- Hasselquist, S., Carlin, J. L., Holtzman, J. A., Shetrone, M., Hayes, C. R., Cunha, K., Smith, V., Beaton, R. L., Sobeck, J., Allende Prieto, C., Majewski, S. R., Anguiano, B., Bizyaev, D., García-Hernández, D. A., Lane, R. R., Pan, K., Nidever, D. L., Fernández-Trincado, J. G., Wilson, J. C., and Zamora, O. (2019). Identifying Sagittarius Stream Stars by Their APOGEE Chemical Abundance Signatures. *The Astrophysical Journal*, 872(1):58.
- Hasselquist, S., Shetrone, M., Cunha, K., Smith, V. V., Holtzman, J., Lawler, J. E., Allende Prieto, C., Beers, T. C., Chojnowski, D., Fernández-Trincado, J. G., García-Hernández, D. A., Hearty, F. R., Majewski, S. R., Pereira, C. B., Placco, V. M., Villanova, S., and Zamora, O. (2016). Identification of Neodymium in the Apogee H-Band Spectra. *The Astrophysical Journal*, 833(1):81.
- Hasselquist, S., Shetrone, M., Smith, V., Holtzman, J., McWilliam, A., Fernández-Trincado, J. G., Beers, T. C., Majewski, S. R., Nidever, D. L., Tang, B., Tissera, P. B., Fernández Alvar, E., Allende Prieto, C., Almeida, A., Anguiano, B., Battaglia, G., Carigi, L., Delgado Inglada, G., Frinchaboy, P., García-Hernández, D. A., Geisler, D., Minniti, D., Placco, V. M., Schultheis, M., Sobeck, J., and Villanova, S. (2017). APOGEE Chemical Abundances of the Sagittarius Dwarf Galaxy. *The Astrophysical Journal*, 845(2):162.
- Helmi, A., Babusiaux, C., Koppelman, H. H., Massari, D., Veljanoski, J., and Brown, A. G. A. (2018). The merger that led to the formation of the Milky Way's inner stellar halo and thick disk. *Nature*, 563(7729):85–88.
- Helmi, A., White, S. D. M., de Zeeuw, P. T., and Zhao, H. (1999). Debris streams in the solar neighbourhood as relicts from the formation of the Milky Way. *Nature*, 402(6757):53–55.
- Heyer, M. and Dame, T. M. (2015). Molecular Clouds in the Milky Way. *Annual Review of Astronomy and Astrophysics*, 53:583–629.
- Holtzman, J. A., Hasselquist, S., Shetrone, M., Cunha, K., Allende Prieto, C., Anguiano, B., Bizyaev, D., Bovy, J., Casey, A., Edvardsson, B., Johnson, J. A., Jönsson, H., Meszaros, S., Smith, V. V., Sobeck, J., Zamora, O., Chojnowski, S. D., Fernandez-Trincado, J., Garcia-Hernandez, D. A., Majewski, S. R., Pinsonneault, M., Souto, D., Stringfellow, G. S., Tayar, J., Troup, N., and Zasowski, G. (2018). APOGEE Data Releases 13 and 14: Data and Analysis. *Astronomical Journal*, 156(3):125.
- Hopkins, P. F. (2014). Some Stars are Totally Metal: A New Mechanism Driving Dust across Star-forming Clouds, and Consequences for Planets, Stars, and Galaxies. *The Astrophysical Journal*, 797(1):59.
- Hummer, D. G. and Rybicki, G. (1971). The Formation of Spectral Lines. *Annual Review of Astronomy and Astrophysics*, 9:237.

- Ibata, R., Malhan, K., Martin, N., Aubert, D., Famaey, B., Bianchini, P., Monari, G., Siebert, A., Thomas, G. F., Bellazzini, M., Bonifacio, P., Caffau, E., and Renaud, F. (2021). Charting the Galactic Acceleration Field. I. A Search for Stellar Streams with Gaia DR2 and EDR3 with Follow-up from ESPaDOnS and UVES. *The Astrophysical Journal*, 914(2):123.
- Ibata, R. A., Gilmore, G., and Irwin, M. J. (1994). A dwarf satellite galaxy in Sagittarius. *Nature*, 370(6486):194–196.
- Ji, S. (2017). *Binding\_energy\_curve\_-\_common\_isotopes.svg*. CC BY-SA 4.0, Wikimedia Commons, <https://commons.wikimedia.org/wiki/File:VoigtPDF.svg>.
- Jiang, D., Han, Z., and Li, L. (2017). Binary interactions and multiple stellar populations in globular clusters. In Charbonnel, C. and Nota, A., editors, *Formation, Evolution, and Survival of Massive Star Clusters*, volume 316, pages 316–319.
- Jönsson, H., Allende Prieto, C., Holtzman, J. A., Feuillet, D. K., Hawkins, K., Cunha, K., Mészáros, S., Hasselquist, S., Fernández-Trincado, J. G., García-Hernández, D. A., Bizyaev, D., Carrera, R., Majewski, S. R., Pinsonneault, M. H., Shetrone, M., Smith, V., Sobeck, J., Souto, D., Stringfellow, G. S., Teske, J., and Zamora, O. (2018). APOGEE Data Releases 13 and 14: Stellar Parameter and Abundance Comparisons with Independent Analyses. *Astronomical Journal*, 156(3):126.
- Jönsson, H., Holtzman, J. A., Allende Prieto, C., Cunha, K., García-Hernández, D. A., Hasselquist, S., Masseron, T., Osorio, Y., Shetrone, M., Smith, V., Stringfellow, G. S., Bizyaev, D., Edvardsson, B., Majewski, S. R., Mészáros, S., Souto, D., Zamora, O., Beaton, R. L., Bovy, J., Donor, J., Pinsonneault, M. H., Poovelil, V. J., and Sobeck, J. (2020). APOGEE Data and Spectral Analysis from SDSS Data Release 16: Seven Years of Observations Including First Results from APOGEE-South. *Astronomical Journal*, 160(3):120.
- Koch, A., Grebel, E. K., and Martell, S. L. (2019). Purveyors of fine halos: Re-assessing globular cluster contributions to the Milky Way halo buildup with SDSS-IV. *Astronomy and Astrophysics*, 625:A75.
- Koch-Hansen, A. J., Hansen, C. J., Lombardo, L., Bonifacio, P., Hanke, M., and Caffau, E. (2021). Purveyors of fine halos. III. Chemical abundance analysis of a potential  $\omega$ Cen associate. *Astronomy and Astrophysics*, 645:A64.
- Koppelman, H. H., Helmi, A., Massari, D., Price-Whelan, A. M., and Starkenburg, T. K. (2019). Multiple retrograde substructures in the Galactic halo: A shattered view of Galactic history. *Astronomy and Astrophysics*, 631:L9.
- Kraft, R. P. (1979). On the nonhomogeneity of metal abundances in stars of globular clusters and satellite subsystems of the Galaxy. *Annual Review of Astronomy and Astrophysics*, 17:309–343.

- Kraft, R. P. and Ivans, I. I. (2003). A Globular Cluster Metallicity Scale Based on the Abundance of Fe II. *Publications of the ASP*, 115(804):143–169.
- Krause, M., Charbonnel, C., Decressin, T., Meynet, G., and Prantzos, N. (2013). Superbubble dynamics in globular cluster infancy. II. Consequences for secondary star formation in the context of self-enrichment via fast-rotating massive stars. *Astronomy and Astrophysics*, 552:A121.
- Kruijssen, J. M. D., Pfeffer, J. L., Chevance, M., Bonaca, A., Trujillo-Gomez, S., Bastian, N., Reina-Campos, M., Crain, R. A., and Hughes, M. E. (2020). Kraken reveals itself - the merger history of the Milky Way reconstructed with the E-MOSAICS simulations. *Monthly Notices of the Royal Astronomical Society*, 498(2):2472–2491.
- Kruijssen, J. M. D., Pfeffer, J. L., Reina-Campos, M., Crain, R. A., and Bastian, N. (2019). The formation and assembly history of the Milky Way revealed by its globular cluster population. *Monthly Notices of the Royal Astronomical Society*, 486(3):3180–3202.
- Krumholz, M. R., McKee, C. F., and Bland-Hawthorn, J. (2019). Star Clusters Across Cosmic Time. *Annual Review of Astronomy and Astrophysics*, 57:227–303.
- Kundu, R., Fernández-Trincado, J. G., Minniti, D., Singh, H. P., Moreno, E., Reylé, C., Robin, A. C., and Soto, M. (2019a). The tale of the Milky Way globular cluster NGC 6362 - I. The orbit and its possible extended star debris features as revealed by Gaia DR2. *Monthly Notices of the Royal Astronomical Society*, 489(4):4565–4573.
- Kundu, R., Minniti, D., and Singh, H. P. (2019b). Search for extra-tidal RR Lyrae stars in Milky Way globular clusters from Gaia DR2. *Monthly Notices of the Royal Astronomical Society*, 483(2):1737–1743.
- Kundu, R., Navarrete, C., Fernández-Trincado, J. G., Minniti, D., Singh, H. P., Sbordone, L., Piatti, A. E., and Reylé, C. (2021). The search for extratidal star candidates around Galactic globular clusters NGC 2808, NGC 6266, and NGC 6397 with Gaia DR2 astrometry. *Astronomy and Astrophysics*, 645:A116.
- Latour, M., Husser, T. O., Giesers, B., Kamann, S., Göttgens, F., Dreizler, S., Brinchmann, J., Bastian, N., Wendt, M., Weilbacher, P. M., and Molinski, N. S. (2019). A stellar census in globular clusters with MUSE: multiple populations chemistry in NGC 2808. *Astronomy and Astrophysics*, 631:A14.
- Leon, S., Meylan, G., and Combes, F. (2000). Tidal tails around 20 Galactic globular clusters. Observational evidence for gravitational disk/bulge shocking. *Astronomy and Astrophysics*, 359:907–931.
- Lind, K., Koposov, S. E., Battistini, C., Marino, A. F., Ruchti, G., Serenelli, A., Worley, C. C., Alves-Brito, A., Asplund, M., Barklem, P. S., Bensby, T., Bergemann, M., Blanco-Cuaresma, S., Bragaglia, A., Edvardsson, B., Feltzing,

- S., Gruyters, P., Heiter, U., Jofre, P., Korn, A. J., Nordlander, T., Ryde, N., Soubiran, C., Gilmore, G., Randich, S., Ferguson, A. M. N., Jeffries, R. D., Vallenari, A., Allende Prieto, C., Pancino, E., Recio-Blanco, A., Romano, D., Smiljanic, R., Bellazzini, M., Damiani, F., Hill, V., de Laverny, P., Jackson, R. J., Lardo, C., and Zaggia, S. (2015). The Gaia-ESO Survey: A globular cluster escapee in the Galactic halo. *Astronomy and Astrophysics*, 575:L12.
- Maercker, M. (2009). *Asymptotic Giant Branch stars viewed up-close and far-off : The physics, chemistry, and evolution of their circumstellar envelopes*. PhD thesis, Stockholm University.
- Majewski, S. R., Schiavon, R. P., Frinchaboy, P. M., Allende Prieto, C., Barkhouser, R., Bizyaev, D., Blank, B., Brunner, S., Burton, A., Carrera, R., Chojnowski, S. D., Cunha, K., Epstein, C., Fitzgerald, G., García Pérez, A. E., Hearty, F. R., Henderson, C., Holtzman, J. A., Johnson, J. A., Lam, C. R., Lawler, J. E., Maseman, P., Mészáros, S., Nelson, M., Nguyen, D. C., Nidever, D. L., Pinsonneault, M., Shetrone, M., Smee, S., Smith, V. V., Stolberg, T., Skrutskie, M. F., Walker, E., Wilson, J. C., Zasowski, G., Anders, F., Basu, S., Beland, S., Blanton, M. R., Bovy, J., Brownstein, J. R., Carlberg, J., Chaplin, W., Chiappini, C., Eisenstein, D. J., Elsworth, Y., Feuillet, D., Fleming, S. W., Galbraith-Frew, J., García, R. A., García-Hernández, D. A., Gillespie, B. A., Girardi, L., Gunn, J. E., Hasselquist, S., Hayden, M. R., Hekker, S., Ivans, I., Kinemuchi, K., Klaene, M., Mahadevan, S., Mathur, S., Mosser, B., Muna, D., Munn, J. A., Nichol, R. C., O'Connell, R. W., Parejko, J. K., Robin, A. C., Rocha-Pinto, H., Schultheis, M., Serenelli, A. M., Shane, N., Silva Aguirre, V., Sobeck, J. S., Thompson, B., Troup, N. W., Weinberg, D. H., and Zamora, O. (2017). The Apache Point Observatory Galactic Evolution Experiment (APOGEE). *Astronomical Journal*, 154(3):94.
- Malhan, K., Ibata, R. A., Sharma, S., Famaey, B., Bellazzini, M., Carlberg, R. G., D'Souza, R., Yuan, Z., Martin, N. F., and Thomas, G. F. (2022). The Global Dynamical Atlas of the Milky Way Mergers: Constraints from Gaia EDR3-based Orbits of Globular Clusters, Stellar Streams, and Satellite Galaxies. *The Astrophysical Journal*, 926(2):107.
- Marcolini, A., Gibson, B. K., Karakas, A. I., and Sánchez-Blázquez, P. (2009). The chemical evolution of globular clusters - I. Reactive elements and non-metals. *Monthly Notices of the Royal Astronomical Society*, 395(2):719–735.
- Marigo, P., Girardi, L., Bressan, A., Rosenfield, P., Aringer, B., Chen, Y., Dussin, M., Nanni, A., Pastorelli, G., Rodrigues, T. S., Trabucchi, M., Bladh, S., Dalcanton, J., Groenewegen, M. A. T., Montalbán, J., and Wood, P. R. (2017). A New Generation of PARSEC-COLIBRI Stellar Isochrones Including the TP-AGB Phase. *The Astrophysical Journal*, 835(1):77.
- Marino, A. F., Milone, A. P., Renzini, A., Yong, D., Asplund, M., Da Costa, G. S., Jerjen, H., Cordon, G., Carlos, M., Dondoglio, E., Lagioia, E. P., Jang, S., and Tailo, M. (2021). Spectroscopy and Photometry of the Least Massive Type

- II Globular Clusters: NGC 1261 and NGC 6934. *The Astrophysical Journal*, 923(1):22.
- Martin, N. F., Ibata, R. A., Bellazzini, M., Irwin, M. J., Lewis, G. F., and Dehnen, W. (2004). A dwarf galaxy remnant in Canis Major: the fossil of an in-plane accretion on to the Milky Way. *Monthly Notices of the Royal Astronomical Society*, 348(1):12–23.
- Massari, D., Koppelman, H. H., and Helmi, A. (2019). Origin of the system of globular clusters in the Milky Way. *Astronomy and Astrophysics*, 630:L4.
- Masseron, T., García-Hernández, D. A., Mészáros, S., Zamora, O., Dell’Agli, F., Allende Prieto, C., Edvardsson, B., Shetrone, M., Plez, B., Fernández-Trincado, J. G., Cunha, K., Jönsson, H., Geisler, D., Beers, T. C., and Cohen, R. E. (2019). Homogeneous analysis of globular clusters from the APOGEE survey with the BACCHUS code. I. The northern clusters. *Astronomy and Astrophysics*, 622:A191.
- Masseron, T., Merle, T., and Hawkins, K. (2016). BACCHUS: Brussels Automatic Code for Characterizing High accUracy Spectra.
- McWilliam, A., Geisler, D., and Rich, R. M. (1992). Abundance Analyses of Three Red Giants in the Metal-Poor Globular Cluster NGC 2298. *Publications of the ASP*, 104:1193.
- Merrill, K. M. and Ridgway, S. T. (1979). Infrared spectroscopy of stars. *Annual Review of Astronomy and Astrophysics*, 17:9–41.
- Mészáros, S., Martell, S. L., Shetrone, M., Lucatello, S., Troup, N. W., Bovy, J., Cunha, K., García-Hernández, D. A., Overbeek, J. C., Allende Prieto, C., Beers, T. C., Frinchaboy, P. M., García Pérez, A. E., Hearty, F. R., Holtzman, J., Majewski, S. R., Nidever, D. L., Schiavon, R. P., Schneider, D. P., Sobeck, J. S., Smith, V. V., Zamora, O., and Zasowski, G. (2015). Exploring Anticorrelations and Light Element Variations in Northern Globular Clusters Observed by the APOGEE Survey. *Astronomical Journal*, 149(5):153.
- Mészáros, S., Masseron, T., Fernández-Trincado, J. G., García-Hernández, D. A., Szigeti, L., Cunha, K., Shetrone, M., Smith, V. V., Beaton, R. L., Beers, T. C., Brownstein, J. R., Geisler, D., Hayes, C. R., Jönsson, H., Lane, R. R., Majewski, S. R., Minniti, D., Munoz, R. R., Nitschelm, C., Roman-Lopes, A., and Zamora, O. (2021). Homogeneous analysis of globular clusters from the APOGEE survey with the BACCHUS code - III.  $\omega$  Cen. *Monthly Notices of the Royal Astronomical Society*.
- Mészáros, S., Masseron, T., García-Hernández, D. A., Allende Prieto, C., Beers, T. C., Bizyaev, D., Chojnowski, D., Cohen, R. E., Cunha, K., Dell’Agli, F., Ebelke, G., Fernández-Trincado, J. G., Frinchaboy, P., Geisler, D., Hasselquist, S., Hearty, F., Holtzman, J., Johnson, J., Lane, R. R., Lacerna, I., Longa-Peña, P., Majewski, S. R., Martell, S. L., Minniti, D., Nataf, D., Nidever, D. L., Pan, K., Schiavon, R. P., Shetrone, M., Smith, V. V., Sobeck, J. S., Stringfellow,

- G. S., Szigeti, L., Tang, B., Wilson, J. C., and Zamora, O. (2020). Homogeneous analysis of globular clusters from the APOGEE survey with the BACCHUS code - II. The Southern clusters and overview. *Monthly Notices of the Royal Astronomical Society*, 492(2):1641–1670.
- Milone, A. P. and Marino, A. F. (2022). Multiple Populations in Star Clusters. *Universe*, 8(7):359.
- Milone, A. P., Piotto, G., Renzini, A., Marino, A. F., Bedin, L. R., Vesperini, E., D'Antona, F., Nardiello, D., Anderson, J., King, I. R., Yong, D., Bellini, A., Aparicio, A., Barbuy, B., Brown, T. M., Cassisi, S., Ortolani, S., Salaris, M., Sarajedini, A., and van der Marel, R. P. (2017). The Hubble Space Telescope UV Legacy Survey of Galactic globular clusters - IX. The Atlas of multiple stellar populations. *Monthly Notices of the Royal Astronomical Society*, 464(3):3636–3656.
- Monty, S., Puzia, T. H., Miller, B. W., Carrasco, E. R., Simunovic, M., Schirmer, M., Stetson, P. B., Cassisi, S., Venn, K. A., Dotter, A., Goudfrooij, P., Perina, S., Peshev, P., Sarajedini, A., and Taylor, M. A. (2018). The GeMS/GSAOI Galactic Globular Cluster Survey (G4CS). I. A Pilot Study of the Stellar Populations in NGC 2298 and NGC 3201. *The Astrophysical Journal*, 865(2):160.
- Mott, A., Steffen, M., Caffau, E., and Strassmeier, K. G. (2020). Improving spectroscopic lithium abundances. Fitting functions for 3D non-LTE corrections in FGK stars of different metallicity. *Astronomy and Astrophysics*, 638:A58.
- Myeong, G. C., Evans, N. W., Belokurov, V., Sanders, J. L., and Koposov, S. E. (2018). The Sausage Globular Clusters. *Astrophysical Journal, Letters*, 863(2):L28.
- Myeong, G. C., Vasiliev, E., Iorio, G., Evans, N. W., and Belokurov, V. (2019). Evidence for two early accretion events that built the Milky Way stellar halo. *Monthly Notices of the Royal Astronomical Society*, 488(1):1235–1247.
- Nemiroff, R. and Jerry, B. (2001). *M55 Color Magnitude Diagram*. [http://www.astronet.ru/db/xware/msg/1166377/m55cmd\\_mochejska\\_big.jpg.html](http://www.astronet.ru/db/xware/msg/1166377/m55cmd_mochejska_big.jpg.html).
- Nguyen, C. T., Costa, G., Girardi, L., Volpato, G., Bressan, A., Chen, Y., Marigo, P., Fu, X., and Goudfrooij, P. (2022). PARSEC V2.0: Stellar tracks and isochrones of low- and intermediate-mass stars with rotation. *Astronomy and Astrophysics*, 665:A126.
- Nidever, D. L., Holtzman, J. A., Allende Prieto, C., Beland, S., Bender, C., Bizyaev, D., Burton, A., Desphande, R., Fleming, S. W., García Pérez, A. E., Hearty, F. R., Majewski, S. R., Mészáros, S., Muna, D., Nguyen, D., Schiavon, R. P., Shetrone, M., Skrutskie, M. F., Sobeck, J. S., and Wilson, J. C. (2015). The Data Reduction Pipeline for the Apache Point Observatory Galactic Evolution Experiment. *Astronomical Journal*, 150(6):173.
- Nomoto, K., Kobayashi, C., and Tominaga, N. (2013). Nucleosynthesis in Stars

- and the Chemical Enrichment of Galaxies. *Annual Review of Astronomy and Astrophysics*, 51(1):457–509.
- Oesch, P. A., Montes, M., Reddy, N., Bouwens, R. J., Illingworth, G. D., Magee, D., Atek, H., Carollo, C. M., Cibinel, A., Franx, M., Holden, B., Labb  , I., Nelson, E. J., Steidel, C. C., van Dokkum, P. G., Morselli, L., Naidu, R. P., and Wilkins, S. (2018). HDUV: The Hubble Deep UV Legacy Survey. *Astrophysical Journal, Supplement*, 237(1):12.
- Pagel, B. E. J. (2009). *Nucleosynthesis and Chemical Evolution of Galaxies*. CAMBRIDGE UNIVERSITY PRESS.
- Pedregosa, F., Varoquaux, G., Gramfort, A., Michel, V., Thirion, B., Grisel, O., Blondel, M., Prettenhofer, P., Weiss, R., Dubourg, V., Vanderplas, J., Passos, A., Cournapeau, D., Brucher, M., Perrot, M., and Duchesnay, E. (2011). Scikit-learn: Machine learning in Python. *Journal of Machine Learning Research*, 12:2825–2830.
- Pejcha, O. (2020). The Explosion Mechanism of Core-Collapse Supernovae and Its Observational Signatures. In *Reviews in Frontiers of Modern Astrophysics; From Space Debris to Cosmology*, pages 189–211. arXiv:2012.11873.
- Piotto, G., Milone, A. P., Bedin, L. R., Anderson, J., King, I. R., Marino, A. F., Nardiello, D., Aparicio, A., Barbuy, B., Bellini, A., Brown, T. M., Cassisi, S., Cool, A. M., Cunial, A., Dalessandro, E., D’Antona, F., Ferraro, F. R., Hidalgo, S., Lanzoni, B., Monelli, M., Ortolani, S., Renzini, A., Salaris, M., Sarajedini, A., van der Marel, R. P., Vesperini, E., and Zoccali, M. (2015). The Hubble Space Telescope UV Legacy Survey of Galactic Globular Clusters. I. Overview of the Project and Detection of Multiple Stellar Populations. *Astronomical Journal*, 149(3):91.
- Plez, B. (2012). Turbospectrum: Code for spectral synthesis. Astrophysics Source Code Library.
- Polster, J., Kor  akov  , D., and Manset, N. (2018). Time-dependent spectral-feature variations of stars displaying the B[e] phenomenon. IV. V2028 Cygni: modelling of H   bisector variability. *Astronomy and Astrophysics*, 617:A79.
- Pritzl, B. J., Venn, K. A., and Irwin, M. (2005). A Comparison of Elemental Abundance Ratios in Globular Clusters, Field Stars, and Dwarf Spheroidal Galaxies. *Astronomical Journal*, 130(5):2140–2165.
- Rani, S., Pandey, G., Subramaniam, A., Chung, C., Sahu, S., and Kameswara Rao, N. (2021). AstroSat Study of the Globular Cluster NGC 2298: Probable Evolutionary Scenarios of Hot Horizontal Branch Stars. *The Astrophysical Journal*, 923(2):162.
- Recio-Blanco, A., Rojas-Arriagada, A., de Laverny, P., Mikolaitis, S., Hill, V., Zoccali, M., Fern  andez-Trincado, J. G., Robin, A. C., Babusiaux, C., Gilmore, G., Randich, S., Alfaro, E., Allende Prieto, C., Bragaglia, A., Carraro, G.,

- Jofré, P., Lardo, C., Monaco, L., Morbidelli, L., and Zaggia, S. (2017). The Gaia-ESO Survey: Low- $\alpha$  element stars in the Galactic bulge. *Astronomy and Astrophysics*, 602:L14.
- Renzini, A., D'Antona, F., Cassisi, S., King, I. R., Milone, A. P., Ventura, P., Anderson, J., Bedin, L. R., Bellini, A., Brown, T. M., Piotto, G., van der Marel, R. P., Barbuy, B., Dalessandro, E., Hidalgo, S., Marino, A. F., Ortolani, S., Salaris, M., and Sarajedini, A. (2015). The Hubble Space Telescope UV Legacy Survey of Galactic Globular Clusters - V. Constraints on formation scenarios. *Monthly Notices of the Royal Astronomical Society*, 454(4):4197–4207.
- RJHall, C. B.-S. . (Retrieved 5 Dec 2008). *Nuclear\_energy\_generation.svg*, via Wikimedia Commons. [https://commons.wikimedia.org/wiki/File:Nuclear\\_energy\\_generation.svg](https://commons.wikimedia.org/wiki/File:Nuclear_energy_generation.svg).
- Roediger, J. C., Courteau, S., Graves, G., and Schiavon, R. P. (2014). Constraining Stellar Population Models. I. Age, Metallicity and Abundance Pattern Compilation for Galactic Globular Clusters. *Astrophysical Journal, Supplement*, 210(1):10.
- Romero-Colmenares, M., Fernández-Trincado, J. G., Geisler, D., Souza, S. O., Villanova, S., Longa-Peña, P., Minniti, D., Beers, T. C., Bidin, C. M., Perez-Villegas, A., Moreno, E., Garro, E. R., Baeza, I., Henao, L., Barbuy, B., Alonso-García, J., Cohen, R. E., Lane, R. R., and Muñoz, C. (2021). CAPOS: The bulge Cluster APOGee Survey. II. The intriguing “Sequoia” globular cluster FSR 1758. *Astronomy and Astrophysics*, 652:A158.
- Rosolowsky, E. (2015). *Stellar Evolution Primer*. <http://low-sky.github.io/stellarev/>.
- Rowland, C., Iliadis, C., Champagne, A. E., Fox, C., José, J., and Runkle, R. (2004). Does an NeNa Cycle Exist in Explosive Hydrogen Burning? *Astrophysical Journal, Letters*, 615(1):L37–L40.
- Salaris, M. and Cassisi, S. (1996). New molecular opacities and effective temperature of RGB stellar models. *Astronomy and Astrophysics*, 305:858.
- Sánchez-Blázquez, P., Marcolini, A., Gibson, B. K., Karakas, A. I., Pilkington, K., and Calura, F. (2012). The chemical evolution of globular clusters - II. Metals and fluorine. *Monthly Notices of the Royal Astronomical Society*, 419(2):1376–1389.
- Sandage, A. (1986). The population concept, globular clusters, subdwarfs, ages, and the collapse of the galaxy. *Annual Review of Astronomy and Astrophysics*, 24:421–458.
- Santana, F. A., Beaton, R. L., Covey, K., Saito, R. K., Hempel, M., Pietrukowicz, P., Ahumada, A. V., Alonso, M. V., Alonso-Garcia, J., Arias, J. I., Bandyopadhyay, R. M., Barbá, R. H., Barbuy, B., Bedin, L. R., Bica, E., Borissova, J., Bronfman, L., Carraro, G., Catelan, M., Clariá, J. J., Cross, N., de Grijs, R., Dékány, I., Drew, J. E., Fariña, C., Feinstein, C., Fernández

- Lajús, E., Gamen, R. C., Geisler, D., Gieren, W., Goldman, B., Gonzalez, O. A., Gunthardt, G., Gurovich, S., Hambly, N. C., Irwin, M. J., Ivanov, V. D., Jordán, A., Kerins, E., Kinemuchi, K., Kurtev, R., López-Corredoira, M., Maccarone, T., Masetti, N., Merlo, D., Messineo, M., Mirabel, I. F., Monaco, L., Morelli, L., Padilla, N., Palma, T., Parisi, M. C., Pignata, G., Rejkuba, M., Roman-Lopes, A., Sale, S. E., Schreiber, M. R., Schröder, A. C., Smith, M., , L. Sodré, J., Soto, M., Tamura, M., Tappert, C., Thompson, M. A., Toledo, I., Zoccali, M., and Pietrzynski, G. (2021). . *The Astrophysical Journal*, in preparation.
- Schatz, H. (2004). Nuclear Astrophysics and Nuclei Far from Stability. In Astbury, A., Campbell, B. A., Khanna, F. C., and Vincter, M. G., editors, *Particles and the Universe*, pages 118–131.
- Schiavon, R. P., Johnson, J. A., Frinchaboy, P. M., Zasowski, G., Mészáros, S., García-Hernández, D. A., Cohen, R. E., Tang, B., Villanova, S., Geisler, D., Beers, T. C., Fernández-Trincado, J. G., García Pérez, A. E., Lucatello, S., Majewski, S. R., Martell, S. L., O'Connell, R. W., Allende Prieto, C., Bizyaev, D., Carrera, R., Lane, R. R., Malanushenko, E., Malanushenko, V., Muñoz, R. R., Nitschelm, C., Oravetz, D., Pan, K., Roman-Lopes, A., Schultheis, M., and Simmons, A. (2017). APOGEE chemical abundances of globular cluster giants in the inner Galaxy. *Monthly Notices of the Royal Astronomical Society*, 466(1):1010–1018.
- Shetrone, M., Bizyaev, D., Lawler, J. E., Allende Prieto, C., Johnson, J. A., Smith, V. V., Cunha, K., Holtzman, J., García Pérez, A. E., Mészáros, S., Sobeck, J., Zamora, O., García-Hernández, D. A., Souto, D., Chojnowski, D., Koesterke, L., Majewski, S., and Zasowski, G. (2015). The SDSS-III APOGEE Spectral Line List for H-band Spectroscopy. *Astrophysical Journal, Supplement*, 221(2):24.
- Smith, H. E. (2007). *Physics 5 - Lecture Summary #9 Stellar Spectra, em\_abs.gif*. University of California, San Diego Physics 5 - Introduction to Astronomy <http://casswww.ucsd.edu/archive/physics/ph5/Stars.html>.
- Smith, V. V., Bizyaev, D., Cunha, K., Shetrone, M. D., Souto, D., Allende Prieto, C., Masseron, T., Meszaros, S., Jonsson, H., Hasselquist, S., Osorio, Y., Garcia-Hernandez, D. A., Plez, B., Beaton, R. L., Holtzman, J., Majewski, S. R., Stringfellow, G. S., and Sobeck, J. (2021). The APOGEE Data Release 16 Spectral Line List. *arXiv e-prints*, page arXiv:2103.10112.
- Smith, V. V., Cunha, K., Shetrone, M. D., Meszaros, S., Allende Prieto, C., Bizyaev, D., García Pérez, A., Majewski, S. R., Schiavon, R., Holtzman, J., and Johnson, J. A. (2013). Chemical Abundances in Field Red Giants from High-resolution H-band Spectra Using the APOGEE Spectral Linelist. *The Astrophysical Journal*, 765:16.
- Sollima, A. (2020). The eye of Gaia on globular clusters structure: tidal tails. *Monthly Notices of the Royal Astronomical Society*, 495(2):2222–2233.

- Strömgren, B. (1966). Spectral Classification Through Photoelectric Narrow-Band Photometry. *Annual Review of Astronomy and Astrophysics*, 4:433.
- Thomas Wijnen<sup>1</sup>, O. Pols, S. P. Z. . E. G. (retrieved 2022). *How efficient is accretion onto a protoplanetary disc? : Dialogue concerning a formation mechanism of two (or more) populations in globular clusters*. IMAPP, Radboud University Nijmegen, Sterrewacht Leiden, Leiden University, [https://astro.uni-bonn.de/~sambaran/DS2014/Modest14\\_Posters/Wijnen.pdf](https://astro.uni-bonn.de/~sambaran/DS2014/Modest14_Posters/Wijnen.pdf).
- Tian, K. P., Zhao, J. L., Shao, Z. Y., and Stetson, P. B. (1998). Determination of proper motions and membership of the open clusters NGC 1750 and NGC 1758. *aaps*, 131:89–98.
- Tsujimoto, T. and Bekki, K. (2012). First Evidence of Globular Cluster Formation from the Ejecta of Prompt Type Ia Supernovae. *Astrophysical Journal, Letters*, 751(2):L35.
- van Regemorter, H. (1965). Spectral Line Broadening. *Annual Review of Astronomy and Astrophysics*, 3:71.
- Ventura, P. and D'Antona, F. (2009). Massive AGB models of low metallicity: the implications for the self-enrichment scenario in metal-poor globular clusters. *Astronomy and Astrophysics*, 499(3):835–846.
- Walker, E. N. (Retrieved 21 May 2019). *CCD PHOTOMETRY*, British Astronomical Association. [https://britastro.org/vss/ccd\\_photometry.htm](https://britastro.org/vss/ccd_photometry.htm).
- Wijnen, T. P. G., Pols, O. R., Pelupessy, F. I., and Portegies Zwart, S. (2016). Face-on accretion onto a protoplanetary disc. *Astronomy and Astrophysics*, 594:A30.
- Wilson, J. C., Hearty, F. R., Skrutskie, M. F., Majewski, S. R., Holtzman, J. A., Eisenstein, D., Gunn, J., Blank, B., Henderson, C., Smeeth, S., Nelson, M., Nidever, D., Arns, J., Barkhouser, R., Barr, J., Beland, S., Bershadsky, M. A., Blanton, M. R., Brunner, S., Burton, A., Carey, L., Carr, M., Colque, J. P., Crane, J., Damke, G. J., Davidson, J. W., J., Dean, J., Di Mille, F., Don, K. W., Ebelke, G., Evans, M., Fitzgerald, G., Gillespie, B., Hall, M., Harding, A., Harding, P., Hammond, R., Hancock, D., Harrison, C., Hope, S., Horne, T., Karakla, J., Lam, C., Leger, F., MacDonald, N., Maseman, P., Matsunari, J., Melton, S., Mitcheltree, T., O'Brien, T., O'Connell, R. W., Patten, A., Richardson, W., Rieke, G., Rieke, M., Roman-Lopes, A., Schiavon, R. P., Sobeck, J. S., Stolberg, T., Stoll, R., Tembe, M., Trujillo, J. D., Uomoto, A., Vernieri, M., Walker, E., Weinberg, D. H., Young, E., Anthony-Brumfield, B., Bizyaev, D., Breslauer, B., De Lee, N., Downey, J., Halverson, S., Huehnerhoff, J., Klaene, M., Leon, E., Long, D., Mahadevan, S., Malanushenko, E., Nguyen, D. C., Owen, R., Sánchez-Gallego, J. R., Sayres, C., Shane, N., Shectman, S. A., Shetrone, M., Skinner, D., Stauffer, F., and Zhao, B. (2019). The Apache Point Observatory Galactic Evolution Experiment (APOGEE) Spectrographs. *Publications of the ASP*, 131(999):055001.

- Wünsch, R., Palouš, J., Tenorio-Tagle, G., and Ehlerová, S. (2017). The Formation of Secondary Stellar Generations in Massive Young Star Clusters from Rapidly Cooling Shocked Stellar Winds. *The Astrophysical Journal*, 835(1):60.
- Xiang, Y., Xi, J., Shao, Z., Wang, M., and Yang, Y. (2021). Open clusters identifying by multi-scale density feature learning. *apss*, 366(2):17.
- Yong, D., Grundahl, F., Nissen, P. E., Jensen, H. R., and Lambert, D. L. (2005). Abundances in giant stars of the globular cluster NGC 6752. *Astronomy and Astrophysics*, 438(3):875–888.
- Yong, D., Roederer, I. U., Grundahl, F., Da Costa, G. S., Karakas, A. I., Norris, J. E., Aoki, W., Fishlock, C. K., Marino, A. F., Milone, A. P., and Shingles, L. J. (2014). Iron and neutron-capture element abundance variations in the globular cluster M2 (NGC 7089)\*. *Monthly Notices of the Royal Astronomical Society*, 441(4):3396–3416.
- Zamora, O., García-Hernández, D. A., Allende Prieto, C., Carrera, R., Koesterke, L., Edvardsson, B., Castelli, F., Plez, B., Bizyaev, D., Cunha, K., García Pérez, A. E., Gustafsson, B., Holtzman, J. A., Lawler, J. E., Majewski, S. R., Manchado, A., Mészáros, S., Shane, N., Shetrone, M., Smith, V. V., and Zasowski, G. (2015). New H-band Stellar Spectral Libraries for the SDSS-III/APOGEE Survey. *Astronomical Journal*, 149(6):181.
- Zasowski, G., Cohen, R. E., Chojnowski, S. D., Santana, F., Oelkers, R. J., Andrews, B., Beaton, R. L., Bender, C., Bird, J. C., Bovy, J., Carlberg, J. K., Covey, K., Cunha, K., Dell’Agli, F., Fleming, S. W., Frinchaboy, P. M., García-Hernández, D. A., Harding, P., Holtzman, J., Johnson, J. A., Kollmeier, J. A., Majewski, S. R., Mészáros, S., Munn, J., Muñoz, R. R., Ness, M. K., Nidever, D. L., Poleski, R., Román-Zúñiga, C., Shetrone, M., Simon, J. D., Smith, V. V., Sobeck, J. S., Stringfellow, G. S., Szigetiáros, L., Tayar, J., and Troup, N. (2017). Target Selection for the SDSS-IV APOGEE-2 Survey. *Astronomical Journal*, 154(5):198.
- Zhang, S., Mackey, D., and Da Costa, G. S. (2022). A search for stellar structures around nine outer halo globular clusters in the Milky Way. *Monthly Notices of the Royal Astronomical Society*, 513(3):3136–3164.
- Zhang, Y., Han, Z., Liu, J., Zhang, F., and Kang, X. (2012). Testing three derivative methods of stellar population synthesis models. *Monthly Notices of the Royal Astronomical Society*, 421(2):1678–1696.
- Zinn, R. (1985). The Globular Cluster System of the Galaxy. IV. The Halo and Disk Subsystems. *The Astrophysical Journal*, 293:424.
- Zinn, R. and West, M. J. (1984). The globular cluster system of the Galaxy. III. Measurements of radial velocity and metallicity for 60 clusters and a compilation of metallicities for 121 clusters. *Astrophysical Journal, Supplement*, 55:45–66.